Year : 2015

ENVIRONMENTAL CONTROL OF THE POM1-DEPENDENT CELL-SIZE REGULATION PATHWAY IN FISSION YEAST

KELKAR Manasi

UNIL | Université de Lausanne

Faculté de biologie
et de médecine

Département de Microbiologie Fondamentale

ENVIRONMENTAL CONTROL OF THE POM1-DEPENDENT CELL-SIZE REGULATION PATHWAY IN FISSION YEAST

Thèse de doctorat ès sciences de la vie (PhD)

présentée à la

Faculté de biologie et de médecine
de l'Université de Lausanne

Par

Manasi KELKAR

Master de l'Université de Pune, Inde

Jury

Prof. John Pannell, Président

Prof. Sophie Martin, Directrice de thèse

Prof. Jürg Bähler, expert

Prof.Claudio De Virgilio, expert

Lausanne 2015

Scientific summary

Cells couple their growth and division rate in response to nutrient availability to maintain a constant size. This co-ordination happens either at the G1-S or the G2-M transition of the cell cycle. In the rod-shaped fission yeast, size regulation happens at the G2-M transition prior to mitotic commitment. Recent studies have focused on the role of the DYRK-family protein kinase Pom1, which forms gradients emanating from cell poles and inhibits the mitotic activator kinase Cdr2, present at the cell middle. Pom1 was proposed to inhibit Cdr2 until cells reached a critical size before division. However when and where Pom1 inhibits Cdr2 is not clear as medial Pom1 levels do not change during cell elongation. Here I show that Pom1 gradients are susceptible to environmental changes in glucose. Specifically, upon glucose limitation, Pom1 re-localizes from the poles to the cell sides where it delays mitosis through regulating Cdr2. This re-localization occurs due to microtubule de-stabilization and lateral catastrophes leading to transient deposition of the Pom1 gradient nucleator Tea4 along the cell cortex. As Tea4 localization to cell sides is sufficient to recruit Pom1, this explains the mechanism of Pom1 re-localization. Microtubule destabilization and consequently Tea4 and Pom1 spread depends on the activity of the cAMP-dependent Protein Kinase A (PKA/Pka1), as *pka1* mutant cells have stable microtubules and retain polar Tea4 and Pom1 under limited glucose. PKA signaling negatively regulates the microtubule rescue factor CLASP/Cls1, thus reducing its ability to stabilize microtubules. Thus PKA signaling tunes CLASP activity to promote microtubule de-stabilization and Pom1 re-localization upon glucose limitation. I show that the side-localized Pom1 delays mitosis and balances the role of the mitosis promoting, mitogen-associated protein kinase (MAPK) protein Sty1. Thus Pom1 re-localization may serve to buffer cell size upon glucose limitation.

Keywords: fission yeast, cell-size regulation, glucose limitation, Pom1, Cdr2, Tea4, microtubules, PKA, CLASP, MAPK

Résumé scientifique

Afin de maintenir une taille constante, les cellules régulent leur croissance ainsi que leur taux de division selon les nutriments disponibles dans le milieu. Dans la levure fissipare, cette régulation de la taille précède l'engagement mitotique et se fait à la transition entre les phases G2 à M du cycle cellulaire. Des études récentes se sont focalisées sur le rôle de la protéine Pom1, membre de la famille des DYRK kinase. Celle-ci forme un gradient provenant des pôles de la cellule et inhibe l'activateur mitotique Cdr2 présent au centre de la cellule. Le model propose que Pom1 inhibe Cdr2 jusqu'à atteindre une taille critique avant la division. Cependant quand et à quel endroit dans la cellulle Pom1 inhibe Cdr2 n'était pas clair car les niveaux médians de Pom1 ne changent pas au cours de la l'élongation des cellules. Dans cette étude, je montre que les gradients de Pom1 sont sensibles aux changements environnementaux du taux de glucose. Plus spécifiquement, en conditions limitantes de glucose, Pom1 se relocalise des pôles de la cellule pour se distribuer sur les côtés de celle-ci. Par conséquent, un délai d'entrée en mitose est observé dû à l'inhibition Cdr2 par Pom1. Cette délocalisation est due à la déstabilisation des microtubules qui va conduire à une déposition transitoire de Tea4, le nucléateur du gradient de Pom1, tout au long du cortex de la cellule. Comme la localisation de Tea4 sur les côtés de la cellule est suffisante pour recruter la protéine Pom1, ceci explique le mécanisme de relocalisation de celle-ci. La déstabilisation des microtubules et par conséquent la diffusion de Tea4 et Pom1 dépendent de l'activité de la protéine kinase A dépendante de l'AMP cyclique (PKA/Pka1). En absence de pka1, la stabilité des microtubules n'est pas affectée ce qui permet la rétention de Tea4 et Pom1 aux pôles de la cellule même en conditions limitantes de glucose. La signalisation via PKA régule négativement le facteur de sauvetage des microtubules CLASP/Cls1 et permet donc de réduire sa fonction de déstabilisation des microtubules. Ainsi la signalisation via PKA affine l'activité des CLASP pour promouvoir la déstabilisation des microtubules et la relocalisation de Pom1 en conditions limitantes de glucose. Je montre que la localisation sur les côtés retarde l'entrée en mitose et compense l'action de la protéine Sty1, connue pour être une MAPK qui induit l'entrée en mitose. Ainsi, la relocalisation de Pom1 pourrait servir à tamponner la taille de la cellule en condition limitantes de glucose.

Public Summary

Various cell types in the environment such as bacterial, plant or animal cells have a distinct cellular size. Maintaining a constant cell size is important for fitness in unicellular organisms and for diverse functions in multicellular organisms. Cells regulate their size by coordinating their growth rate to their division rate. This coupling is important otherwise cells would get progressively smaller or larger after each successive cell cycle. In their natural environment cells may face fluctuations in the available nutrient supply. Thus cells have to coordinate their division rate to the variable growth rates shown under different nutrient conditions. During my PhD, I worked with a single-celled rod shaped yeast called the fission yeast. These cells are longer when the nutrient supply is abundant and shorter when the nutrient supply is scarce. A protein that senses changes in the external carbon source (glucose) is called Protein Kinase A (PKA). The rod shape of fission yeast cells is maintained thanks to a structural backbone called the cytoskeleton. One of the components of this backbone is called microtubules, which are small tube like structures spanning the length of the cell. They transport a protein called Tea4, which in turn is important for the proper localization of another protein Pom1 to the cell ends. Pom1 helps to maintain proper shape and size of these rod shaped yeast cells.

My thesis work showed that upon reduction in the external nutrient (glucose) levels, microtubules become less stable and show an alteration in their organization. A significant percentage of the microtubules contact the side of the cell instead of touching only the cell tip. This leads to the spreading of the protein Pom1 away from the tips all around the cell periphery. This helps fission yeast cells to maintain the proper size required under these conditions of limited glucose supply. I further showed that the protein PKA regulates microtubule stability and organization and thus Pom1 spreading and maintenance of proper cell size. Thus my work led to the discovery of a novel pathway by which fission yeast cells maintain their size under limited supply of glucose.

Resumé grand public

Divers types cellulaires dans l'environnement tels que les bactéries, les plantes ou les cellules animales ont une taille précise. Le maintien d'une taille cellulaire constante est importante pour le fitness des organismes unicellulaire ainsi que pour multiples fonctions dans les organismes multicellulaires. Les cellules régulent leur taille en coordonnant le taux de croissance avec le taux de division. Ce couplage est essentiel sinon les cellules deviendraient progressivement plus petites ou plus grandes après chaque cycle cellulaire. Dans leur habitat naturels les cellules peuvent faire face a des fluctuations dans le taux de nutriment disponible. Les cellules doivent donc coordonner leur taux de division aux taux variables de croissances perçus dans les différentes conditions nutritionnels.

Pendant ma thèse, j'ai travaillée sur une levure unicellulaire, en forme de bâtonnet, nommé levure fissipare ou levure de fission. La taille de ces cellules est plus grande quand le taux de nutriments est grand et plus courte quand celui-ci est plus faible. Une protéine qui perçoit les changements dans le taux externe de la source de carbone (glucose) est nommée PKA pour protéine kinase A. La forme en bâtonnet de la cellule est due aux caractères structuraux du cytosquelette. Une composante importante de ce cytosquelette sont les microtubules, dont la structures ressemble à des petit tubes qui vont d'un bout à l'autre de la cellule. Ces microtubules transportent une protéine importante nommée Tea4 qui à leur tour importante pour la bonne localisation d'une autre protéine Pom1 aux extrémités de la cellule. La protéine Pom1 aide à maintenir la taille appropriée des levures fissipares.

Mon travail de thèse a montré qu'en présence de taux faible de nutriments (glucose) les microtubules deviennent de moins en moins stables et montrent une désorganisation globale. Un pourcentage significatif des microtubules touche les côtés de la cellule aux lieu d'atteindre uniquement les extrémités. Ceci a pour conséquence une diffusion de Pom1 tout au long du cortex de la cellule. Ceci aide les levures fissipares à maintenir la taille appropriée pendant ce stress nutritionnel. De plus, je montre que PKA régule la stabilité et l'organisation des microtubules et par conséquent la diffusion de Pom1 et le maintien d'une taille constante. En conclusion, mon travail a conduit à la découverte d'un nouveau mécanisme par lequel la levure fissipare maintient sa taille dans des conditions limitantes en glucose.

Table of Contents

Chapter 1

Introduction

Regulation of cell size in fission yeast

The size of a cell is a fundamental attribute that contributes to function in multicellular organisms and fitness in unicellular organisms (Jorgensen and Tyers, 2004). To maintain a constant size cells have to couple their growth rate to their division rate. This co-ordination helps maintaining size homeostasis and is seen across a large number of unicellular organisms. Regulation of cell size occurs at two phases of the cell cycle: at the G1-S transition and/or the G2-M transition. These cell cycle checkpoints ensure that a cell has reached a certain threshold for cell size before entering either the S or the M phase. They govern the time that a cell spends in either the G1 or the G2 phase thus providing a constant cellular size. The highly divergent unicellular eukaryotes: the budding and fission yeasts have been ideal genetic model systems to study size regulation. In *Saccharomyces cerevisiae*, the budding yeast, cytokinesis is asymmetric and produces a large mother cell and a much smaller daughter cell. To compensate for this asymmetry, the small daughter cells grow more than their mother cells before dividing. This growth happens exclusively in the G1 phase, in which daughter cells spend a longer time to attain a critical cell size than their mothers. Once this size threshold is achieved, cells commit to division at a point in late G1 called the 'Start' (Pringle and Hartwell, 1981). Thus the G1-S transition is the most crucial step of size regulation in budding yeast.

Cell-size regulation in the rod-shaped *Schizosaccharomyces pombe*, the fission yeast has also been extensively studied. Indeed fission yeast was the first organism in which cell cycle mutants (wee1/wee2) were isolated that caused advanced entry into mitosis (Nurse, 1975). *S.pombe* makes an ideal model system to study cell size and cell cycle control as cells exhibit a stereotypical growth and division pattern: they grow by elongation exclusively at the cell ends/poles with a constant diameter during interphase, and then stop growth to divide medially. Medial fission occurs after they reach a critical length/size (~14 μm) to produce two daughter cells of equal size. Thus the length at septation can be considered as a measure of cell size (Fantes and Nurse, 1977; Fantes, 1977; Mitchison, 2003). After division both daughter cells initiate growth only at the end that was present in the mother cell prior to division (old end). Only in early G2, the end generated by the previous cell division cycle (new end) starts growing in a process called as New-End Take Off (NETO) which marks the

transition between monopolar to bipolar growth (Mitchison and Nurse, 1985).

Regulation of cell size in fission yeast primarily occurs at the G2-M transition (MacNeil and Nurse, 1997) with the G1-S control being cryptic under favorable conditions. In nutrient rich conditions, when cells exit mitosis they are sufficiently large enough to pass the size threshold required for S phase and thus immediately enter the S phase (Fantes and Nurse, 1977; MacNeil and Nurse, 1997). They then enter the long G2 phase adjusting the time they spend there depending on their birth sizes. Smaller cells spend longer time in G2 compared to longer cells. Once they reach a critical cell size they initiate mitosis. Entry into mitosis depends on the timely activation of the cyclin/cyclin-dependent kinase (cyclin-Cdk1) complex. The activation of CDK1 (Cdc2) in fission yeast depends on the phosphorylation status of its tyrosine residue: Tyr15. Phosphorylation of this residue by a kinase Wee1 keeps Cdc2 in an inhibitory state while de-phosphorylation by a protein phosphatase Cdc25 leads to its activation at G2/M transition. Thus Cdk1 activity and mitotic entry depends on the concerted activities of the activatory phosphatase Cdc25 and the inhibitory kinase Wee1 (MacNeil and Nurse, 1997; Rupes, 2002).

Nutrient-dependent modulation of cell size

Cell size regulation is also subject to the fluctuating external environment in which cells grow. As nutrient supply in the environment may be uncertain cells have to coordinate their division rate with the widely variable growth rates exhibited under different external conditions. This coupling is important otherwise cells would get progressively smaller or larger with every successive generation (Rupes, 2002). In budding yeast, unfavorable external conditions lead to an elongation of the G1 phase of the cell cycle giving cells enough time to reach the new threshold of cell size set under those conditions. Modulation of the external environment has a strong impact on the target size in fission yeast as well, such that cells growing in nutrient-rich medium divide at a longer cell length than the ones growing in nutrient-poor medium. This occurs mainly due to an elongation in the G1 or the G2 phase of the cell cycle in the nutrient-poor medium, thus giving cells enough time until they attain the required critical cell size. If wild type cells are shifted to a medium lacking nitrogen cells divide approximately two times without growing, producing short and round cells that

arrest in G1. The lengthening of G1 is advantageous to cells as it allows for an important response to starvation: if cells are compatible they undergo mating and meiosis from G1 to form haploid resistant spores. If cells are heterosexual however, they remain in the G0 state (Costello *et al.*, 1986; Su *et al.,* 1996; Yanagida, 2009). If cells are shifted from a rich nitrogen source to a poor one (glutamate to proline) they also divide at a shorter cell-size.

A reduction of the favored carbon source in fission yeast, glucose, leads to cell length shortening. A decrease in glucose levels from the normal 2% to as low as 0.08% leads to largely normal growth rates, however the size at division is reduced by 20-30%. In these limited glucose conditions, cells transiently stop division for one or two generations and then resume their division at rates similar to those in high glucose. There is a transient decrease in the septation index following the shift, suggesting either a cell cycle delay or arrest, however it gets restored within 4 hours of the shift (Saitoh and Yanagida, 2014). If the glucose concentration is reduced even further, cells get shorter however the nature of divisions is stochastic. Under very low glucose concentration of 0.03% cells are mostly quiescent and only a small population undergoes division. A complete removal of glucose causes an immediate arrest in cell division (Yanagida *et al.*, 2011).

Signaling pathways regulating cell size upon nutrient depletion

Apart from the intrinsic homeostasis mechanisms, stress regulated pathways also impinge on the cell-cycle machinery to contribute towards size regulation. In eukaryotic cells the two well studied and conserved pathways that respond to the changing environment are the Mitogen Activated Protein Kinase (MAPK) pathway and the Target Of Rapamycin (TOR) pathway. A third one that responds to external glucose levels is the cAMP- dependent Protein Kinase A (cAMP/PKA) pathway.

The MAPK pathway gets activated in response to stress and nutrient deprivation. In fission yeast cells, the MAP kinase protein (Spc1/Sty1) was shown to be important for mitotic onset, as cells deficient for Spc1 show a G2 delay under steady state conditions. This phenotype gets exacerbated under conditions of stress, such as, high osmolarity medium (KCl) and nutrient (nitrogen) limitation. Spc1 was shown to promote mitotic onset thus linking the external environment to the cell-cycle

machinery (Shiozaki and Russell, 1995).

TOR also coordinates cell size and growth under nutrient limitation. Inhibition of TOR has been shown to increase cell numbers and reduce cell size at division in *Drosophila* and mammalian cell cultures (Wu *et al*., 2007, Fingar *et al*., 2004). This is true even for fission yeast cells: when wild type cells are shifted from a good to a poor nitrogen source (glutamate to proline), they divide at a reduced cell size. This nutrient modulated control of mitotic onset is mediated through reduced TOR signaling causing an increased activation of the MAPK protein-Sty1 (Fig 1.1). This in turn leads to recruitment of the Polo kinase at the spindle pole body (SPB) and subsequent Cdk1 activation (Petersen and Hagan, 2005; Petersen and Nurse, 2007).
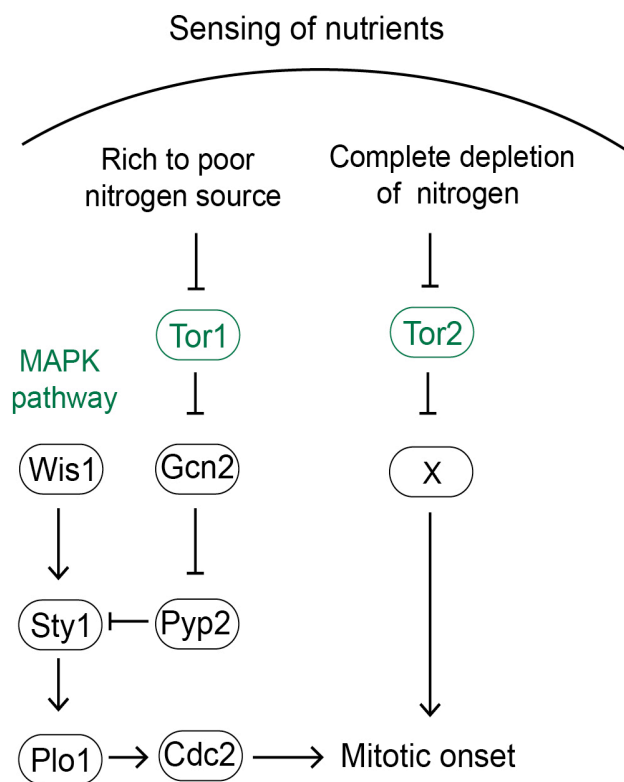
Figure1.1 Nutrient dependent modulation of cell-size via the TOR and MAPK pathway Shift of fission yeast cells from a rich to a poor nitrogen source, leads to inhibition of the TOR signaling. This leads to de-repression of Gcn2 an effector of TOR and a modulator of translation to inhibit the Pyp2 phosphatase. This further causes activation of the MAPK (Sty1/Spc1) to recruit Polo kinase (Plo1) to the spindle pole bodies (SPBs) to advance mitosis. Complete removal of nitrogen source causes inhibition of Tor2 and accelerated mitosis for 2 generations after which cells arrest in G1.

Adapted from Petersen and Nurse, 2007

Fission yeast cells shifted from a glucose-rich medium (2%) to a glucose-poor environment (0.08%) divide at a shorter cell size (Yanagida, 2009), but the exact mechanism of such an adaptation remains unclear. Hanyu *et al.,* in 2009 reported that the putative CaMKK in fission yeast- Ssp1, that regulates G2-M control and response

to stress, is required for cell growth under limited glucose conditions. They observed that *ssp1Δ* cells remained long and failed to reduce their cell size upon glucose limitation. They also showed that Sds23: an inhibitory regulator of the type 2 phosphatases, which itself is requited for tolerance to limited glucose, acts as a suppressor of the *ssp1* phenotype. Recent studies using genome wide transcriptome analysis, show an up-regulation of genes coding for transcription factors and proteins like Ssp1 and the glucose transporter Ght5 (Saitoh and Yanagida, 2014; Saitoh *et al.*, 2014). The TOR pathway has also been implicated in tolerance to limited glucose. Specifically, the TORC1 and the TORC2 pathways were shown to have opposing effects on mitotic entry in limited glucose. The TORC1 mutant *tor2-S* was shown to undergo accelerated mitosis while the TORC2 mutant *tor1-D* was shown to remain long under limited glucose (Ikai *et al.*, 2011). Thus although a lot of proteins have been implicated in altering cell-size in response to limited glucose, the exact mechanisms by which they directly or indirectly affect CDK1 (Cdc2) activity are not completely clear.

Glucose signaling in fission yeast: the cyclic-AMP/Protein Kinase A pathway

Carbon source sensing has been extensively studied in the context of catabolite repression in which microorganisms first utilize a favorable carbon source by repression of the enzymes required to metabolize the unfavorable carbon source (Magasanik, 1961). Once the favorable source is over, this repression gets relieved and cells can use the second favored carbon source. In fission yeast like in many microorganisms the preferred carbon source is glucose and detection of glucose causes the repression of enzymes involved in utilization of other less optimal carbon sources. Glucose detection in fission yeast leads to a transient increase in the levels of cAMP to activate the cAMP-dependent Protein Kinase A (PKA). Studies of catabolite repression suggest that glucose detection acts largely through the PKA pathway as strains with reduced PKA activity fully mimic glucose-starved cells (Hoffman and Winston, 1991; Maeda *et al.*, 1990).

Most of the components of the PKA pathway have been characterized based on their functional homology to orthologous genes in budding yeast by hybridization studies. Also much of their functions have been determined through the study of glucose

repression of genes involved in sexual reproduction or the *fbp1* gene that encodes a fructose-1,6-bisphosphatase required in gluconeogenesis. Glucose detection occurs via a canonical G-protein coupled receptor pathway (Fig 1.2). Git3, the receptor with 7 trans-membrane domains, is coupled to a heterotrimeric G-protein consisting three subunits, Gpa2, Git5 and Git11 (Gα, Gβ and Gγ) (Hoffman, 2005; Welton and Hoffman, 2000). Binding of glucose to the receptor, Git3, leads to release and activation of the Gα subunit Gpa2 for downstream signaling. Gpa2 signals activation of adenylyl cyclase Cyr1 to produce the secondary messenger cyclic-AMP (cAMP). cAMP binds the inactive PKA complex (Cgs1 bound to Pka1) to trigger release of Cgs1 (the negative regulator of Pka1), thereby leading to Pka1 activation (Hoffman, 2005; DeVoti *et al*., 1991). Finally cAMP levels and thus Pka1 activity are regulated by a cAMP phospho-di-esterase (PDE encoded by Cgs2) that degrades cAMP to AMP to dampen the signaling. Thus Pka1 is active when glucose levels are high and proposed to be largely inactive under limited glucose. Interestingly Pka1 also changes its cellular localization under various stresses. Whereas in normal steady state nutrient conditions its largely nuclear it gets exported to the cytoplasm upon nutrient starvation and hyperosmotic stress. Cgs1 was shown to be important in this nuclear export of Pka1 under hyperosmotic stress but not stationary phase induced stress conditions (Matsuo *et al*., 2008). The localization of Pka1 explains its transcriptional role, where the nuclear-localized pool in high glucose represses transcription of a number of genes involved in sexual reproduction and meiosis, gluconeogenesis and stress response (Maeda *et al*., 1994; Matsuo *et al*., 2008; Higuchi *et al*., 2002; Kunitomo *et al*., 2000). Thus *pka1Δ* cells undergo hyper-mating and sporulation even in rich media, show high levels of *fbp1* transcription and are resistant to various stresses and stationary phase adaptation.

Apart from these functions PKA also regulates the cell cycle. Indeed *pka1Δ* cells are small and overexpression of PKA causes cell elongation. Previous studies suggest a role for cAMP to delay mitosis (Kishimoto and Yamashita, 2000). This study showed that cAMP causes a reduction in the protein levels of Cdc25 thus delaying mitosis. Thus cAMP regulates the cell cycle in part by regulating the protein stability of Cdc25, which is an activator of mitosis. This presumably happens due to activation of PKA thus mimicking overexpression of Pka1 leading to mitotic delay and longer cells. However the exact mechanism of how PKA regulates cell cycle and cell size is

far from understood.
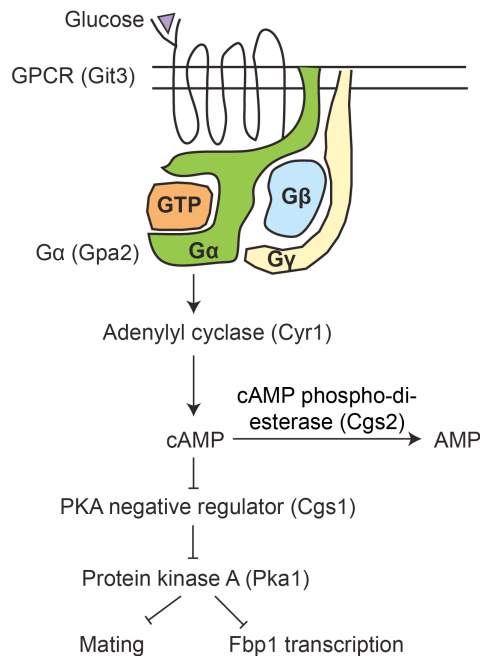
Role of Pom1 in cell size regulation under steady state conditions

The *pom1* (polarity misplaced) gene was first identified in a genetic screen looking at *S.pombe* mutants defective in morphology. The *pom1-1* allele was defective in positioning and orienting the division septum and formed aberrant T-shaped cells (Bähler and Pringle, 1998). Pom1 encodes a protein of 1087 amino acids with the kinase domain in the C-terminal region. It belongs to a dual specificity-tyrosine-regulated family of kinases (DYRK) conserved in eukaryotes. These kinases first auto-phosphorylate on a tyrosine residue in their activation loop, before phosphorylating serine/threonine residues on their target proteins (Lochhead *et al*., 2005). Although the specific targets of DYRKs show wide variation, their common functions are to regulate cell growth, cell division and differentiation (Aranda *et al*., 2011). Further characterization of the *pom1-1* allele revealed that these cells grow exclusively from one cell end (monopolar growth) and a large percentage of cells show a misplaced septum close to the non-growing end thus generating two cells of

20

unequal length following cell division (Bähler and Pringle, 1998).

Apart from Pom1's role in morphogenesis and placement of the division septum, recent studies have elucidated its function in regulating the cell cycle and cell-size. It was noted that *pom1Δ* cells have a shorter size at division compared to wild type cells and small increases in the levels of Pom1 caused a dose-dependent increase in cell size in both wild type and *cdc25-22* cells. In addition, forced localization of Pom1 to cell sides causes mitotic delay. This indicated that Pom1 is a dose-dependent inhibitor of the G2-M transition (Martin and Berthelot-Grosjean, 2009; Moseley *et al.*, 2009). By carrying out epistasis analysis between *pom1Δ* and mutants affecting the G2-M cell cycle transition these studies showed that *cdr2Δ* is epistatic to *pom1Δ*. Cdr2, a member of the SAD-family kinase is localized to a band of cortical nodes in the middle of interphase cells and it negatively regulates the Cdc2 inhibitory kinase Wee1 (Breeding *et al.*, 1998; Kanoh and Russel, 1998). Another kinase that negatively regulates Wee1 is Cdr1 (Nim1) (Wu and Russel, 1993; Parker *et al.*, 1993; Coleman *et al.*, 1993, Russell and Nurse, 1987), which also localizes to the nodes, however deletion of Cdr1 was not fully epistatic to Pom1, suggesting that Pom1 regulates specifically Cdr2 for G2-M regulation. Pom1 regulates the localization of Cdr2 as well, such that in *pom1Δ* cells the medial nodes of Cdr2 are seen in one half of the cell towards the non-growing end. Additionally both *in vivo* and *in vitro* experiments show that Pom1 directly phosphorylates Cdr2 in the C-terminal region (Martin and Berthelot-Grosjean 2009; Bhatia *et al.*, 2013). Further studies on the mechanism of the Pom1-Cdr2 regulation indicate a role for the Ca^{2+}/Calmodulin dependent kinase kinase (CaMKK) Ssp1 to cause a direct activation of Cdr2 by phosphorylation at threonine-166 to promote mitotic entry. Phosphorylation of the Cdr2 C-terminal tail by Pom1 was shown to block Ssp1 mediated activation of Cdr2 thus inhibiting mitotic commitment (Deng *et al.*, 2014). Pom1 also modulates the cortex binding of Cdr2 and its ability to form clusters (Rincon *et al.*, 2014).

Earlier studies showed that the medial levels of Pom1 reduce with increasing cell size by doing whole cell fluorescent quantifications of Pom1-GFP (Martin and Berthelot-Grosjean, 2009; Moseley *et al.*, 2009). This data led to the proposal of a model in which Pom1 inhibits Cdr2 in short cells where the medial levels of Pom1 are relatively high, thus activating Wee1, allowing for growth and thus a G2 delay. As the

cell-size increases, the medial levels of Pom1 drop and release the inhibition on Cdr2 to allow for Cdk1 activation and mitotic commitment (Fig1.3). These studies proposed Pom1 to be a cell size sensor that couples cell growth to cell cycle progression (Martin and Berthelot-Grosjean, 2009; Moseley *et al.*, 2009).
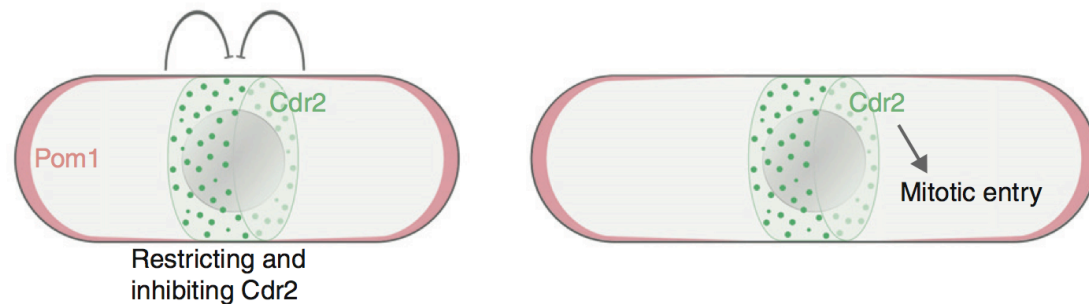
Figure 1.3 A geometric control for mitotic entry In short cells Pom1 gradients negatively regulate the mitotic inducer Cdr2 to inhibit Cdk1 and entry into mitosis. As cells get longer, this inhibition is relieved and active Cdr2 inhibits Wee1, thus promoting mitotic entry.

However, the role of Pom1 as a sensor for cell size has been recently questioned. This is because *pom1Δ* cells have the same cell size variability and size homeostasis capacity (time required to return to normal length after perturbation) as wild type cells. This study argued that if Pom1 was indeed the sole cell size sensor then *pom1Δ* cells would be expected to show slower or even no recovery to normal conditions after perturbations (Wood and Nurse, 2013). Additionally recent data using cortical Pom1 intensity quantifications, have detected no change in the medial concentration of Pom1 with an increase in cell length (Bhatia *et al.*, 2013; Pan *et al.*, 2014). Thus where and when Pom1 naturally inhibits Cdr2 is not clear.

Mechanism of Pom1 gradient formation

The microtubule cytoskeleton in fission yeast appears to be involved in regulation of polarized growth. Indeed mutations in the tubulin gene or disruption using microtubule depolymerizing drugs leads to bent or T-shaped cells (Umesono *et al.*, 1983; Hiraoka *et al.*, 1984). Microtubules serve to transport landmark polarity

proteins to the cell tips. The kelch repeat protein Tea1, which was originally identified through screens for morphogenetic mutants, gets transported to the cell poles by microtubules (Mata and Nurse, 1997). Biochemical purification of Tea1 led to the identification of Tea4, an SH3-domain containing protein. The Tea1-Tea4 complex gets delivered to cell tips by binding to the plus end of microtubules and gets deposited there upon microtubule-cortex contact (Behrens and Nurse, 2002; Feierbach *et al.*, 2004; Martin *et al.*, 2005; Tatebe *et al.*, 2005). The Tea1-Tea4 complex is essential for the proper localization and gradient formation of Pom1 to cell tips, indeed mutations in Tea4 lead to cytoplasmic Pom1 and *Tea1* mutants have both cortex-localized and cytosolic Pom1.

The positioning of microtubules and the localization of the Tea1-Tea4 complex dictates the formation of Pom1 gradients. Tea4 associates with and recruits the type I phosphatase Dis2 to the cell tips (Alvarez-Tabarés *et al.*, 2007). The binding of Pom1 to the cell tips relies on its phosphorylation status. The Tea4-Dis2 complex mediates de-phosphorylation of Pom1 exposing a positively charged basic region that binds to the negatively charged plasma membrane. Upon binding to the cell tips, Pom1 moves laterally through the membrane via diffusion and auto-phosphorylates itself on multiple residues mainly in the basic region. Auto-phosphorylation leads to an increase in its negative charge and promotes detachment from the membrane. Inside the cytoplasm Pom1 diffuses and interacts with Tea4 to initiate another round of membrane association-detachment thus shaping its concentration gradient (Fig 1.4A-B, Hachet *et al.*, 2011). Recent data suggest the importance of Pom1 cluster formation and intermolecular auto-phosphorylation as mechanisms to reduce noise and provide robustness to the gradient (Saunders *et al.*, 2012; Hersch *et al.*, 2015).
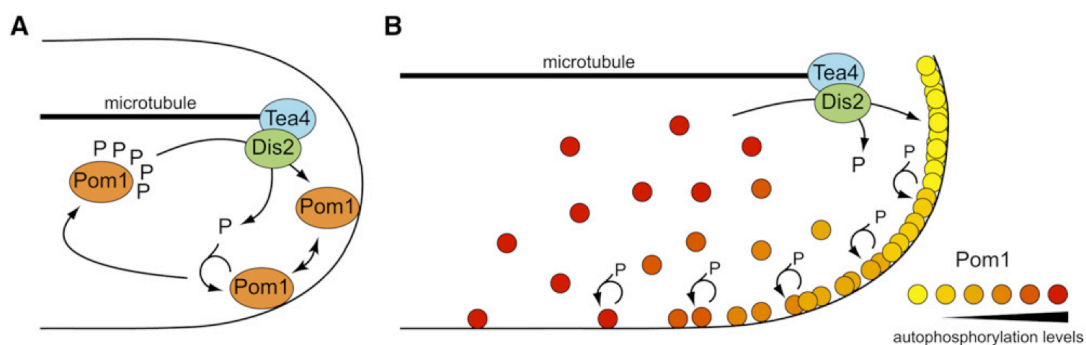
Adapted from Hachet *et al*., 2011

Figure 1.4 Mechanism of Pom1 gradient formation (A) Microtubules deposit Tea4 to the cell tips where it recruits the type I phosphatase Dis2. This complex mediates local de-phosphorylation of Pom1 leading to its binding to the negatively charged plasma membrane. There, Pom1 binds to the membrane and diffuses along it laterally. Auto-phosphorylation of Pom1 leads to its detachment from the membrane and in the cytoplasm it encounters Tea4, to mediate another round of membrane association-detachment thereby forming a gradient. **(B)** Multiple events of auto-phosphorylation may serve as a timer to shape Pom1 gradients. These events increase the probability of Pom1's detachment from the membrane. The various degrees of auto-phosphorylation are shown in colors of increasing intensities, with yellow for dephosphorylated state and red for a fully phosphorylated state.

The microtubule cytoskeleton in fission yeast

<u>Structure and dynamics</u>

As in all eukaryotic cells, the cytoskeleton in fission yeast is important to maintain the rod shape of these cells and for cellular morphogenesis. Morphogenesis depends on the capacity of a cell to establish and maintain polarity, which involves asymmetric distribution of regulators. Distinct molecules perform distinct functions and lead to spatial differences in the shape and function of a cell. Thus cell polarity underlies trafficking of molecules towards different parts of a cell, which is mainly achieved through the cytoskeleton comprising of actin and microtubules. Motor proteins can then 'walk' on these cytoskeletal tracks and regulate transport of molecules in a cell.

As most of my work is related to the microtubule cytoskeleton, it will be my focus in this part of the Introduction. Microtubules in general consist of polymers of α and β tubulin. The γ tubulin is found at the microtubule-organizing center (MTOC) and acts as a template to nucleate microtubules (Pereira and Schiebel, 1997). The α and β tubulin dimers polymerize end-to-end to form linear proto-filaments, which associate laterally, normally 13 of them, to form a single microtubule. Microtubule bundles have a distinct polarity with the end in which the β-tubulin is exposed called the plus (+) end and the α-tubulin called the minus (-) end. At the MTOC or the spindle pole body (SPB) in fission yeast, the γ tubulin along with a host of other proteins form the γ- tubulin ring complex (γ-TuRC). This acts as a template for the α/β -dimers to begin polymerization. This complex provides a cap at the – end, while growth continues away from the SPB at the + end (Desai and Mitchison, 1997).

24

Microtubules undergo a process of dynamic instability at their plus ends, both in vitro and in vivo, which means that they can dynamically switch between growth (assembly) and shrinkage (disassembly) (Fig 1.5, Mitchison and Kirschner, 1984; Sammak and Borisy, 1988; Walker *et al.*, 1988). During polymerization or growth the tubulin dimers are in a GTP-bound state, however hydrolysis of the β-tubulin GTP to GDP at the tip of a microtubule can lead to its de-polymerization or shrinkage (Hyman *et al.*, 1992). This transition from growth to shrinkage is called 'catastrophe'. However if a GTP-bound tubulin begins adding onto an existing microtubule tip protecting it from disassembly, this is termed 'rescue'. In 1984, Mitchison and Kirschner proposed that microtubules use this dynamic instability at the plus end to probe their surroundings/space in a cell. Microtubule dynamics, *i.e.*, growth, shrinkage, catastrophe and rescue are regulated by a host of microtubule associated proteins (MAPs) that bind to various regions on a microtubule and motor proteins that move along the length of a microtubule. I will focus on these regulatory proteins in a later part of this chapter.
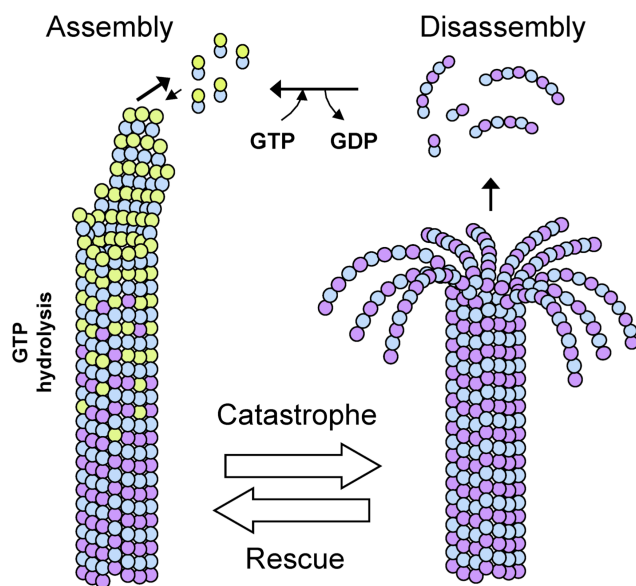
Figure1.5 Dynamic instability of microtubules During assembly GTP bound tubulin dimers bind to the microtubule plus end forming a GTP-cap. Hydrolysis of the GTP to GDP results in microtubule disassembly, and the GDP-tubulin peels off from the plus ends. The transition from assembly (growth) to disassembly (shrinkage) is called 'catastrophe' and from shrinkage to growth is called 'rescue'.

Adapted from Al-Bassam and Chang, 2011

Organization and function

Microtubules in interphase fission yeast cells are cytoplasmic and organized in about 3-6 antiparallel bundles parallel to the long axis of the cell, nucleated from the nuclear periphery (Fig1.6A, Marks *et al.*, 1986). Interphase microtubules are held in an

antiparallel fashion thanks to microtubule overlap close to the nuclear periphery in the middle of the cell (Drummond and Cross 2000; Tran *et al.*, 2001). The plus ends constantly exhibit dynamic instability, probe the surroundings and contact the cell poles/tips. Interphase microtubules help to center the nucleus by exerting pushing forces on it (Daga *et al.*, 2006) and also help to serve as tracks for directed delivery of polarity proteins. Thus even though microtubules are not essential for polarized growth in fission yeast they play an instructive role by delivering key proteins to active sites of polarity. At mitosis these interphase microtubules arrange themselves into an intra-nuclear spindle that helps chromosome segregation and nuclear division (Fig1.6B). After spindle elongation and finally disassembly the microtubule network forms an aster-like structure called the post-anaphase array (Fig1.6C) that along with the actin cytoskeleton leads to contractile ring assembly (CAR), the constriction of which leads to cell separation (Hagan, 1998).
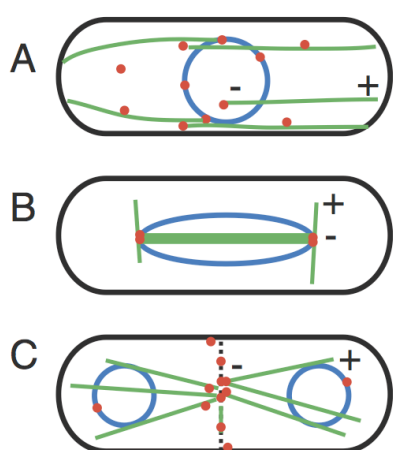
Figure1.6 Microtubule (MT) organization in fission yeast (A) In interphase, MTs are arranged in an antiparallel bundle (green), MTOCs (red) are close to the nuclear envelope or on existing MTs, the - end is in the middle and the + end is free, towards the cell tips **(B)** In mitosis intra-nuclear MTs form the mitotic spindle and astral MTs are nucleated from SPBs **(C)** At the end of mitosis, equatorial MTOCs assemble at the division site to assemble a post-anaphase MT array

Adapted from Sawin and Tran, 2006

Microtubules contribute in maintaining the rod shape of *S.pombe* cells. Disruption of the microtubule cytoskeleton does not cause loss of polarity, however results in aberrant growth. Mutation in the tubulin genes or disruption of microtubule regulatory proteins leads to misshapen cells: T shaped or curved (Umesono *et al.*, 1983; Radcliffe *et al.*, 1998; Zimmerman *et al.*, 2004). The branched shapes are also predominant after stress or recovery from starvation (Sawin and Snaith 2004; Tatebe *et al.*, 2005). Studies from various groups have showed that microtubules in fission yeast help in transporting the 'Tea' polarity proteins- Tea1 and Tea4 to the cell ends.

Their plus end localization depends on a +TIP protein Tip1 (CLIP-170), which is deposited on microtubules by a kinesin-Tea2. At the cortex this complex directly or indirectly recruits other factors such as the formin For3 to drive actin polymerization and Pom1 to regulate cell cycle progression, thus regulating cell polarity and morphogenesis (Mata and Nurse 1997; Behrens and Nurse 2002; Feierbach *et al.*, 2004; Martin *et al.*, 2005; Tatebe *et al.*, 2005; Browning *et al.*, 2000; Brunner and Nurse 2000; Browning *et al.*, 2003; Busch *et al.*, 2004).

Regulation of microtubule dynamics

As mentioned in the earlier part, microtubule plus-end dynamics are regulated by a host of proteins including MAPs and motors. They either stabilize or destabilize microtubules and regulate dynamics in time and space. In this section I will particularly focus on the role of the + TIP protein complex that binds the plus end of microtubules, the kinesin-8 family of proteins that destabilize microtubules and the well-conserved microtubule rescue factor CLASP.

Role of +TIP proteins- Mal3, Tip1, Tea2 and Alp14

Plus-end tracking proteins (+TIPs) are a set of MAPs that are conserved amongst eukaryotes and bind specifically to the microtubule plus end. In the 1990's, the first +TIP protein that was discovered was the Cytoplasmic Linker Protein of 170 kDa (CLIP-170) (Tip1 in fission yeast) (Rickard and Kreis, 1990). Since its discovery other +TIP proteins have also been discovered. Another family is named after the end binding protein (EB1) (Mal3 in fission yeast) that was originally identified as a binding partner to the tumor suppressor protein APC (Su *et al.*, 1995). The other plus end directed motor protein, the kinesin-like protein Tea2, helps to transport the CLIP-170 on microtubules thus maintaining proper cell shape and polarity (Busch *et al.*, 2004). Thus in fission yeast the +TIP complex includes Mal3/EB1, Tip1/CLIP-170 and Tea2/Kinesin.

EB1 proteins are involved in spindle formation, chromosome segregation and orientation by regulating astral microtubule dynamics but they also affect dynamics of interphase microtubules. In fission yeast, Mal3 binds and stabilizes the microtubule seam, inhibits shrinkage and promotes rescue (Katsuki *et al.*, 2009; Sandblad *et al.*, 2006). Indeed *mal3* mutants have shortened microtubules and high frequency of

catastrophe, indicating that Mal3 stabilizes microtubules (Beinhauer *et al.*, 1997; Busch and Brunner, 2004). The CLIP-170 family protein Tip1 localizes onto microtubules through Mal3 and the kinesin Tea2. *Tip1* mutant cells also show shortened microtubules and show premature catastrophe at the cell cortex outside the cell tip region (Brunner and Nurse, 2000). Loss of *Tip1* results in Tea1/Tea4 not reaching the cell ends thereby causing T-shaped cells. Finally the kinesin Tea2 helps to transport Tip1 onto microtubules, thus loss of *Tea2* also leads to shortened microtubules and alterations in cell shape (Busch and Brunner, 2004). In conclusion, these three proteins are required for microtubule growth and stability and loss of either of them causes shortened microtubules, reduction in growth rate and an increase in catastrophe rate. Additionally, another protein belonging to the XMAP215/Dis1 family, which are conserved tubulin binding TOG domain proteins, also regulate + end dynamics. The fission yeast orthologue, Alp14 was shown to localize to microtubule plus ends and acts as a dose-dependent microtubule polymerase (Al-Bassam *et al.*, 2012).

Role of kinesin-8 family proteins

Kinesin superfamily proteins (KIFs) are a class of molecular motor proteins that move directionally along microtubules to transport organelles and molecules that are essential for cellular functions. These motor proteins use energy derived from ATP hydrolysis to power processive movements along microtubules (Vale *et al.*, 1985). The conserved motor domain is the one that binds both ATP and microtubules, and the hydrolysis of ATP to release ADP generates motion. Apart from their ability to transport cargo, some families of kinesins are also important for chromosome segregation, bipolar spindle assembly and regulation of microtubule dynamics. In particular kinesin-8 and kinesin-13 families have been shown to possess microtubule de-polymerizing activities (Wordeman, 2005; Howard and Hyman, 2007; Gardner *et al.*, 2008).

In fission yeast, the two proteins that belong to the kinesin-8 family are called Klp5 and Klp6. Although most of the kinesins function as homodimers, Klp5 and Klp6 are the only members reported so far that function as obligate heterodimers, co-localizing throughout the entire cell cycle (Garcia *et al.*, 2002b; Li and Chang, 2003). They

localize to cytoplasmic microtubules in interphase and to the kinetochores and the spindle in mitosis. They have been shown to regulate chromosome segregation by regulating microtubule dynamics. Indeed deletion mutants though viable, have chromosome congression defects and show long, hyper stable microtubules that can curl along cell ends (Garcia *et al*., 2002; West *et al*., 2001; Sanchez-Perrez *et al*., 2005). Additionally, orthologs of kinesin-8 family proteins in both the budding yeast, and in human cells, Kip3 and Kif-18A respectively, have been shown to possess de-polymerization activity. Kip3 was shown to depolymerize microtubules in a length-dependent manner (Gupta *et al*., 2006; Varga *et al*., 2006; Mayr *et al*., 2007). In fission yeast, recent studies *in vivo* have shown that Klp5-Klp6 induce a microtubule length-dependent increase in catastrophe frequency by being specifically more enriched on long microtubules (Tischer *et al*., 2009). Although deletion mutants display no major changes in growth or shrinkage rates, the catastrophe and rescue frequencies are indeed diminished compared to wild type (Unsworth *et al*., 2008) thus corroborating their role in inducing catastrophes at cell ends. However *in vitro* characterization, did not detect noticeable depolymerase activity and it was proposed that Klp5-Klp6 could promote both microtubule nucleation at the cell center and catastrophe at cell ends (Erent *et al*., 2012; Grissom *et al*., 2009). Thus the mechanism of kinesin-8 family proteins to induce microtubule catastrophe in fission yeast, seems to be different from its conserved role as a depolymerase in other species.

Role of CLASPs

CLASPs (CLIP-170 ASsociated Proteins) as the name suggests, were initially identified in a yeast two-hybrid screen looking for partners of CLIP-170 in mammalian cells. They bind to microtubules stabilizing them and are well conserved from yeast to mammalian and plant cells. CLASPs in animal cells are localized to the interphase microtubule plus ends, the lattice and other parts where they stabilize microtubules by causing rescue (Akhmanova, 2001). They are also important during mitosis (localizing at the kinetochore and spindle), as loss of CLASP results in spindle collapse forming a monopolar spindle (Inoue *et al*., 2004; Maiato *et al*., 2003).

The sole fission yeast CLASP is Cls1/Peg1 and it localizes to the microtubule lattice

at regions of antiparallel microtubule overlap of interphase microtubules and the spindle. It accumulates to the overlaps thanks to its recruitment by the MAP65/PRC1-family protein Ase1 that bundles microtubules (Bratman and Chang, 2007; Loiodice *et al.*, 2005). However, dynein-dependent Cls1 localization near microtubule plus-ends was also reported (Grallert *et al*., 2006). Cls1 is responsible for almost all the rescue events at the spindle and interphase microtubules, indeed in *cls1* mutants rescues do not occur, however, other dynamic parameters remain unaltered. *In vitro* studies suggest that Cls1 reduces catastrophe and increases rescue frequency by binding the microtubules and directly recruiting tubulin dimers. Cls1 binds microtubule through its basic S/R rich region and tubulin through its TOG domains. Unlike animal cells, the fission yeast Cls1 binds to the overlaps and does not track plus ends. Overexpression of Cls1 causes it to bind all along the lattice and increases rescue frequencies (Bratman and Chang, 2007; Al-Bassam *et al*., 2010; Al-Bassam and Chang, 2011). Thus both *in vivo* and *in vitro* studies suggest that Cls1 acts as a microtubule rescue factor.

Background

When I started my PhD, one of the mechanisms, by which cells couple growth to division under steady state conditions, was proposed by the Martin and the Nurse labs. This involves as previously described the DYRK-family kinase Pom1 regulating its substrate the mitotic inducer kinase Cdr2. This mechanism was proposed to act as a cell size sensor in fission yeast. However what was unknown was whether this mechanism of size regulation was subject to modifications from the external environment in which cells grow and if so, what were the mechanisms of this regulation. As changes in external environment affect cell size, we wondered if the Pom1-Cdr2 pathway might be involved in this regulation. Further, both Pom1 and Cdr2 were previously described to be affected by modulation of the environment. Pom1 was shown to be distributed throughout the cell after pheromone treatment (Niccoli and Nurse, 2002) and cdr1/cdr2 mutant cells were initially identified to remain elongated even after nitrogen starvation (Young and Fantes, 1987; Rupes *et al*, 1997). This suggested that the pathway might be susceptible to changes in the external environmental conditions.

Main goals

With this in mind the two main questions that my PhD thesis tried to answer are:

1) **Whether and how Pom1 gradients are susceptible to changes in the external environment?**

2) **What are the physiological implications of the above for fission yeast cells?**

Introduction to Chapters

In the following Chapter 2, I will present the major Results of my PhD work. In the beginning I will describe how Pom1 localization is specifically affected by glucose limitation via the PKA pathway. Then I will try to address the question of when and where PKA activity is required for Pom1 re-localization. In the later part I will focus on the role of Tea4 and microtubules, which are required for Pom1 gradient formation. I will demonstrate that Pka1 destabilizes microtubules upon glucose limitation. I will then talk about the role of kinesin-8 family proteins Klp5/Klp6 and CLASP-Cls1, which I found to be epistatic to Pka1, in regulating microtubule dynamics. Finally I will investigate the physiological importance of Pom1 re-localization by looking at cell size at division as a proxy for the cell cycle.

Next in Chapter 3, I will discuss the main findings of my thesis work and also propose some future perspectives.

Finally in Chapter 4, I will describe the Materials and Methods that I have used in this work.

Chapter 2

Results

PKA antagonizes CLASP-dependent microtubule stabilization to re-localize Pom1 and buffer cell size upon glucose limitation

Pka1-dependent reversible re-localization of Pom1 around the cell cortex upon glucose limitation

While studying the role of Pom1, we serendipitously observed that, in contrast to the polar gradients formed in exponentially growing cells, Pom1 is detected all around the medial cortex in saturated cultures (Fig S2.1A). This suggested that nutrient starvation may trigger Pom1 re-localization. Thus I examined the effect of the two major nutrient sources: carbon and nitrogen on Pom1 localization. Depletion of nitrogen for up to 36h or shift from a good to a poor nitrogen source (glutamate to proline up to 70 minutes) did not modify Pom1 distribution (Fig S2.1C). By contrast, depletion of the preferred carbon source, glucose, to levels similar to those measured in the saturated cultures resulted in Pom1 re-localization (Fig 2.1A, C-D; S2.1B). Pom1 was almost homogenous around the cell periphery in 0.03% glucose, a condition in which cells grow very little, and was also less confined to cell poles in 0.08% glucose, in which cells proliferate at very similar rates as in 2% glucose (Pluskal *et al*., 2011). Pom1 re-localization occurred quickly within 10 minutes, and was reversible, thus could be rescued by replenishing glucose levels in the medium (Fig 2.1A). Measurement of protein levels both by fluorescent imaging and western blotting showed no major change in global Pom1 levels in the three glucose conditions tested (Fig S2.1D). Other stresses, such as heat shock at a higher temperature (36ºC) or osmotic stress (1M sorbitol) did not affect Pom1 localization (Fig S2.1I). Thus, Pom1 localization responds to changes in external glucose levels.

The mechanism of glucose detection in fission yeast cells is well studied. It occurs via a well-conserved cAMP-PKA pathway. Briefly, glucose is sensed by a dedicated G-protein-coupled receptor (GPCR) at the plasma membrane, Git3, which activates the Gα subunit Gpa2, in turn activating the adenylyl cyclase, Cyr1 (Hoffman, 2005). Cyr1 activation leads to the production of cyclic AMP (cAMP), which eventually leads to PKA activation. In *pka1Δ* cells grown to saturation or shifted to 0.08% or 0.03%G, Pom1 remained restricted to cell tips (Fig 2.1B, Fig S2.1A), indicating that the PKA pathway may be required for Pom1 re-localization upon glucose limitation. I further confirmed that the PKA pathway is required for Pom1 re-localization by looking at mutants upstream to Pka1.All the mutants of this pathway: *git3Δ*, *gpa2Δ*, *cyr1Δ*, failed to re-localize Pom1 upon shift to low glucose (Fig 2.1 D-E).

By contrast, cells deleted for the regulatory subunit of PKA, Cgs1, which exhibit constitutive Pka1 activity (DeVoti *et al*., 1991), displayed normal tip-localized Pom1 in glucose-rich conditions and Pom1 re-localization in low glucose (Fig 2.1E). To test if Pka1 could regulate Pom1 through direct phosphorylation, I mutated the three predicted serine residues (S449, S566 and S669) on Pom1 to alanine. Mutation of these sites either individually or in various combinations however, resulted in Pom1 re-localization in low glucose like in the wild type background. This finding lead me to hypothesize that Pka1 may regulate Pom1 indirectly through one or more protein/s.

To verify further whether the re-localization of Pom1 depends specifically on the PKA pathway, I studied the role of TOR and MAPK: two other major pathways that transduce information about nutrient availability (Shiozaki, 2009; Yanagida *et al*., 2011). Mutations in both the TORC1 and the TORC2 pathways, using the *tor2-S* and *tor1-D,* at the restrictive temperature (37°C), showed cell-tip restricted Pom1 in 2% glucose, while complete re-localization in 0.03% glucose much like wild type cells (Fig S2.1F). I also tested the effect of TOR using an inhibitor torin1 that blocks both the pathways (Atkin *et al*., 2013).
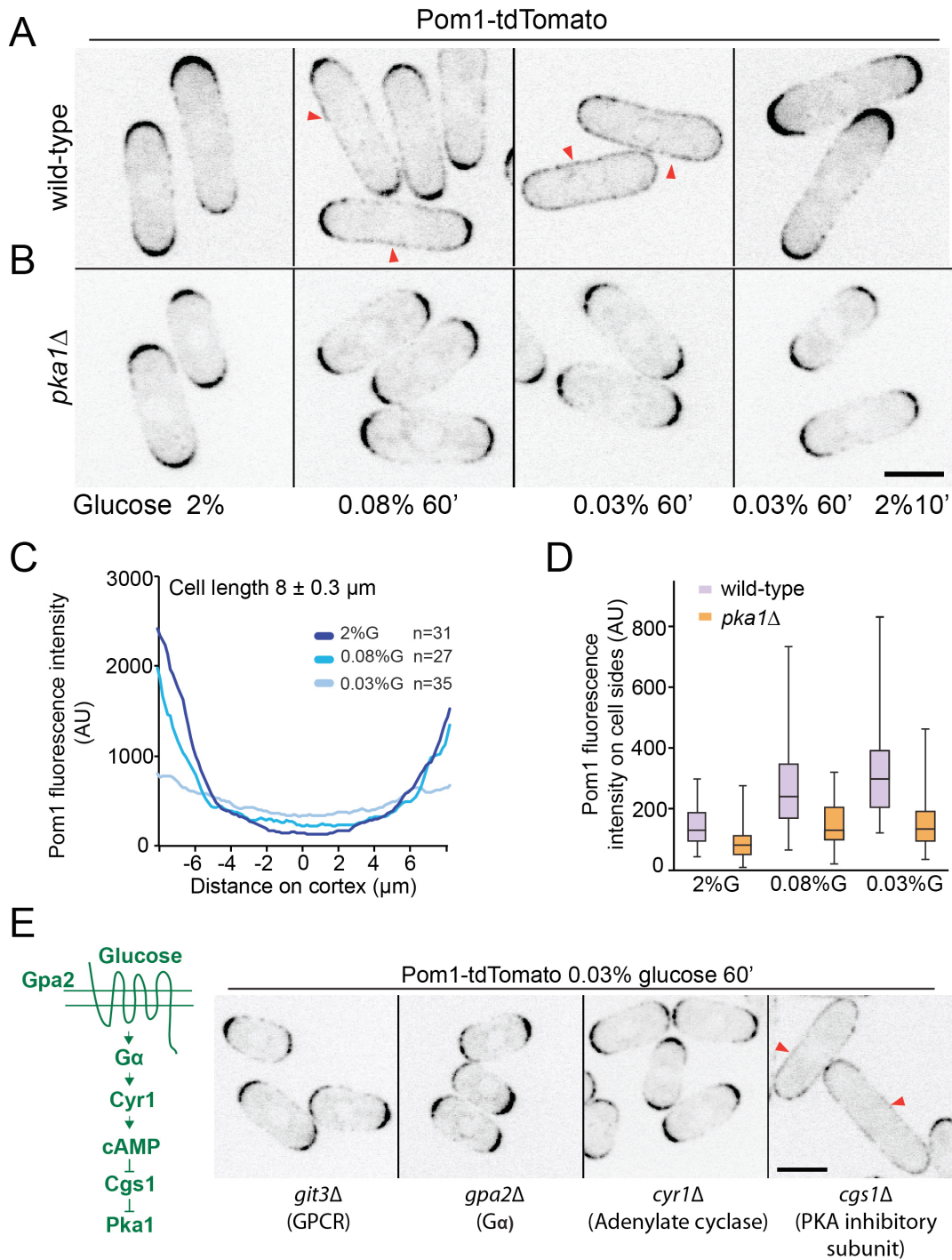
Figure 2.1: Pka1 dependent reversible re-localization of Pom1 in limited glucose (A) Sum of 5 medial spinning disk confocal images taken over 30 seconds of Pom1-tdTomato in wild type cells grown in 2% or 0.08% or 0.03% glucose for 1h. The last panel shows polar Pom1 upon 2% glucose replenishment for 10min. **(B)** Pom1-tdTomato in *pka1Δ* cells grown and imaged as in (A) **(C)** Distribution of cortical Pom1 from one cell tip to the other (0 = cell middle) in wild type cells obtained with the Cellophane plugin. Average of indicated number of profiles in 8μm-long cells. Profiles obtained from other cell lengths are similar **(D)** Box and whisker plot of cortical Pom1 fluorescence intensity in the middle 2μm region in both wild type (n=31, 27, 35 cells) and *pka1Δ* (n=34, 24, 42

This treatment did not cause Pom1 re-localization in high glucose. A double treatment of elevated Pka1 activity (using cAMP) and inhibition of TOR (using torin1) was also not sufficient to rescue Pom1 re-localization in steady state levels suggesting that TOR may not regulate Pom1 re-localization (Fig S2.1J). Deletion of the MAPK, Sty1/Spc1, did not prevent Pom1 re-localization in low glucose, though Pom1 remained fairly enriched at cell tips. Similar results were obtained upon treatment with the MAPK inhibitor SP600125, to acutely inhibit Sty1 (Hartmuth *et al.*, 2009). Interestingly hyper-activation of the MAPK pathway using the *wis1^{DD}* allele (Shiozaki *et al.*, 1998), led to a drastic reduction in global levels of Pom1 (Fig S2.1E). Thus, I concluded that the cAMP-PKA pathway is the major regulator of Pom1 re-localization upon glucose limitation with some contribution from the MAPK pathway. In my thesis I decided to focus on the role of the PKA signal regulating Pom1.

I also examined the localization of Cdr2, which is the known substrate of Pom1. Cdr2, which in steady-state glucose conditions is localized to the medial cell cortex forming nodes, was distributed more widely around the cell cortex upon glucose limitation, in a *pka1*-dependent manner (Fig S2.1G-H). The medial localization of Cdr2 depends on Pom1 in steady state conditions, with Cdr2 seen towards the non-growing end in *pom1Δ* cells. This regulation remained unaltered upon glucose limitation (Fig S2.1G). This is consistent with the proposed role of Pom1 in regulating the cortex binding of Cdr2 (Rincon *et al.*, 2014).

PKA activity is required in low glucose to signal Pom1 re-localization

Previous data showed that nuclear-localized Pka1 represses transcription in presence of glucose, with de-repression observed upon glucose depletion (Byrne and Hoffman, 1993; Hoffman and Winston, 1991; Higuchi *et al.*, 2002). However, the cortical, fast and reversible dynamics of Pom1 re-localization upon glucose depletion suggest this may not be a transcriptional response. Published data suggests that Pka1 gets exported

A

wild-type | pka1Δ

2%G 24h | 2%G 36h | 2%G 24h | 2%G 36h

B

Percentage glucose vs Time (hours)
— wild-type
— pka1Δ

C

Glutamate | Proline 15' | Proline 30' | Proline 70'

-N | t=0 | 60' | 24h | 36h

D

Normalized Pom1 levels (imaging)
wild-type | pka1Δ
2%G | 0.08%G | 0.03%G | 2%G | 0.08%G | 0.03%G

Pom1-GFP — 148kDa
α-tubulin — 50kDa
wild-type | pka1Δ

Normalized Pom1 levels (western blot)
2%G | 0.08%G | 0.03%G | 2%G | 0.08%G | 0.03%G

E

Pom1 td-Tomato

sty1Δ | SP600125 | wis1.DD
2%G | 0.03%G 60' | 2%G | 0.03%G 60' | 2%G | 0.03%G 60'

F

Pom1 td-Tomato

tor1-D
tor2-S
2%G | 0.03%G 60'

G

Cdr2-GFP

wt
pom1Δ
pka1Δ

Glucose 2% | 0.08% 60' | 0.03% 60'

H

Cell length 8±0.3 μm
Cdr2 fluorescence intensity in WT cells (AU) vs Distance on cortex (μm)
2%G n=30
0.08%G n=28
0.03%G n=36

I

36°C 60'
Pom1- td Tomato

1M Sorbitol 60'

J

Pom1- td Tomato

cgs2Δ
cgs2Δ pka1Δ

2% glucose | solvent control (DMSO) | 30mM cAMP | 25μM torin1 | 30mM cAMP+ 25μM torin1
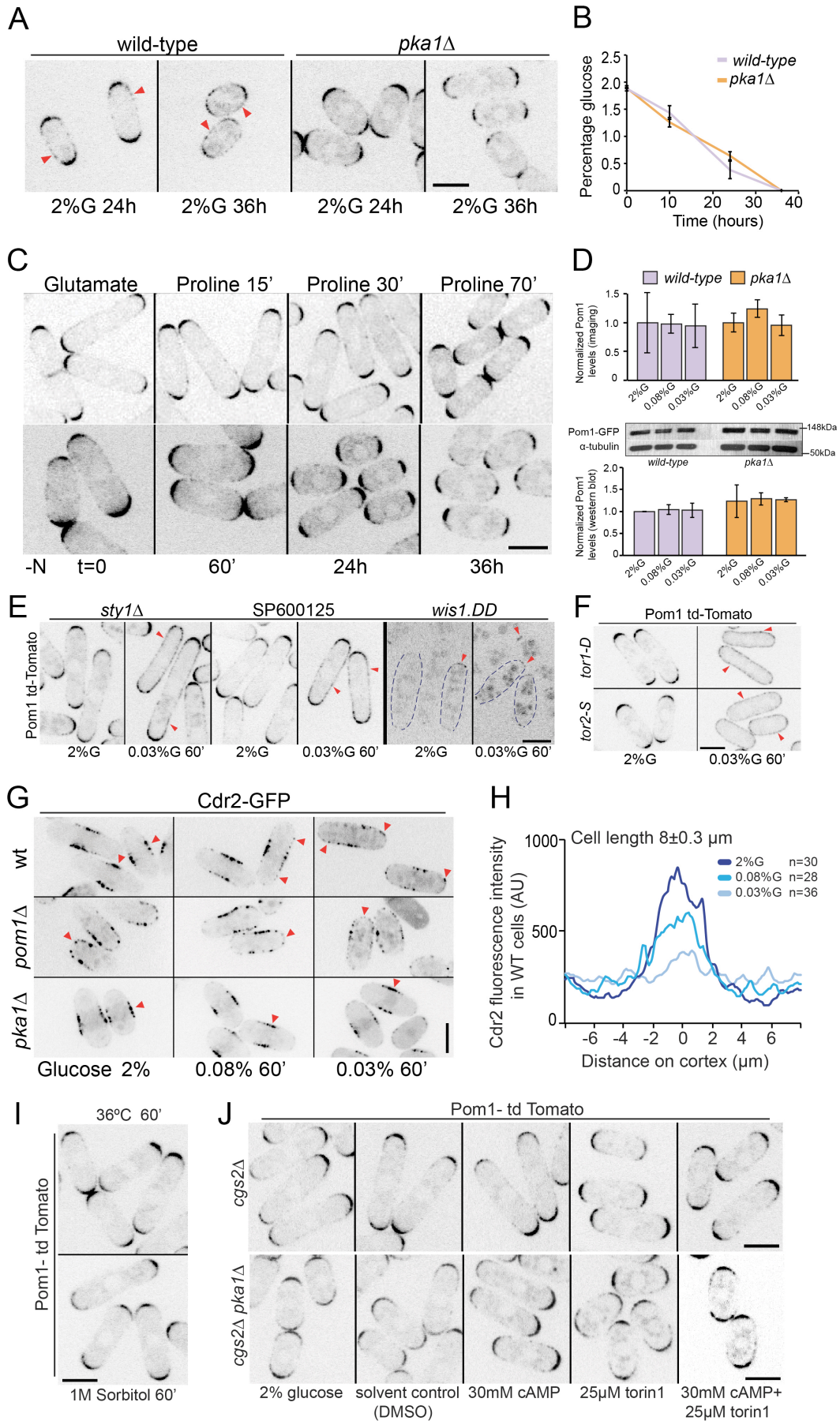
40

Figure S2.1: **Pom1 re-localization upon glucose limitation is specific to the PKA pathway (A)** Localization of Pom1-tdTomato in wild type and *pka1Δ* cells grown to saturation at indicated time points. **(B)** Measurement of glucose levels in wild type and *pka1Δ* grown to saturation **(C)** Localization of Pom1-tdTomato in wild type cells before or after shift from glutamate to proline (top) or after nitrogen withdrawal (bottom) at indicated time points. **(D)** Mean global Pom1-tdTomato levels in wild type and *pka1Δ* cells grown in 2% or 0.08% or 0.03% glucose (G) for 1h as measured by imaging (top) and mean Pom1-GFP levels as measured by western blotting. Levels were normalized to that in 2%G. (n>28) for top panel **(E)** Localization of Pom1-tdTomato, in *sty1Δ,* wild type cells treated with SP600125 and *wis1^{DD}* cells in 2% or 0.03%G for 1h. The panel of *wis1^{DD}* is imaged in the same way as the other panels, but contrasted differently, as the fluorescent signal is very weak. **(F)** Localization of Pom1-tdTomato in mutants of the TOR pathway, *tor1-D and tor2-S* mutants grown at 25ºC and shifted to 37ºC for 1h in 2% or 0.03%G. Arrowheads indicate Pom1 at cell sides. Images shown are medial spinning disk confocal sections. Images shown are medial spinning disk confocal sections. **(G)** Sum of 5 medial spinning disk confocal images taken over 30 seconds of Cdr2-GFP in wild-type, *pom1Δ* and *pka1Δ* cells grown in 2% or 0.08% or 0.03%G for 1h. **(H)** Distribution of cortical Cdr2 from one cell tip to the other (0 = cell middle) in wild type cells (n=30, 28, 36) obtained with the Cellophane plugin. Average of indicated number of profiles in 8µm-long cells. Profiles obtained from other cell lengths are similar. **(I)** Localization of Pom1-tdTomato in wild type cells subjected to heat shock (36ºC) or osmolarity stress (1M Sorbitol) for 1h. **(J)** Localization of Pom1-tdTomato in *cgs2Δ* and *cgs2Δ pka1Δ* cells in 2%G treated for 1h in the indicated manner. Simultaneous or individual treatment with cAMP and torin1 did not result in Pom1 re-localization. Scale bars represent 5µm. Error bars show standard deviation.

to the cytoplasm upon glucose limitation (Matsuo *et al*., 2008; Gupta *et al*., 2011). Consistently, Pka1-GFP localized to the nucleus in presence of 2% glucose, but was also present in the cytosol. This cytosolic concentration increased as it exited the nucleus upon glucose starvation (Fig 2.2A). Cgs1 was shown to have a role in nuclear export of Pka1 in glycerol and hyperosmotic stress but not when cells were grown to stationary phase (Matsuo *et al*., 2008). I found that in *cgs1Δ* cells, nuclear and cytosolic levels of Pka1-GFP remained constant in all glucose conditions tested (Fig S2.2A). As these cells showed a wild type-like Pom1 distribution (Fig 2.1E), I concluded that Pka1 may signal Pom1 re-localization from the cytosol, but that an increase in cytosolic Pka1 levels cannot be the direct trigger for Pom1 re-localization.

I decided to address when Pka1 activity is required in two ways. First, I used cells lacking cAMP, and thus PKA activity, due to deletion of the adenylyl cyclase cyr1. To ensure no exogenous cAMP degradation, I combined this to the deletion of the
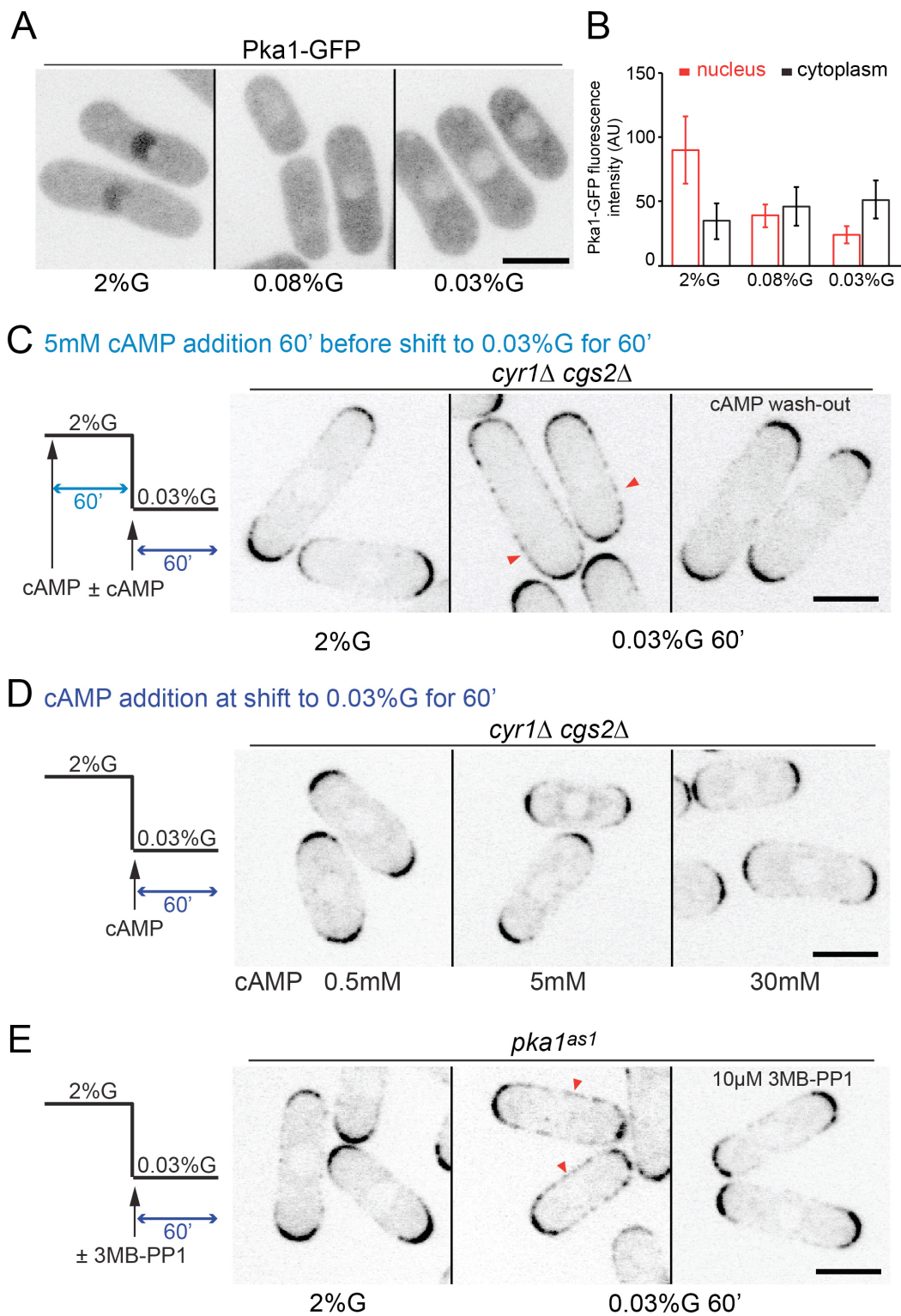
Figure 2.2: Pka1 is active in low glucose to promote Pom1 side-localization (A) Maximum intensity spinning disk projections of Pka1-GFP in wild type cells grown in 2%G or 0.08% or 0.03%G for 1h. **(B)** Graph shows measurement of cytoplasmic and nuclear Pka1-GFP levels in the same cells as in A (n>20) **(C)** Medial spinning disk confocal section of Pom1-tdTomato in *cyr1Δcgs2Δ* cells incubated with 5mM cAMP in 2%G for 1h (left) and shifted to 0.03%G for 1h with the same amount of cAMP

(middle) or without cAMP (right). Arrowheads indicate Pom1 at cell sides **(D)** Medial spinning disk confocal section of Pom1-tdTomato in *cyr1Δcgs2Δ* cells grown in 2%G and incubated with increasing amounts of cAMP at the time of shift 0.03%G for 1h **(E)** Medial spinning disk confocal section of Pom1-tdTomato in *pka1-as1* cells grown in 2%G (left) and shifted to 0.03%G without (middle) or with 10μM 3MB-PP1 (right). Arrowheads indicate Pom1 at cell sides. Scale bars are 5μm. Error bars are standard deviations.

cAMP phospho-diesterase gene cgs2, making a double mutant (c*yr1Δ cgs2Δ*). As expected, *cyr1Δ cgs2Δ* cells failed to re-localize Pom1 exactly mimicking *pka1Δ* cells. However, addition of exogenous cAMP both before and throughout glucose limitation restored PKA activity and resulted in Pom1 re-localization over the entire cell cortex. However, if cAMP was washed out specifically at the time of shift to low glucose, Pom1 failed to re-localize. This suggested that PKA activity is required in low glucose (Fig 2.2C; S2.2C). Addition of up to 30mM cAMP selectively at the time of shift to low glucose was not sufficient to trigger Pom1 re-localization (Fig 2.2D). This indicated to me that PKA activity is required both during the glucose-rich and glucose-poor phase to signal Pom1 spread. Control *pka1Δ cgs2Δ* cells treated the same way retained polar Pom1, confirming that the action of cAMP occurs through PKA activation (Fig S2.2B-C).

Second, I constructed an analog-sensitive Pka1 mutant allele (*pka1^{as1}*), whose activity can be selectively inhibited by addition of an ATP-analogue (Bishop *et al.*, 2001). Untreated *pka1^{as1}* cells behaved largely like wild type cells, with polar Pom1 in rich glucose and Pom1 spreading in low glucose (Fig 2.2E). However I observed that these cells were somewhat shorter than wild type, suggesting that Pka1^{as1} is not fully functional (Fig S2.2D). Prolonged treatment with 10μM 3MB-PP1 mimicked a *pka1* deletion (Fig S2.2E). Selective Pka1^{as1} inhibition only upon glucose limitation also blocked Pom1 re-localization, indicating that PKA is active to promote Pom1 side-localization in glucose-limiting conditions (Fig2.2E). Together these data demonstrate that cytosolic Pka1 is active during glucose limitation and its activity is required to signal Pom1 re-localization.

A *cgs1Δ* Pka1-GFP

2%G 0.08%G 0.03%G 2%G 0.08%G 0.03%G

B 5mM cAMP addition 60' before shift to 0.03%G for 60'

pka1Δ cgs2Δ

cAMP wash-out

2%G 0.03%G 60'

C 0.5mM cAMP addition 240' before shift to 0.03%G for 60'

cyr1Δ cgs2Δ

cAMP wash-out

pka1Δ cgs2Δ

cAMP wash-out

2%G 0.03%G 60'

D wild-type *pka1as1*

E *pka1as1*

2%G 4h 0.03%G 1h
Prolonged treatment with10μM 3MB-PPP1 in
both glucose-rich and poor phase
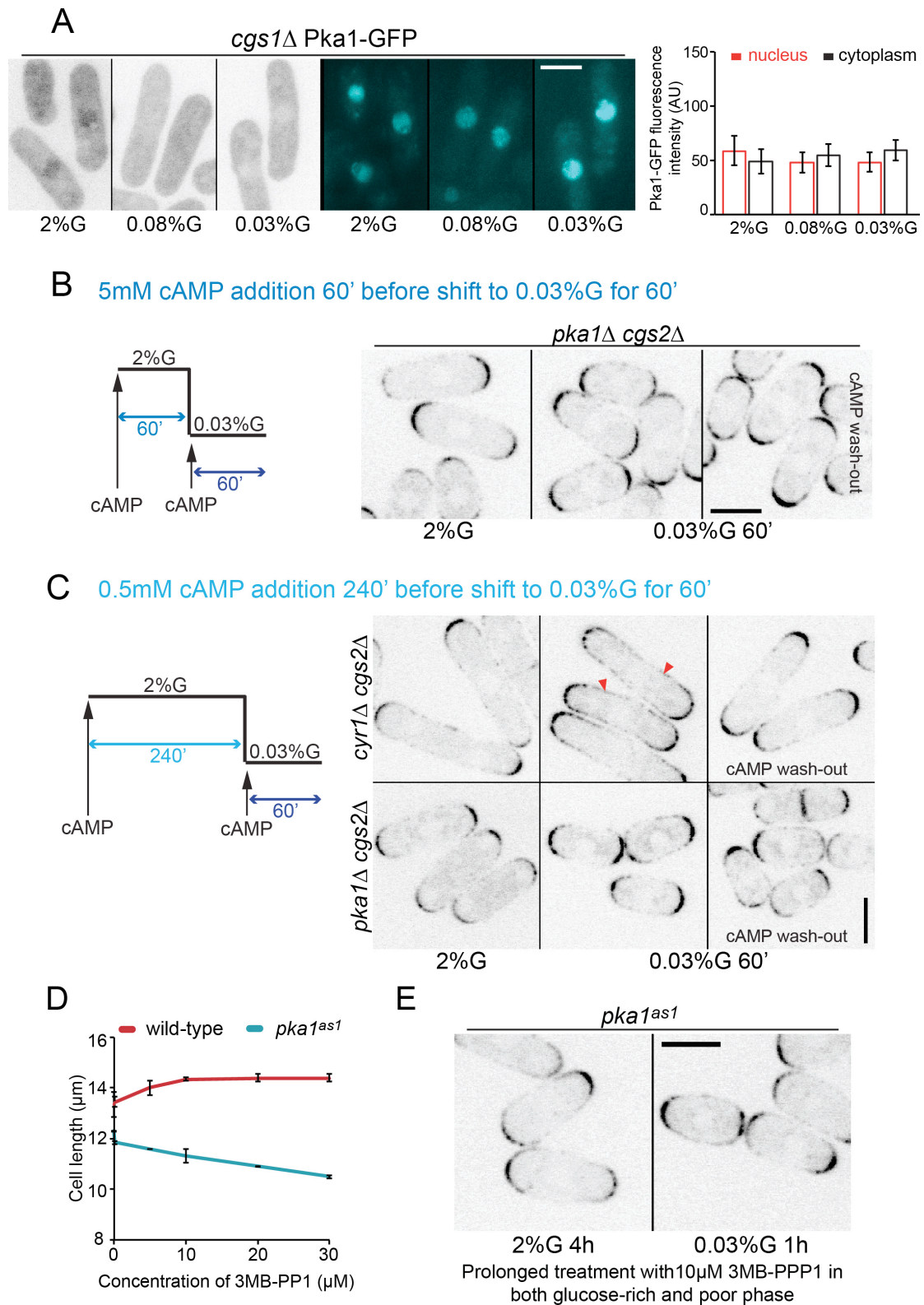
Figure S2.2: Pka1 is active in low glucose to promote Pom1 side-localization (A) Left: Images are maximum intensity spinning disk projection of Pka1-GFP in *cgs1Δ* cells grown in 2%G or 0.08% or 0.03%G for 1h. Images show Pka1 in the GFP channel and Hoechst staining for chromatin in the UV channel (cyan). Right: Measurement of cytoplasmic and nuclear Pka1-GFP levels in the same cells

(n>20). **(B)** Localization of Pom1-tdTomato in control *pka1Δ cgs2Δ* cells incubated with 5mM cAMP in 2%G (left panel) and shifted to 0.03%G with (middle) or without (right) cAMP. **(C)** Localization of Pom1-tdTomato in *cyr1Δ cgs2Δ* and in control *pka1Δ cgs2Δ* cells incubated with 0.5mM cAMP in 2%G (left panel) and shifted to 0.03%G with (middle) or without (right) cAMP. Arrowheads indicate Pom1 at cell sides. **(D)** Mean cell length at division of wild type and *pka1-^{as1}* cells treated with increasing concentrations of 3MB-PP1 for 4h (n>75). Error bars are standard deviations **(E)** Localization of Pom1-tdTomato in *pka1-^{as1}* cells treated with 10μM 3MB-PP1 in 2%G and imaged after 4h in 2%G or after 4h in 2%G + 1h in 0.03%G. All images shown are medial spinning disk confocal sections. Scale bars represent 5μm.

Mechanism of Pom1 re-localization upon glucose limitation

I considered three possible mechanisms of Pom1 re-localization: First, glucose limitation may lead to Pom1 inactivation, causing its delocalization from the cell tips as observed for the Pom1 *kinase-dead* (Pom1^{kd}) allele (Bahler and Pringle, 1998; Hachet *et al*., 2011). Previous work had shown using the Pom1-^{kd} allele, that inactivation of Pom1 slows down its FRAP, yielding a longer recovery half-time ($t_{1/2}$). This is because inactive Pom1 is in an un-phosphorylated state and binds the plasma membrane more tightly than active Pom1 (Hachet *et al*., 2011). Thus I decided to use FRAP measurements as a way to test Pom1 activity in low glucose using the same parameters as described in Hachet *et al*., 2011. Glucose depletion did not alter Pom1 FRAP dynamics in wild type cells, which remained significantly higher than those of Pom1^{kd} (Fig S2.3A-B). This indicates that Pom1 remains active in low glucose, and the re-localization observed is not due to a loss of Pom1's ability to auto-phosphorylate and detach from the membrane. The second possibility is that glucose limitation may alter the membrane composition or potential thus increasing the intrinsic affinity of Pom1 for the plasma membrane. To verify this hypothesis, and to uncouple the role of Pom1 activity from binding, I did FRAP measurements on the pom1^{kd} allele in all glucose conditions. As mentioned above, Pom1^{kd} recovers significantly slower than wild type Pom1 in 2% glucose (Fig S2.3A-B). Upon glucose limitation, the recovery was even slower suggesting an increase in the intrinsic affinity of Pom1 for the plasma membrane, independently of its phosphoregulation. This may be due to changes in the membrane composition or potential.

Previous work showed that Pom1 is cytosolic in *tea4Δ* cells in 2%G, because it cannot be dephosphorylated and thus fails to associate with the membrane. In
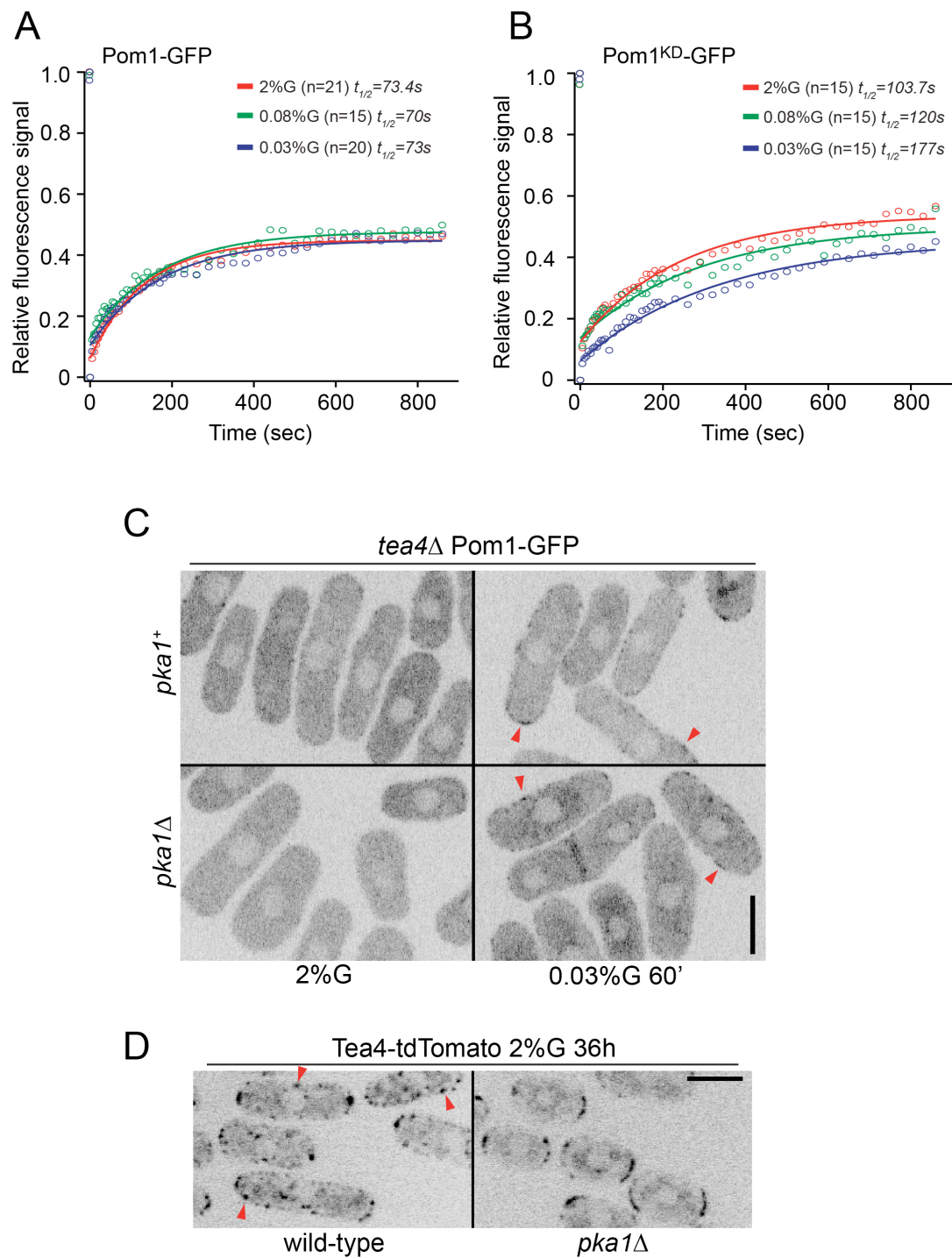
Figure S2.3: Pom1 remains active and its localization depends on Tea4 upon glucose limitation
(A) Fluorescence recovery after photo-bleaching (FRAP) analysis on wild type cells expressing Pom1-GFP grown in 2%G or 0.08%G or 0.03%G for 1h. **(B)** FRAP analysis on the Pom1[kd]–GFP allele grown in the same conditions as in (A) **(C)** Localization of Pom1-GFP in *tea4Δ* and *tea4Δ pka1Δ* cells grown in 2%G or 0.03%G for 1h **(D)** Localization of Tea4-tdTomato in wild-type and *pka1Δ* cells grown to saturation. Arrowheads indicate Tea4 dots present at cell sides. All images shown are medial spinning disk confocal sections. Scale bars represent 5μm.

0.03%G, Pom1 also remained largely cytosolic, though a weak signal was detected at the cell cortex (Fig S2.3C, arrowheads). Thus in agreement with data shown in panel B, glucose limitation modestly increases the intrinsic affinity of Pom1 for the plasma membrane, possibly through changes in membrane potential. However, this modest effect is unlikely to explain the important redistribution observed in wild type glucose-starved cells. In addition, the localization of Pom1 was identical in *pka1Δ tea4Δ*, suggesting that the modest increase in Pom1's affinity for the membrane in low glucose is independent of Pka1. Additionally, as *pka1Δ tea4Δ* cells behave exactly like *tea4Δ* for Pom1 localization, I concluded that Pka1 regulates Tea4 to modulate Pom1 localization.

I thus considered the third possibility of the delivery of Tea4 being altered upon glucose limitation. Indeed the localization of Tea4 was drastically changed upon glucose withdrawal (Fig 2.3A,C): in 0.08% glucose, there was an increase in the cortical levels of Tea4 in the middle of the cell and in 0.03% glucose, Tea4 was delocalized from cell poles and distinct Tea4 dots were present around the cell periphery. Further, microtubule tracks could not be detected in 0.03%G. Tea4 re-localization reversibly occurred within 10 minutes of shift to low glucose and was *pka1*-dependent (Fig 2.3B, D). Thus in *pka1Δ* cells, active Tea4 transport towards the cell tips could be observed. The time required for Tea4 re-localization corresponds well to that observed for Pom1. Tea4 was also present on cell sides in wild-type cells grown to saturation (Fig S2.3D). As the localization of Tea4 on cell sides is sufficient to recruit Pom1 (Hachet *et al.*, 2011), I concluded that upon glucose limitation, Pka1 regulates Tea4 localization, which in turn recruits Pom1.

Pka1 controls microtubule stability

To understand the mechanism of Tea4 re-localization, I studied microtubule behavior under limited glucose conditions. Since microtubule stability is sensitive to external conditions, I made use of flow-chambers to maintain a uniform glucose concentration. In steady state conditions of 2% glucose, microtubules formed 3-4 antiparallel bundles extending from one tip to the other. A shift to 0.03% glucose caused a dramatic, rapid, reversible loss of long interphase microtubules in less than 5 minutes, with 37% cells exhibiting short dynamic microtubules and 63% displaying only

47
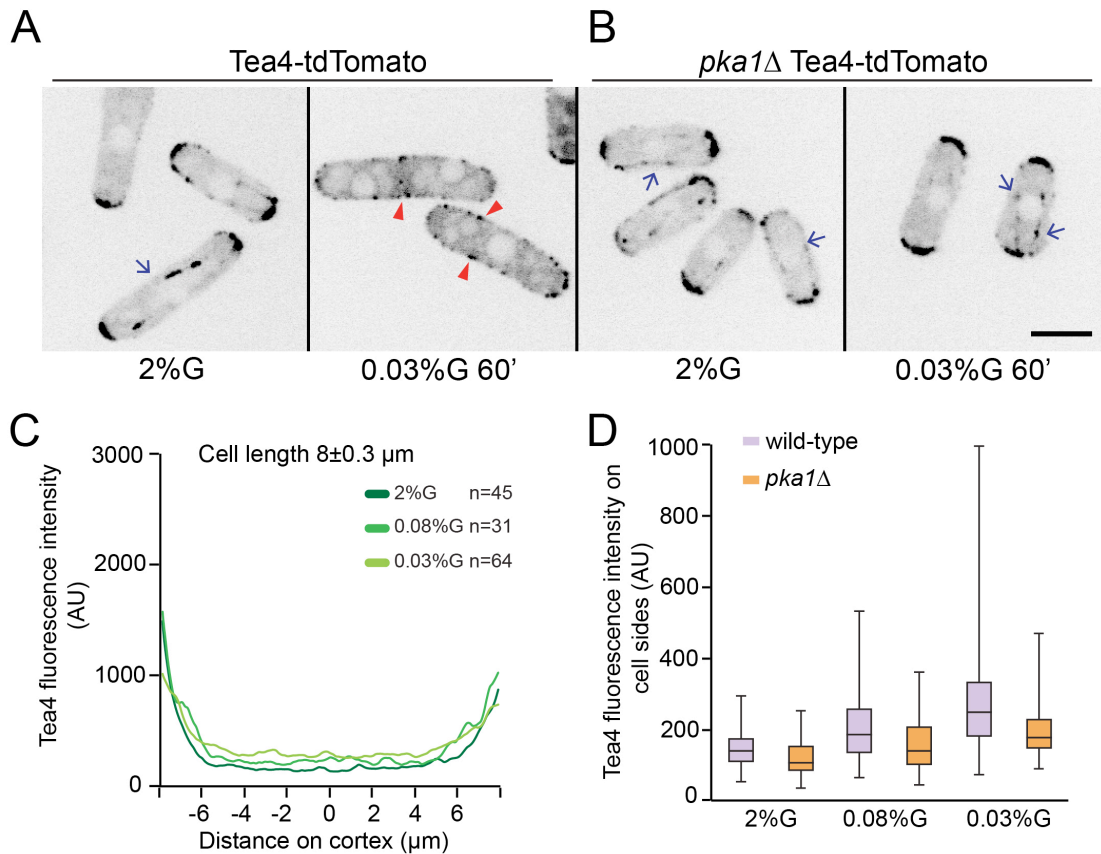
Figure 2.3: Pka1-dependent reversible Tea4 re-localization around the cell cortex upon glucose limitation (A) Sum of 5 medial spinning disk confocal images taken over 30 seconds of Tea4-tdTomato in wild-type cells grown in 2%G or 0.03%G for 1h. Arrows indicate Tea4 tracks on microtubules. Arrowheads indicate Tea4 dots at cell sides **(B)** Localization of Tea4-tdTomato in *pka1Δ* cells grown as in (A) **(C)** Distribution of cortical Tea4 from one tip to the other (0 = cell middle) in wild type cells obtained with the Cellophane plugin. Average of indicated number of profiles in 8μm-long cells. Profiles obtained from other cell lengths are similar **(D)** Box and whisker plot of cortical Tea4 fluorescence intensity in the middle 2μm region in both wild type (n=45, 31, 64) and *pka1Δ* (n=71, 66, 62) cells. Scale bars represent 5μm.

microtubule stubs (stable regions of microtubule overlap) (Fig 2.4A, C). As medium exchange in the flow-chamber takes about 3 minutes, the effect occurred within 2 minutes of glucose deprivation. Mitotic spindles however were resistant and kept elongating under these conditions. Short dynamic microtubules were observed in cells kept in 0.03%G for up to 20h, after which microtubules disappeared completely from all cells presumably due to depletion of energy.

In 0.08% glucose, microtubules remained long but were also destabilized. First, they were de-polymerized by sub-optimal MBC levels (1μg/ml) that did not affect microtubules in 2% glucose (Fig 2.4D). Second, they showed increased shrinkage rate and dynamicity (length change of microtubules in any direction over time), as compared to cells grown in 2% glucose (Fig 2.4E). Finally, 23.8% of microtubule catastrophes occurred upon contact at the lateral cortex (vs. only 9.2 % in 2% glucose; Fig2.4F). These catastrophes at cell sides led to sustained Tea4 contact and temporary deposition at the lateral cortex (Fig 2.4G). Thus, frequent microtubule catastrophes at cell sides may promote Tea4 and thus Pom1 re-localization upon glucose starvation.

Microtubule destabilization upon glucose limitation was entirely dependent on Pka1. In *pka1Δ* cells, microtubules remained long when cells were shifted to 0.03% glucose for up to 30h, after which microtubules disappeared completely as in the wild type situation (Fig 2.4B-C). In 0.08% glucose, they were not de-polymerized by sub-optimal dosage of MBC (Fig 2.4D), the dynamic microtubule parameters and location of catastrophes at cell sides were not altered as compared to *pka1Δ* cells grown in 2% glucose (Fig 2.4E-F). Even in 2% glucose, microtubules were significantly more stable in *pka1Δ* than wild type cells, displaying higher resistance to MBC treatment and slower shrinkage rate and dynamicity (Fig 2.4D-E).

Conversely, Pka1 over-expression caused faster microtubule shrinkage rates, higher dynamicity and 30.2% of catastrophes occurring along the lateral cell cortex (Fig S2.4A; Table1). As *pka1* overexpression causes cell elongation, I controlled for the effect that cell length may have on microtubule dynamics by using elongated *cdc25-22* cells. In these cells, microtubules showed largely wild-type dynamic parameters, with 20% side catastrophes, a percentage significantly lower than that observed upon *pka1* overexpression (Fig S2.4A; Table1). These data indicate that Pka1 negatively regulates microtubule stability.

I next asked the question if microtubule de-stabilization was sufficient to trigger both Tea4 and Pom1 side-relocation. Indeed, Tea4 and Pom1 partly re-localized to cell sides in glucose-starved *pka1Δ* cells when microtubules were destabilized either by a 10 min MBC treatment (Fig S2.4C-D), or by deletion of the microtubule stabilizing +TIP complex (Fig S2.4E). Similarly, Pom1 localized along cell sides in *pka1*-overexpressing cells even in 2% glucose, but not in control *cdc25-22* mutant cells (Fig
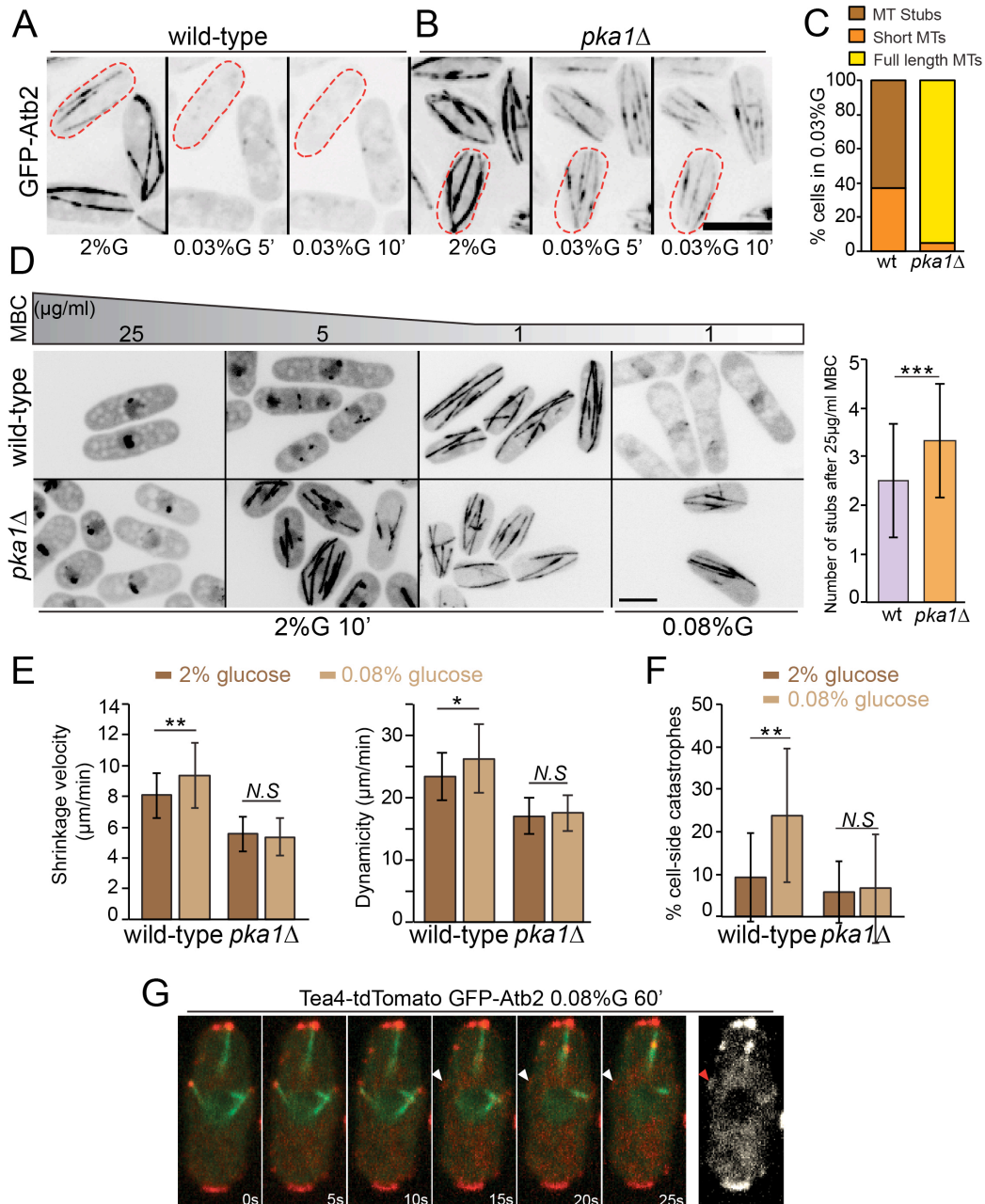
Figure 2.4: Pka1 negatively regulates microtubule stability (A) Epifluorescence deconvolved maximum intensity projection images of wild type cells expressing GFP-Atb2 grown in microfluidic chambers in 2%G and 5 and 10 min after shift to 0.03%G **(B)** GFP-Atb2 in *pka1Δ* cells grown as in (A) **(C)** Percentage of wild type (n=68) and *pka1Δ* (n=59) cells with indicated microtubule organization in 0.03%G for 10min in microfluidic chambers **(D)** Maximum projection of spinning disk confocal images of wild type and *pka1Δ* cells expressing GFP-Atb2 treated with the indicated concentrations of MBC for 10min in 2% or 0.08%G. The graph (right) shows the number of microtubule stubs left after 10min 25μg/ml MBC treatment (n>45 cells) (*p*=0.001) **(E)** Mean microtubule shrinkage velocity (left) (*p*=0.008, *p*=0.56) and dynamicity (right) (*p*=0.031, *p*=0.54) in wild type and *pka1Δ* cells grown under 2%G or 0.08%G for 1h (n>27 microtubules) **(F)** Percentage of microtubule catastrophes occurring at the cell-sides in wild-type and *pka1Δ* cells (n>100 catastrophe events) grown as in (E) (*p*=0.002,

50

S2.4B). Thus, Pka1 promotes microtubule destabilization, which causes Tea4 and thus Pom1 re-localization to cell sides.

Pka1 regulates microtubule stability independently of the +TIP complex

To dissect the mechanism by which Pka1 destabilizes microtubules, I conducted a limited epistasis screen between *pka1Δ* and mutations in known microtubule associated proteins (MAPs) in 2% glucose, initially measuring microtubule shrinkage rates as read-outs. I reasoned that if Pka1 regulates a MAP, the double mutant of *MAPΔ pka1Δ* would show the same phenotype as the single *MAPΔ*. If however, a MAP is not regulated by Pka1, the phenotype would be additive. As mentioned above, single, double and triple deletions of genes encoding the +TIP complex (the kinesin-like protein-Tea2, the CLIP170 family protein-Tip1 and the EB1 homologue-Mal3), in which microtubules are destabilized (Beinhauer *et al.*, 1997; Browning *et al.*, 2000; Brunner and Nurse, 2000), restored Pom1 side-localization to glucose-starved *pka1Δ* cells. However all deletions showed additive effects with *pka1Δ* for microtubule shrinkage velocities. Similarly, deletion of the TOG-domain protein Alp14/XMAP215, shown to accelerate microtubule assembly (Al-Bassam *et al.*, 2012) was additive with *pka1Δ*. (Table1) These additive phenotypes indicate that Pka1 does not modulate microtubule stability through these MAPs.

Pka1 regulates microtubule dynamics through CLASP and Kinesin-8

Interestingly, single and double deletions of kinesin-8 family members, *klp5Δ* or *klp6Δ*, and mutation in the essential *cls1/peg1* gene, which encodes a CLASP homologue, masked the effect of *pka1Δ* for microtubule shrinkage rates. Kinesin-8 proteins belong to a conserved kinesin sub-family shown to possess microtubule de-
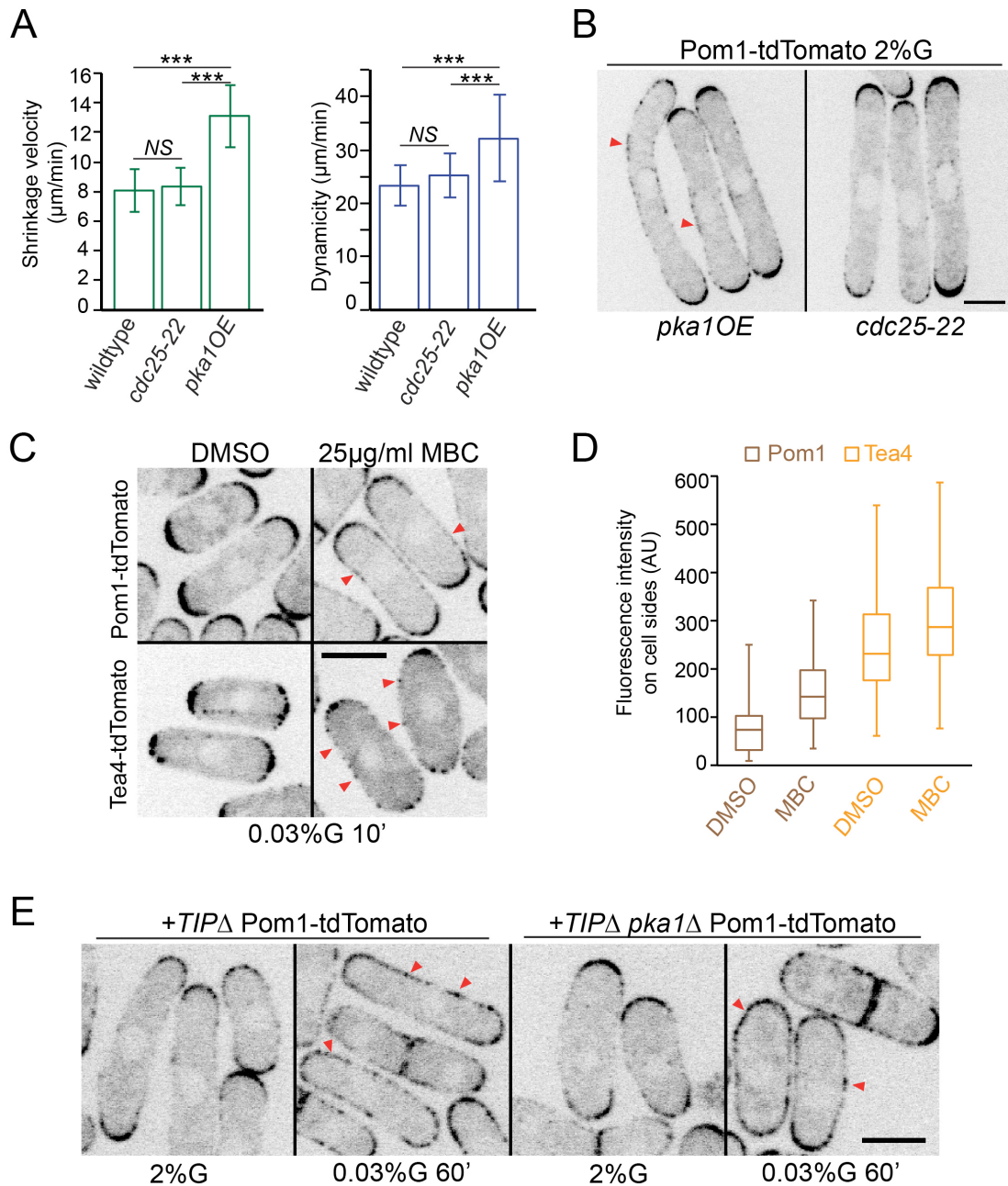
Figure S2.4: Microtubule destabilization is sufficient to restore Tea4 and Pom1 side-localization in *pka1Δ* cells (A) Mean microtubule shrinkage velocity (left) and dynamicity (right), in wild-type, *cdc25-22* and pka1OE cells grown in 2%G (n=30, 20, 24) *(p=0.2, p<10⁻¹¹, p<10⁻⁷)*. Statistical significance was derived using student's *t*-test. Error bars are standard deviations. **(B)** Medial spinning disk confocal images of Pom1-tdTomato Pka1 over-expressing cells grown in 2%G (left). Elongated *cdc25-22* cells are used as control (right). Arrowheads mark Pom1 at cell sides. **(C)** Sum of 5 medial spinning disk confocal images taken over 30 seconds of Pom1-tdTomato and Tea4-tdTomato in *pka1Δ* cells grown in 2%G, shifted to 0.03%G for 10min, and treated with DMSO (control) or 25μg/ml MBC at the time of shift. Arrowheads indicate Pom1 and Tea4 side localization in MBC treated cells. **(D)** Box and whisker plot of cortical Pom1 and Tea4 fluorescence intensity in the middle 2μm region in *pka1Δ* cells treated as in (C). **(E)** Medial spinning disk confocal images

polymerization activity (Gupta *et al*., 2006; Mayr *et al*., 2007; Varga *et al*., 2006). In fission yeast, Klp5 and Klp6 form hetero-dimers that regulate chromosome segregation by controlling microtubule dynamics (Garcia *et al*., 2002; West *et al*., 2001). *In vivo* evidence has further shown that the Klp5/Klp6 heterodimer provides a length-dependent regulation of microtubule catastrophe, by being more enriched on and specifically enhancing the catastrophe rate of long microtubules (Tischer *et al*., 2009). However, in vitro characterization of fission yeast kinesin-8 proteins did not detect noticeable depolymerase activity (Erent *et al*., 2012; Grissom *et al*., 2009).

Remarkably, though *klp5Δ* and *klp6Δ* mutants displayed only modestly diminished microtubule dynamics compared to wild type cells (Unsworth *et al*., 2008) *pka1Δ* failed to modify any of the global growth or shrinkage rates, and catastrophe or rescue frequency parameters in these deletions. Consequently, microtubule dynamicity was identical in *klp5Δ klp6Δ pka1Δ* triple mutants and in *klp5Δ klp6Δ* double mutants. This epistasis held true when cells were grown in 0.08% glucose (Fig 2.5A, Table1). Significantly, in this growth condition, microtubule catastrophes frequently occurred at the sides of both *klp5Δ klp6Δ* and *klp5Δ klp6Δ pka1Δ*, in contrast to the cell tip-restricted catastrophes of *pka1Δ* cells (Fig 2.5B). These data thus suggest that Pka1 controls microtubule dynamics by regulating the kinesin-8 heterodimer.

However, kinesin-8 mutations did not mask all aspects of the *pka1Δ* phenotypes. First, *klp5Δ klp6Δ pka1Δ* triple mutant cells displayed more stable microtubules than *klp5Δ klp6Δ* double mutants, upon incubation of cells in 0.03% glucose (Fig 2.5C-D), suggesting PKA has additional targets for regulation of microtubule stability. Second, even though both the double and triple mutants showed a large percentage of microtubules contacting the cell-side in low glucose, Tea4 dots could not be detected at the lateral cortex in all cells of *klp5Δ klp6Δ* (Fig 2.5C, E). A large percentage of cells showed polar Tea4 while some showed cortical dots all around the periphery. Thus, quantification of Tea4 revealed a mild increase on cell sides compared to wild type cells in limited glucose. By contrast the triple mutant showed polar Tea4
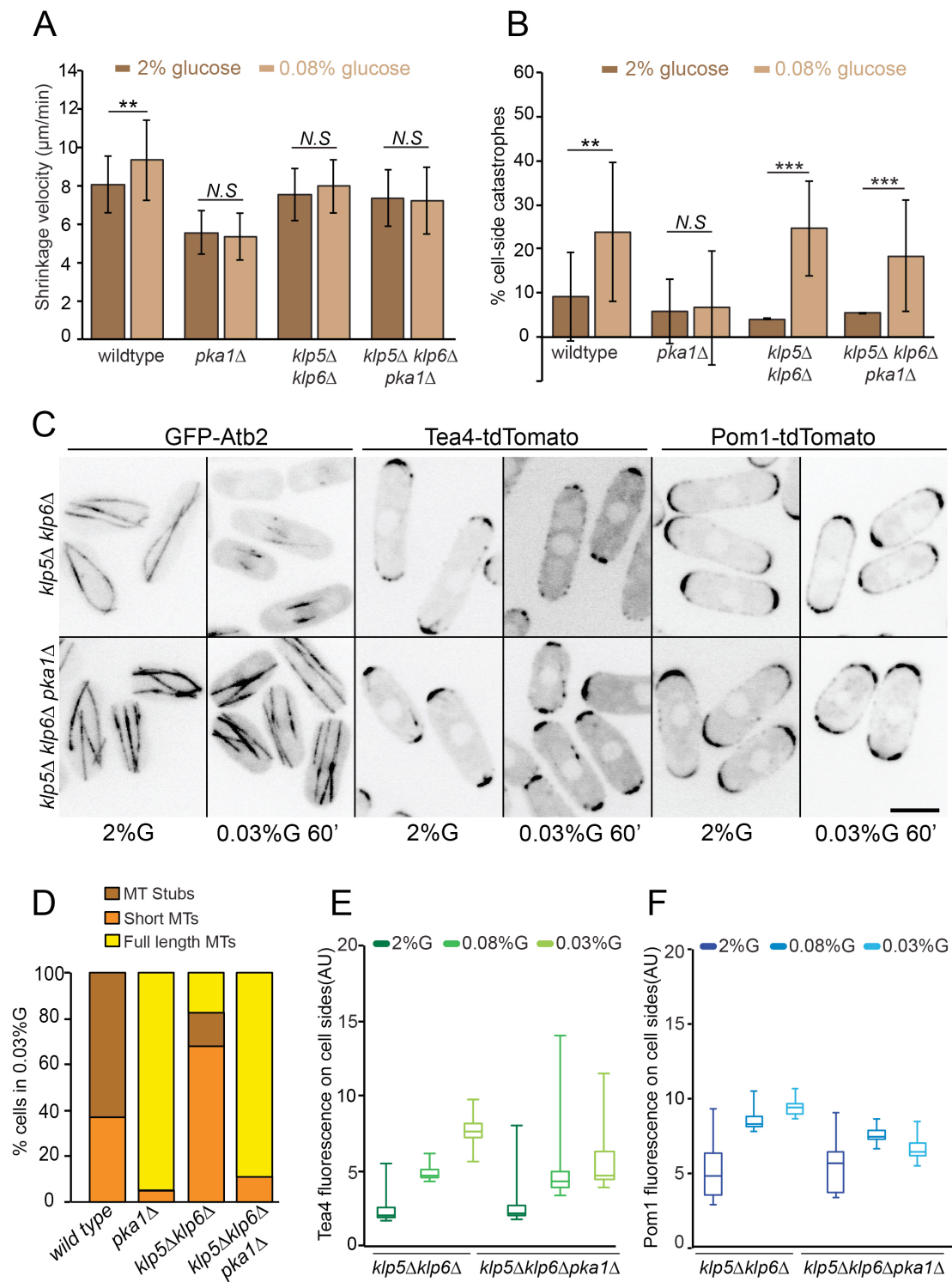
Figure 2.5: Pka1 regulates microtubule dynamics through the kinesin-8 family proteins (A) Mean microtubule shrinkage velocity in wild-type, *pka1Δ*, *klp5Δklp6Δ* and *klp5Δklp6Δpka1Δ* strains grown in 2%G or 0.08%G for 1h (n>25 microtubules) (*p*=0.008, *p*=0.56, *p*=0.65, *p*=0.44). **(B)** Percentage of microtubule catastrophes occurring at cell sides in the same strains, grown as in (A) (n>100 catastrophe events) (*p*=0.002, *p*=0.926, *p*=10^{-7}, *p*=0.0002). Statistical significance is derived using student's *t*-test. Error bars are standard deviations. **(C)** Maximum intensity projection of spinning disk images of GFP-

Atb2, and sum of 5 medial spinning disk confocal images taken over 30 seconds of Tea4-tdTomato and Pom1-tdTomato in *klp5Δ klp6Δ* and *klp5Δ klp6Δ pka1Δ* cells grown in 2%G and shifted to 0.03%G for 1h. Scale bar represents 5 μm. **(D)** Percentage of wild-type (n=68), *pka1Δ* (n=59), *klp5Δklp6Δ* (n=103) and *klp5Δklp6Δpka1Δ* (n=64) cells showing the indicated microtubule organization after shift to 0.03%G for 10min at 36°C. **(E)** Box and whisker plot of cortical Tea4 fluorescence intensity in the middle 2μm region in both *klp5Δ klp6Δ* and *klp5Δ klp6Δ pka1Δ* cells in 2%G and shifted to 0.08%G and 0.03%G for 1h **(F)** Box and whisker plot of cortical Pom1 fluorescence intensity in the middle 2μm region in both *klp5Δ klp6Δ* and *klp5Δ klp6Δ pka1Δ* cells grown as in (E).

---

consistent with the more stable microtubules. As a consequence, Pom1 was largely restricted to cell ends in 0.03%G with a modest increase observed at cell sides in the double mutant and almost none in the triple mutant (Fig 2.5C, F). Thus in spite of microtubules undergoing catastrophe at cell sides, these mutants largely fail to deposit Tea4 and re-localize Pom1 to cell sides. One hypothesis, which should be investigated in future studies is whether kinesins-8 are involved in the transfer of Tea4 from the microtubule plus end to the cell cortex.

I then turned my attention to CLASP, a conserved microtubule stabilizer (Al-Bassam and Chang, 2011). CLASP was initially identified as a cytoplasmic linker (CLIP)-associated protein, and tracks microtubule plus ends in many animal cells (Akhmanova *et al*., 2001) The sole fission yeast CLASP, Cls1/Peg1 (Cls1 below), is an essential protein that localizes prominently to zones of antiparallel microtubule overlap and promotes the rescue of microtubules (Al-Bassam *et al*., 2010; Bratman and Chang, 2007). Several lines of evidence showed that Pka1 modulates microtubule dynamics through CLASP. As Cls1 is an essential gene I used a published temperature-sensitive mutant *cls1-36*, at the restrictive temperature of 36°C. Consistent with previous observations, inactivation of Cls1, revealed no or only minor effect on microtubule dynamics (Bratman and Chang, 2007 and Table 1). Surprisingly however, *cls1-36* masked the effect of *pka1Δ* for all microtubule dynamic parameters in both 2% and 0.08% glucose (Fig 2.6A). The *cls1-36* mutant also restored frequent side-catastrophes in *pka1Δ* cells in 0.08% glucose (Fig 2.6B), and microtubule destabilization in 0.03% glucose (Fig 2.6 C-D). Thus, in absence of PKA, CLASP modulates microtubule dynamics. However, more long microtubules were observed in double *cls1-36 pka1Δ* than the single *cls1-36* mutant in 0.03% glucose (Fig 2.6D), suggesting PKA may signal through additional MAPs for microtubule de-
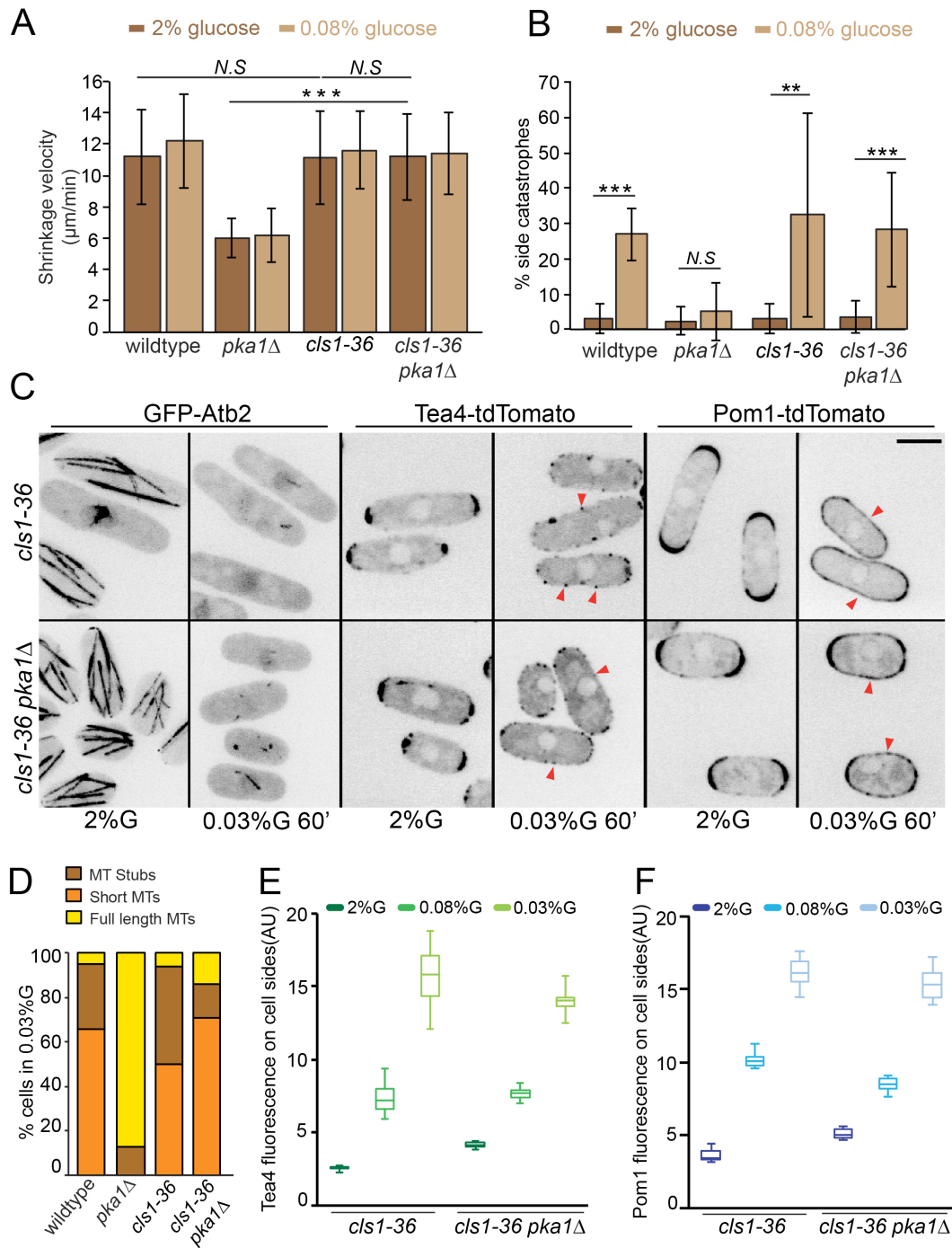
Figure 2.6: Pka1 regulates microtubule dynamics through CLASP to trigger Tea4 and Pom1 side-localization (A) Mean microtubule shrinkage velocity in wild-type, *pka1Δ*, *cls1-36* and *cls1-36 pka1Δ* strains grown in 2%G or 0.08%G for 1h at 36°C (n>15 microtubules) (*p*=0.9, *p*=0.93, *p*<10⁻⁹).
(B) Percentage of microtubule catastrophes occurring at cell sides in the same strains, grown as in (A) (n>70 catastrophe events) (*p*<10⁻⁸ *p*=0.46 *p*=0.015 *p*= 0.00013). Statistical significance is derived using student's *t*-test. Error bars are standard deviations. **(C)** Maximum intensity projection of spinning disk images of GFP-Atb2, and sum of 5 medial spinning disk confocal images taken over 30 seconds of Tea4-tdTomato and Pom1-tdTomato in *cls1-36* and *cls1-36 pka1Δ* cells grown in 2%G at 25°C and

shifted to 36ºC for 1h in either 2%G or 0.03%G. Arrowheads indicate Tea4 or Pom1 side-localization. Scale bar represents 5 µm. **(D)** Percentage of wild-type (n=38), *pka1∆* (n=32), *cls1-36* (n=100) and *cls1-36 pka1∆* (n=119) cells showing the indicated microtubule organization after shift to 0.03%G for 10min at 36°C. **(E)** Box and whisker plot of cortical Tea4 fluorescence intensity in the middle 2µm region in both *cls1-36* and *cls1-36 pka1∆* cells at 36°C with cells grown in 2%G at 25ºC and shifted to 36ºC for 1h in either 2%G or 0.08%G or 0.03%G. **(F)** Box and whisker plot of cortical Pom1 fluorescence intensity in the middle 2µm region in both *cls1-36* and *cls1-36 pka1∆* cells at 36°C with cells grown as in (E).
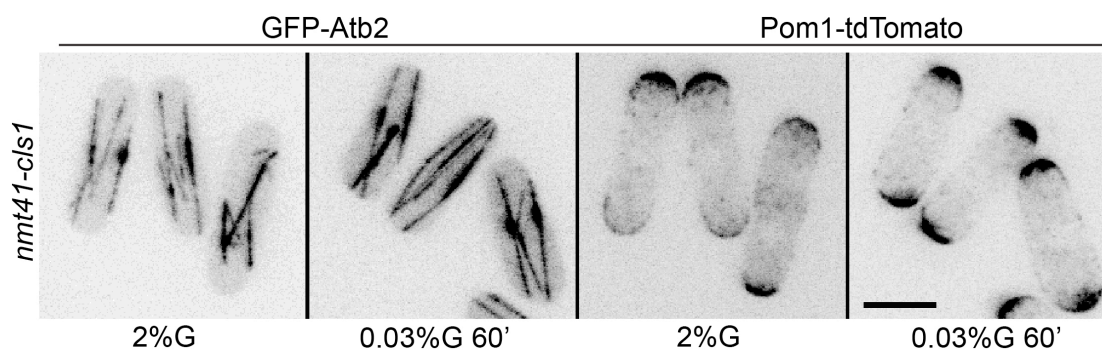
Figure S2.6: Microtubule stabilization through CLASP over-expression mimics a *pka1∆* phenotype: Maximum intensity spinning disk images of GFP-Atb2 and Pom1-tdTomato in cls1-overexpressing (*nmt41-cls1*) cells grown in 2%G or shifted to 0.03%G for 1h. *cls1* expression was induced by thiamine removal for 16-18h before low-glucose shift. Scale bar represents 5 µm.

stabilization. CLASP inactivation further restored both Tea4 and Pom1 side-localization upon glucose starvation in *pka1∆* cells (Fig 2.6C, E-F). Conversely, *cls1* overexpression, which promotes microtubule stabilization, led to restriction of Pom1 at cell tips even upon glucose limitation, mimicking the *pka1∆* phenotype (Fig S2.6).

CLASP binds the microtubule lattice with high affinity through its S/R-rich region and also binds to the tubulin dimer through its N-terminal TOG domains. CLASP thus recruits tubulin dimers to promote rescue (Bratman and Chang, 2007; Al-Bassam *et al.*, 2010). In vivo, Cls1 is recruited to zones of microtubule overlaps by the microtubule bundling protein Ase1 and exhibits little movement on the microtubule lattice (Bratman and Chang, 2007). Dynein-dependent Cls1 localization near microtubule plus-ends was also reported (Chiron *et al.*, 2008; Grallert *et al.*, 2006). Cls1 localization was significantly altered both in low-glucose and in *pka1∆* cells. In *pka1∆* cells, Cls1 showed increased levels on microtubules and often formed multiple,
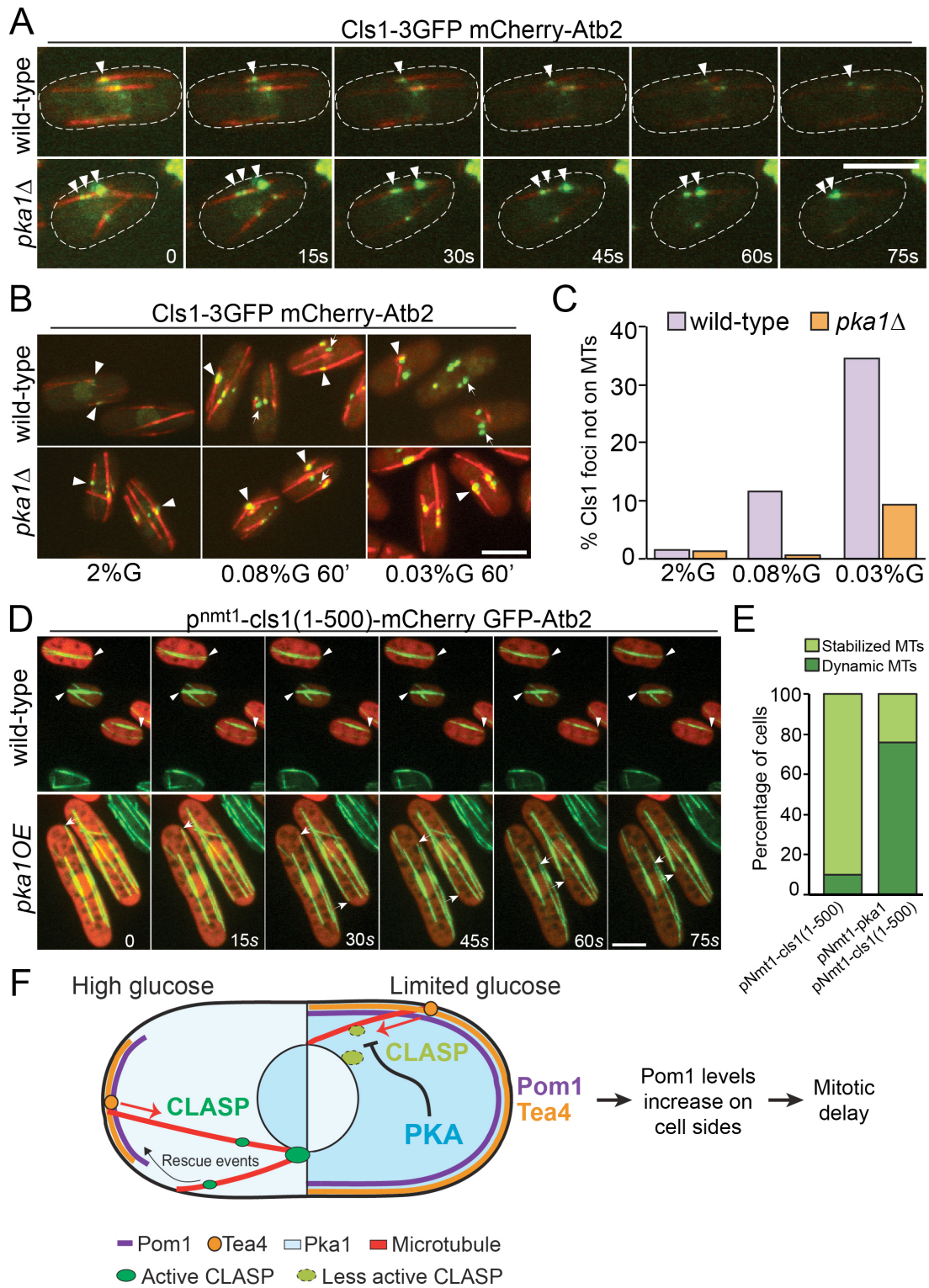
Figure 2.7: Pka1 promotes microtubule destabilization by negatively regulating Cls1 (A) Maximum intensity spinning disk projections showing time-lapse imaging of Cls1-3GFP and mCherry-Atb2 in wild-type and *pka1Δ* cells grown in 2%G. Arrowheads highlight Cls1 dots on microtubules. **(B)** Maximum intensity spinning disk projections of Cls1-3GFP and mCherry-Atb2 in wild-type and

pka1Δ cells grown in in2%G or 0.08%G or 0.03%G for 1h. Arrowheads indicate Cls1 dots present on microtubule overlaps. Arrows point to Cls1 foci not on microtubules. **(C)** Percentage of Cls1 foci not on microtubules in cells as in (B) (n>96). **(D)** Time-lapse imaging of GFP-Atb2 in wild-type and *pka1* over-expressing (pka1OE) cells transformed with p^{nmt1}-cls1(1-500)-mCherry grown in 2%G and induced without thiamine for 14-16h. Arrowheads indicate stable microtubules in wild type (upper panel) and arrows track microtubule shrinkage events in pka1OE (bottom panel) cells. Scale bar represents 5 µm. **(E)** Percentage of cells showing dynamic or at least one stabilized microtubule bundle in strains as in (D). Cells with similar range of Cls1 fluorescence levels were chosen for this analysis. **(F)** Schematic depicting the mechanism of Pom1 side-localization under glucose limitation conditions. The left part of the cell shows the situation in high glucose, when CLASP rescues microtubules allowing them to reach cell ends. The right part of the cell shows the situation in low glucose, when PKA activity antagonizes the microtubule-stabilizer CLASP. Microtubules thus become destabilized and undergo catastrophe at the lateral cortex, depositing Tea4 there. Tea4 mediated de-phosphorylation of Pom1 leads to an increase in its levels at cell sides, promoting mitotic delay.

more mobile dots on a single microtubule, though global Cls1 levels were only modestly changed compared to wild type (Fig 2.7A, Fig S2.7 A-C). In low glucose, Cls1 also showed enhanced local levels and formed strong foci near the cell middle (Fig 2.7B). Whereas most of these foci localized on microtubule bundles in *pka1Δ* cells, 12-35% were at sites lacking microtubules in wild type cells (Fig 2.7C). These foci that do not contain microtubules may represent less active or inactive Cls1 in agreement with the less stable microtubule bundles seen in these conditions in wild type cells. I was unable to test for the presence of Ase1 in these foci, as co-localization experiments using Ase1-mCherry and Cls1-3GFP showed synthetic effects. However, deletion of neither Ase1 nor the dynein Dhc1 masked the effect of *pka1Δ* on microtubule dynamics and Pom1 localization, suggesting Pka1 does not regulate Cls1 through these targeting factors (Table 1). Thus PKA may render Cls1 less active for microtubule rescue, leading to complete loss of the microtubule bundle. Additionally, I also found that Pka1 overexpression was able to mitigate the Cls1 TOG domains-dependent microtubule stabilization (Fig 2.7D-E), suggesting Pka1 reduces the activity of Cls1 in microtubule stabilization.
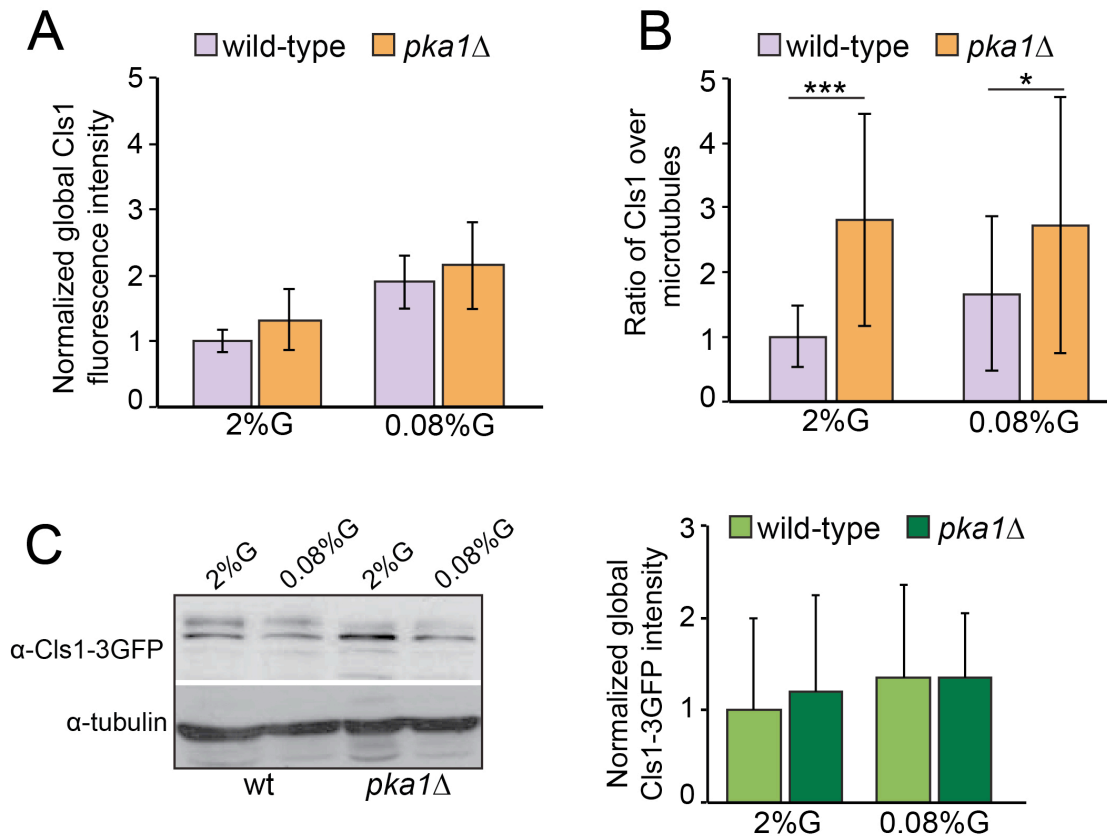
Figure S2.7: Local and global Cls1-GFP levels in wild-type and pka1Δ cells. (A) Mean global levels of Cls1-3GFP in wild-type and *pka1Δ* cells in 2% or 0.08% glucose, normalized to wild-type level in 2% glucose (n>26). **(B)** Mean ratio between Cls1 and Atb2 local fluorescence on microtubule bundles in wild-type and *pka1Δ* cells in 2% or 0.08% glucose, normalized to wild-type level in 2% (n>27) **(C)** Western blot quantifications of Cls1-3GFP in wild-type and *pka1Δ* cells in 2% or 0.08% glucose, normalized to wild-type level in 2% glucose Statistical significance was derived using students *t*-test. Error bars are standard deviations.

Pom1 re-localization buffers against excessive cell shortening upon glucose limitation

I examined the physiological consequences of Pom1 re-localization in low glucose, by examining cell length at division as a proxy of cell cycle length (Fantes, 1977). I measured cell length at division in the standard conditions of 2% glucose and in 0.08% glucose, in which cells show reliable growth and division patterns, though at shorter size (Pluskal *et al.*, 2011, Table 2).

Pka1 plays an ill-understood function in cell cycle progression. Indeed, *pka1Δ* cells

are short, and *pka1* overexpression yields long cells, suggesting Pka1 delays the cell cycle (Maeda *et al.*, 1994; Yu *et al.*, 1994). Previous work placed Pka1 upstream of MAPK signaling (Navarro *et al.*, 2012; Stettler *et al.*, 1996). Consistently, in 2% glucose, deletion of the MAPK Sty1 was largely epistatic over Pka1, with *sty1Δ pka1Δ* double mutants dividing at a length similar to *sty1Δ* single mutants. Pom1 and Pka1 seem to regulate cell length through parallel pathways as *pom1Δ* and *pka1Δ* were additive, with double mutants dividing at shorter size than either single mutant. By contrast, in 0.08% glucose, *sty1Δ pka1Δ* double mutants were significantly shorter than *sty1Δ* single mutants, suggesting that in these conditions Pka1 plays an additional role that is not upstream of Sty1. Interestingly *pom1Δ pka1Δ* double mutant divided at the same length as *pom1Δ* single mutant, suggesting Pom1 is largely epistatic over Pka1 in these conditions. I thus concluded that Pka1 regulates both MAPK and Pom1 pathways, with contributions depending on glucose conditions.

To better understand the changes in cell size upon glucose limitation, I devised an adaptation index representing the percent difference in cell lengths between 2% and 0.08% glucose. Wild type cells reduce in length by about 12%. As is the case upon nitrogen limitation (Petersen and Hagan, 2007; Petersen and Nurse, 2007; Shiozaki and Russel, 1995), MAPK likely promotes mitotic entry upon glucose limitation, as *sty1Δ* cells did not shorten in 0.08% glucose. Instead, these cells became longer, yielding a negative adaptation index. Remarkably, this negative adaptation was abolished by *pom1* deletion. Consistently, *pom1* deletion or inactivation caused hyper-adaptation with cells loosing 25% of their length in low glucose, suggesting Pom1 plays a comparatively more important role to delay mitosis in glucose-limiting conditions. I further confirmed that the newly recruited, membrane-associated Pom1 activity delays mitosis through Cdr2 regulation, as in cells grown in glucose-rich medium. First, *pom1^{KD}* cells bearing a kinase-dead allele were indistinguishable from *pom1Δ*, indicating Pom1 kinase activity is required. Second, *tea4* mutant cells, in which Pom1 is largely cytosolic (Hachet *et al.*, 2011), showed hyper-adaption to glucose limitation like *pom1Δ*, indicating that Pom1 signals from the plasma membrane. Third, mutation of 6 Pom1 auto-phosphorylation sites in *pom1^{6A}*, previously shown to delocalize active Pom1^{6A} around the cell cortex even in rich medium (Hachet *et al.*, 2011) severely dampened cell length adaption to low glucose. Fourth, *cdr2Δ* was epistatic to *pom1Δ* under limiting glucose, like in rich medium,

and also showed dampened adaptation. Finally, I found that the $cdr2^{T166A}$ allele, carrying a mutation of the activation loop preventing phosphorylation by the activating kinase Ssp1 (Deng *et al.*, 2014), showed hyper-adaption to glucose limitation, similar to *pom1Δ*. This is consistent with the proposed model that Pom1 blocks activation of Cdr2 by Ssp1 (Deng *et al.*, 2014). However, mutation of the C-terminal Pom1 phosphorylation sites in $cdr2^{S755A-758A}$, through which Pom1 was proposed to inhibit Cdr2 activity (Bhatia *et al.*, 2013; Deng *et al.*, 2014), was epistatic to *pom1Δ* in high, but not low glucose, and did not show hyper-adaption to glucose limitation, suggesting other modes of Cdr2 regulation by Pom1 exist. Together these data suggest that the higher levels of Pom1 along cell sides in low glucose conditions impose a stronger inhibition on Cdr2, balancing the mitosis-promoting effect of the MAPK pathway.

Table1: Microtubule dynamic parameters of the indicated strains

	%G	Genotype	Shrinkage rate	Growth rate	Freq. catastrophe	Freq. rescue	Dynamicity	% side catastrophes
25°C	2	WT	8.06±1.47	3.3±0.57	0.53±0.13	0.51±0.14	23.4±3.84	9.17±10.5
	0.08	WT	9.34±2.1	2.9±0.83	0.63±0.28	0.61±0.2	26.2±5.5	23.80±15.7
	2	*pka1Δ*	5.55±1.13	2.95±0.56	0.53±0.13	0.6±0.19	17.06±2.9	5.80±7.3
	0.08	*pka1Δ*	5.36±1.23	3.06±0.70	0.36±0.12	0.36±0.14	17.53±2.9	6.60±12.9
	2	*klp5Δ klp6Δ*	7.55±1.37	3.08±0.51	0.3±0.16	0.31±0.13	20.47±5.25	4.1±0.07
	0.08	*klp5Δ klp6Δ*	7.97±1.39	2.97±0.48	0.48±0.12	0.37±0.14	24.5±4.7	25.6±10.8
	2	*klp5Δklp6Δ pka1Δ*	7.36±1.47	3.05±0.56	0.28±0.14	0.26±0.13	21.07±3.48	5.4±0.09
	0.08	*klp5Δklp6Δ pka1Δ*	7.21±1.73	3.14±0.58	0.34±0.14	0.26±0.19	23.5±6.7	18.5±12.7
36°C	2	WT	11.2 ± 3.04	4.6 ± 1.37	0.59 ± 0.2	0.58 ± 0.15	31.83±8.25	3.07±4.2
	0.08	WT	12.2 ± 3.0					26.8±7.3
	2	*pka1Δ*	6.03 ± 1.25	3.8 ± 0.68	0.41 ± 0.09	0.47 ± 0.11	19.63±2.14	2.4±3.9
	0.08	*pka1Δ*	6.19 ± 1.7					4.9±8.1
	2	*cls1-36*	11.13 ± 2.9	4.45 ± 0.8	0.47 ± 0.16	0.44 ± 0.15	31.89±6.16	3.1±4.3
	0.08	*cls1-36*	11.7 ± 2.5					32.4±28.8
	2	*cls1-36 pka1Δ*	11.19 ± 2.7	4.09 ± 0.9	0.5 ± 0.14	0.48 ± 0.12	31.33±6.59	3.58±4.58
	0.08	*cls1-36 pka1Δ*	11.4 ± 2.6					28.1±16.05

	%G	Genotype	Shrinkage rate	Growth rate	Freq. catastrophe	Freq. rescue	Dynamicity	% side catastrophes
25°C	2	*Pka1-OE*	13.1±2.1	3.59±0.45	0.71±0.15	0.7±0.17	32.1±8.1	30.2±24.3
		cdc25-22	8.35±1.3	3.93±0.98	0.37±0.2	0.39±0.17	25.2±4.2	20.1±16.9
		mal3Δ	6.09±1.45					
		mal3Δ pka1Δ	4.5±0.85					
		tea2Δ	10.09±2.23					
		tea2Δ pka1Δ	6.98±1.26					
		tip1Δ	7.74±1.03					
		tip1Δ pka1Δ	5.98±0.83					
		tip1Δ tea2Δ mal3Δ	8.4±2.0					
		tip1Δ tea2Δ mal3Δpka1Δ	5.0±0.18					
		alp14Δ	4.7±0.58					
		alp14Δ pka1Δ	3.7±0.58					
		ase1Δ	8.3±1.67					
		ase1Δ pka1Δ	5.7±1.24					
		dhc1Δ	8.0±1.23					
		dhc1Δpka1Δ	4.62±1.12					

Table 2: Mean cell length at division of the strains used in this thesis

Genotype	Mean cell length at division		Adaptation index	*p* value
	2%G	0.08%G		
WT	13.9±1.33	12.2±1.57	12.23	>10^{-14}
pka1Δ	11.14±1.9	10.94±3.03	1.79	0.56
sty1Δ	23.04±2.61	24.6±5.4	-6.77	0.0002
sty1Δ pka1Δ	22.7±3.1	21.2±3.2	6.6	>10^{-7}
pom1Δ	11.58±1.7	8.69±1.26	24.95	>10^{-49}
pom1Δ pka1Δ	9.07±1.77	8.64±2.17	4.74	0.12
pom1Δ sty1Δ	17.4±1.99	16.6±2.08	4.59	0.0048
cdr2Δ	22.25±1.86	21.24±3.9	4.5	>10^{-8}
pom1Δ cdr2Δ	21.8±3.02	20.5±2.95	6.3	>10^{-6}
pom1^{6A}	19.38±1.38	18±3.5	7.12	>10^{-5}
pom1^{KD}	11.5±1.5	8.2±1.7	28.69	>10^{-34}
tea4Δ	15.1±1.01	9.6±0.9	36.5	>10^{-82}
tea4^{RVXF*}	15.1±0.9	10.5±1.1	30.67	>10^{-60}
cdr2^{T166A}	18.22±1.57	14.34±1.7	21.42	>10^{-37}
WT (YSM2224)	13.08±1.55	11.69±2.31	10.6	0.0003
pom1Δ	11.25±1.38	8.34±1.46	25.8	>10^{-18}

(YSM2229)				
cdr2^{S755A-758A} *(YSM2226)*	12.46±1.08	11.03±2.16	11.47	$>10^{-7}$
pom1∆ cdr2^{S755A-758A} *(YSM2234)*	12.11±2.24	8.52±1.24	20.71	$>10^{-31}$

The *p* value was calculated by using the student's *t-test* comparing the cell length at division in 2%G vs 0.08%G for the same strain. A p value less than 0.05 was considered to indicate a significant difference. All strains used are prototrophs, except for the bottom four (YSM2224, YSM2226, YSM2229 and YSM2234), which are auxotrophs for leucine and uracil.

Chapter 3

Discussion and Future perspectives

In this thesis work I tried to answer the two main questions set forth which were to understand the mechanism of Pom1 re-localization and its physiological implication for the cell, upon glucose limitation, a condition that fission yeast cells may face routinely in the wild. In the first part of this work, I discovered a novel PKA-signaling dependent destabilization and change in the organization of microtubules. This occurs via a negative regulation of the microtubule rescue factor CLASP. I demonstrated that upon glucose limitation, microtubules get destabilized and contact the lateral cell cortex, where they transiently deposit the type I phosphatase regulatory subunit Tea4. This in turn may recruit Pom1 at the cell sides shedding light on the mechanism of Pom1 re-localization in these conditions. In the later part of this work, I focused on the implication of this side-localized Pom1 on the cell cycle in limited glucose. I showed that Pom1 plays a more important role to delay cell division in these limiting conditions through regulating Cdr2. Finally I proposed that a balance in the mitotic delay function of Pom1 and the mitosis promoting function of the stress-responsive MAPK pathway, is important for cells to attain a critical size under these conditions.

Pom1 gradients are modulated by external glucose levels

Pom1 in steady state conditions forms gradients emanating from cell poles and its concentration decays as it reaches the cell middle. At the cell middle it regulates its substrate the mitotic inducer kinase Cdr2. It is not very clear how these low medial levels of Pom1 may regulate Cdr2 in the cell middle. Indeed Pom1 delays mitosis and artificial recruitment of Pom1 to the cell side imposes a G2 delay acting via Cdr2 and Wee1 (Martin and Berthelot-Grosjean, 2009). However changes in the medial levels of Pom1 have not been naturally observed in interphase cells. Previous data has shown Pom1 to be distributed/diffused more generally in the cell upon treatment with P-factor, however this was in shmoo forming cells and in a protease mutant background (Niccoli and Nurse, 2002). Also initial observations from Sophie Martin showed that its localization was unaffected in interphase cells upon nitrogen depletion or sorbitol stress. Instead it was seen all over the cortex upon glucose depletion.

Thus modulation in the medial levels of Pom1 is a natural response to glucose limitation. Indeed in 0.08% glucose, there is an increase in the medial levels of Pom1 and it shows an important effect on cell size: causing cell-elongation through Cdr2. In

0.03% glucose, Pom1 is seen all over the cell cortex, mimicking the localization of the kinase-dead (^{kd}) allele. However FRAP experiments (in both 0.08%G and 0.03%G) show that the dynamics of Pom1 remain faster compared to the slower recovery of the Pom1^{kd} allele, suggesting that Pom1 remains active in these conditions though delocalized. Although these experiments suggest Pom1 to be still active, immunoprecipitation of Pom1 from cells grown under various glucose conditions and doing direct *in-vitro* kinase assays using Cdr2 fragments as substrates, would be a direct test to assess its activity. FRAP experiments using the Pom1^{kd} allele also suggested that there may be intrinsic changes in the plasma membrane properties or lipid composition upon glucose limitation. Recent studies have evoked a major interest in the role of lipids in regulating cell polarity (reviewed in Martin and Arkowitz, 2014). In particular sterol rich domains are enriched at tips and cell-division site and thought to contribute to polarity and cytokinesis in fission yeast (Wachtler, 2003). Interestingly in this study, they also observed a reduction in the fluorescence levels of filipin (used to mark sterol domains) in glucose-starved cells. Further studies by manipulating these domains and using mutants would be required to see if this could have an impact on localization of polarity proteins including Pom1 upon glucose depletion.

Where and when does PKA signaling regulate Pom1?

In this work, I showed that under limiting glucose conditions Pom1 re-localizes around the cell cortex in a *pka1*-dependent manner. However under these conditions Pka1 is expected to be largely inactive. Indeed previous studies have shown that nuclear localized Pka1 is active in glucose-rich conditions where it represses the transcription of target genes, whereas, in glucose-poor conditions cytosolic Pka1 is expected to be transcriptionally inactive (Byrne and Hoffman 1993; Higuchi *et al.*, 2002; Matsuo *et al.*, 2008). My findings using exogenous cAMP addition to *cyr1* mutant cells and inhibiting Pka1 activity using the analog-sensitive (*pka1^{as1}*) allele suggest however that cytosolic Pka1 is active and required to trigger Pom1 side-localization. I further show that Pka1 regulates microtubule stability and organization to cause Tea4 deposition to cell sides thereby causing Pom1 side-localization. Pka1 does regulate microtubule stability as *pka1Δ* cells show increased stability while

overexpression of Pka1 leads to less stable microtubules compared to wild type cells. In addition the PKA-dependent regulation of microtubule stability is reversible and occurs very quickly (within 2 minutes) and is thus unlikely to be a transcriptional response (Coulon *et al.*, 2013). Thus cytosolic Pka1 seems to be active to destabilize microtubules. However this may be more complicated as *cgs1Δ* cells do not show much change in nuclear and cytosolic levels of Pka1 yet shows tip-restricted Pom1 in high glucose and re-localized Pom1 in limited glucose like wild type cells, indicating that Pka1 may signal Pom1 re-localization from the cytosol, but that an increase in cytosolic Pka1 cannot be the trigger for Pom1 re-localization. Thus though PKA activity is necessary for microtubule destabilization it is certainly not sufficient for this phenomenon.

It is therefore very likely that other signaling pathways apart from PKA also regulate microtubule dynamics and Pom1 localization. This other signal is unlikely to be the Target of Rapamycin (TOR) pathway, as mutants in either the TORC1 (*tor2-S*) or the TORC2 (*tor1-D*) behave like wild type cells for Pom1 re-localization. Further I show that inhibition of TOR using torin1 with or without simultaneous activation of PKA using exogenous cAMP is not enough to trigger Pom1 side-localization in glucose-rich cells. The prime candidate for this additional signal may be the stress responsive MAPK pathway. This is because a) in the hyperactive mutant of the MAPKK, Wis1 (*wis1^{DD}*) Pom1 levels were very reduced, b) in both the MAPK mutant- *sty1Δ*, and in cells treated with the MAPK inhibitor SP600125, Pom1 re-localizes although to a lesser extent than wild type cells and c) in glucose rich conditions *sty1Δ* is largely epistatic to *pka1Δ*. Further studies should investigate the role of the MAPK pathway in regulating Pom1 localization.

External glucose levels affect microtubule dynamics and organization

Reduction in glucose levels leads to an alteration in microtubule dynamics and organization. Indeed in 0.08% glucose, both the shrinkage rate and dynamicity of microtubules are significantly higher than those in steady state conditions. Microtubule disruption experiments using MBC also indicate destabilization of microtubules in these conditions. Additionally about a quarter of the total percentage of microtubules contact the cell side where they transiently deposit the polarity

protein Tea4 thereby recruiting Pom1. Furthermore, in 0.03% glucose, microtubules are completely depolymerized. Thus while spindle microtubules are resistant, cytoplasmic microtubules are destabilized upon glucose limitation. I hypothesize that re-localized Pom1 may serve to buffer cell-size under these conditions. This finding seems to be very distinct from a very recent report that suggests that carbon exhaustion (leading to quiescence) for up to 6-7 days results in the formation of a 'Q-MT' bundle, which is composed of extremely stable microtubules. This bundle is associated to the SPB and retains an antiparallel organization of microtubules. When quiescent cells were re-fed with rich medium, the bundle rapidly (~5 min) elongated from both extremities and in ~15 minutes, new interphase microtubules were assembled (LaPorte *et al.*, 2015). This study proposed that the Q-bundle elongation was important to reestablish polarity upon quiescence exit as cells failing to do so formed T-shapes. Thus microtubule organization and stability seem to be very sensitive to glucose levels. In case of glucose limitation, destabilization of microtubules may favor the required cell-size shortening observed in such conditions, whereas upon complete glucose depletion for long periods of time, the formation of a hyper-stable microtubule bundle regulates proliferation upon quiescence exit. Therefore cells may employ different strategies to regulate the microtubule cytoskeleton depending on changes in their external environment.

An important consequence of having the polarity machinery (Tea4, Pom1) at cell sides in limited glucose could be an alteration in cell shape via recruitment of the growth machinery. Although in 0.08% glucose cells remain rod-shaped, would a further reduction in glucose levels, lead to sustained Tea4-Pom1 contact at the lateral cortex, recruitment of Cdc42 (the master polarity protein) and the polarity machinery to induce growth at cell sides? Would this eventually form T-shaped cells over longer time periods? Future studies should address this exciting question.

The role of kinesin-8 family proteins

Kinesin-8 family proteins have been shown to possess microtubule de-polymerization activity in yeast and mammalian cells (Gupta *et al*., 2006; Mayr *et al*., 2007; Varga *et al*., 2006). However, *in vitro* characterization of Klp5-Klp6 in fission yeast did not detect noticeable depolymerase activity (Erent *et al*., 2012; Grissom *et al*., 2009). *In*

vivo evidence has shown that this heterodimer provides a length-dependent regulation of microtubule catastrophe, by being more enriched on and specifically enhancing the catastrophe rate of long microtubules (Tischer *et al.*, 2009). Remarkably *klp5Δ klp6Δ* were epistatic to *pka1Δ* for all the microtubule dynamic parameters including position of catastrophes, suggesting that PKA may regulate microtubule dynamics through these proteins. However in spite of a high percentage of side catastrophes, Tea4 levels only mildly increased at the cell middle in the double mutant. This response seems to be non-homogenous, as some cells clearly showed Tea4 dots in the middle while in others Tea4 remained polarized to the cell tips. Consequently Pom1 too showed a very mild re-localization in these cells. This data suggests that maybe the kinesin-8 family proteins apart from regulating microtubule dynamics may have a role in offloading Tea4 from the microtubule ends onto the cell cortex. Indeed microtubules in these mutants tend to curl around the cell tips and dwell for a much longer time at the poles compared to wild type cells before undergoing catastrophe. This could be reflected due to either a delay in deposition of the Tea1/Tea4 complex onto the cortex or a higher affinity for MAPs in general or changes in the capture/anchoring mechanisms of Tea1/Tea4 at the cortex (e.g., Mod5 levels/activity) or changes in the force exerted by the cell cortex on the microtubules in these mutants. Further investigation may lead to an interesting function of these proteins in regulating cell polarity.

PKA signaling likely antagonizes CLASP-dependent microtubule stability

CLASP-dependent microtubule stabilization is a likely target of the PKA signal. Previous work doing *in-vitro* studies showed that CLASP (Cls1) promotes microtubule rescue and suppresses catastrophe by recruiting tubulin dimers onto microtubules (Al-Bassam *et al.*, 2010). *In vivo*, Cls1 is recruited to zones of antiparallel overlap through Ase1 (the microtubule bundling protein) where it promotes rescue and stabilization of the microtubule bundle (Bratman and Chang, 2007). This is in striking contrast to the situation in animal cells where Cls1 localizes to plus ends by CLIP-170 and prevents catastrophe (Akhmanova, 2001) or in plant cells where it promotes growth at cell edges (Ambrose *et al.*, 2011). A recent study by Grallert *et al.*, 2006, in fission yeast, reported a dynein heavy chain 1(dhc1)-

dependent weak localization of Cls1 at the microtubule plus ends, however using the same Cls1 allele both Bratman and Chang, 2007 and my data did not detect Cls1 dots at plus ends even when co-localized using a plus tip protein. Consistently inactivation of Cls1 does not appear to affect plus end microtubule dynamics. Instead, here I show that in *pka1Δ* cells, CLASP inactivation restores microtubule dynamics and catastrophes at cell sides, as well as Tea4 and Pom1 relocation, in low glucose. Thus my data suggests that CLASP promotes microtubule growth persistence in fission yeast as well, but that this activity is normally inhibited by PKA signaling. Therefore tuning of CLASP activity underlies distinct microtubule organization.

PKA most likely antagonizes the microtubule stabilizing function of CLASP. Indeed, Cls1 showed an altered localization in wild type glucose-starved cells where a significant number of Cls1 foci do not contain microtubule bundles. I interpret these sites to be inactive Cls1 foci that cannot promote microtubule rescue thus causing de-polymerization of the bundle seen under these conditions. On the contrary most Cls1 foci in *pka1* mutant cells contain microtubules, thus active in causing rescue and stabilization as seen in these cells. In addition, Pka1 overexpression antagonizes the microtubule-stabilizing effect of the N-terminal CLASP TOG domains, which directly bind tubulin dimers. PKA signaling may also antagonize CLASP microtubule binding, as Cls1 localization on microtubule overlaps is significantly enhanced in *pka1Δ* cells. Although I did not observe any Cls1 foci directly at the plus ends, in *pka1* mutant cells Cls1 forms multiple dots that show a wider spread away from the overlaps, as compared to wild type cells. Thus, I propose that similar to *in vitro* observations, in absence of PKA, direct binding by a few CLASP molecules near a microtubule plus end leads to rescue events promoting further growth of microtubules contacting cell sides.

One thing to be followed up is to understand if CLASP is a direct PKA target. Mutation of the five predicted PKA phosphorylated sites in Cls1 N-terminus did not alter Cls1's ability to stabilize microtubules *in vivo*, and immunoprecipitated Pka1-GFP failed to phosphorylate Cls1 fragments *in vitro*. However, this does not exclude the presence of other additional phospho sites on Cls1 *in vivo* and also it is not completely clear if immunoprecipitated Pka1 is active. This is because even a kinase-dead version was able to phosphorylate myelin basic protein (MBP), a synthetic substrate. Thus the relationship between PKA and CLASP needs to be further

investigated. PKA may also indirectly modulate microtubules by regulating the cell energy levels. Indeed, recent data in the budding yeast has shown that cells lacking PKA activity exhibit higher ATP stores. Whether this happens in fission yeast as well is unknown. However, the complete loss of microtubules observed after long-term starvation in 0.03% glucose may reflect a loss of cellular energy, which indeed happens later in the *pka1* deleted cells. Thus, PKA may regulate microtubule dynamics in direct and indirect ways.

Another aspect that is not entirely clear is how CLASP, being localized at the overlap of microtubules, regulates microtubule catastrophes at the plus end? Indeed though Cls1 inactivation in both high and low glucose does not significantly alter microtubule plus end dynamics (growth, shrinkage, catastrophe and recue), the position of lateral catastrophes is significantly higher in 0.08% glucose. One hypothesis is that CLASP may directly or indirectly regulate kinesin-8 proteins (klp5, klp6), which are proposed to regulate the position of catastrophes favoring more cell-pole catastrophes. Further studies should investigate if CLASP inactivation causes a change in the activity of Kinesin-8 or other plus end proteins regulating cortex catastrophes. Another hypothesis could be that when microtubules get destabilized, they contact the lateral cell cortex more often before undergoing complete de-polymerization. Indeed time-lapse imaging of wild type cells in 0.03% glucose suggests this. Of course, this is very preliminary and more work will be needed to test these hypotheses.

Regulation of cell size by external glucose levels

The cAMP-PKA pathway is known to modulate the cell cycle. Indeed *pka1Δ* cells are short and overexpression of Pka1 induces cell length elongation (Maeda *et al.*, 1994; Yu *et al.*, 1994). Previous studies suggested that cAMP negatively regulates Cdc25 protein levels thus inducing a mitotic delay causing cell elongation (Kishimoto and Yamashita, 2000). Pka1 has been proposed to act upstream of the MAPK pathway through unknown mechanisms (Navarro *et al.*, 2012; Stettler *et al.*, 1996). The MAPK Sty1 further modulates mitotic entry again through mechanisms that are not completely clear although it can act independently of both Wee1 and Cdc25 (Shiozaki and Russel, 1995). Under nitrogen stress, Sty1 was shown to recruit Plo1 to the SPBs to promote mitosis through Cdc25 (Petersen and Hagan 2005; Petersen and Nurse,

2007). My data suggests that the contribution of PKA depends on glucose levels. When glucose levels are high, Pka1 acts mainly through the stress-responsive MAPK pathway as *sty1Δ* show epistasis to *pka1Δ* cells, consistent with previous studies. On the contrary, when glucose levels are limiting, Pka1 acts upstream of Pom1 (*pom1Δ pka1Δ* divide at the same size as *pom1Δ*) to regulate cell size likely by modifying its localization. Pom1 spread causing Cdr2 inhibition would be predicted to activate Wee1 and cause mitotic delay. This would cause cell size elongation instead cells get shorter in limited glucose. I propose that this mitotic delay is counterbalanced by the activation of MAPK, which happens only under limited glucose conditions, thus promoting mitosis. Indeed deletion of *sty1* leads to cells becoming longer upon glucose limitation which may be explained due to Pom1 re-localization inhibiting Cdr2. Thus a balance of these two pathways may help cells to attain a critical cell size with the Pom1-Cdr2 pathway ensuring that cells do not get successively shorter over generations thereby providing a buffering mechanism. Future work should reveal whether this is due to the modification of a homeostatic sizer system.

Finally, the question of why size regulation is so important for a cell is far from understood. Indeed, Pom1 may prevent cells from getting successively shorter over generations in low glucose conditions, however this needs to be tested. One can imagine that reduction in cell size may lead to space constrains for essential processes like DNA duplication or chromosome segregation and may lead to errors in cell division. Conversely if cells keep getting longer over generations, they may require excess energy production to transport essential proteins over long distances. However these are mere ideas which should be tested for instance by doing competition assays between short and long sized mutants with wild type cells to assess for viability and fitness under various growth conditions.

Chapter 4

Materials and Methods

Strain construction, media and growth conditions

All *S.pombe* strains used are listed in Supplementary Table 1. All plasmids used are listed in Supplementary Table 2. Strains were made by either tetrad dissection or random spore analysis and replication on appropriate antibiotic plates. Gene tagging and deletions were done using a PCR-based approach and confirmed by diagnostic PCR (Bähler *et al.*, 1998). Transformations were done using the lithium-acetate-DMSO method (Bähler *et al.*, 1998). Pka1-overexpressing strains were obtained as follows: For *KanMX-3nmt1-GFP-Pka1* strain (FigS2.4A-B), the first 547 bp of Pka1-open reading frame (ORF) and the last 500 bp of Pka1-promoter were cloned in a pFA6a-KanMX6-P3nmt1-GFP plasmid using BamHI/SalI sites in frame after GFP and SacII/EcoRV sites before the kanMX cassette, respectively. The plasmid was cut with SacII/SalI to excise the cassette with the homology and transformed in appropriate yeast strains, wherein the integration was checked by diagnostic PCR. For the *NatMX-3nmt1-Pka1 strain* (Fig 2.7D lower panel), the kanMX6 cassette from pFA6a-kanMX6-P3nmt1 was replaced by the natMX cassette, excised from pFA6a-natMX6 with EcoRV/BglII, followed by the same strategy as above.

To generate the *pka1-as1* strain, the ORF of Pka1 and 618bp of the 3'UTR were cloned in a small plasmid using BamHI/SalI sites and the gatekeeper residue aa278 (Met) was mutated to (Gly) M278G (Bishop *et al.*, 2000) by site-directed mutagenesis and checked by sequencing. The cassette was then excised using the same enzymes and transformed into a *pka1::ura4+* strain which still retains the first 200bp of the Pka1-ORF. Colonies were selected on 5'FOA plates and correct integration was checked by diagnostic PCR.

Cells were grown in standard Edinburgh minimal media (EMM) with appropriate supplements adenine, leucine, uracil (A,L,U) when required. For glucose limitation assays, cells were grown in 2% glucose to mid-log, washed three times in either 0.08%G or 0.03%G and then incubated in the same medium before imaging. For measurement of glucose in the medium (FigS2.1B), cells were grown in EMM-2%G to saturation and glucose concentration in the medium was measured using the Glucose (HK) Assay Kit (Sigma) at the indicated time-points. For nitrogen depletion experiments, cells were first grown in EMM medium containing nitrogen, washed thrice in a medium lacking nitrogen and incubated for the indicated time-points.

In Fig 2.4A-B cells were first grown in EMM with proper supplements, containing 2%G to mid-log phase. They were diluted to an O.D of 0.1-0.2, and 100µl of cells were loaded onto ONIX microfluidic chambers (Y04C plates, CellAsic). After loading, the medium flux was kept constant at 2psi, at which the chamber refresh time is just above 3 min (*CellAsic* Y04C specifications). These cells were first allowed to adapt to the chambers by letting them grow for 3-4 hours prior to imaging. GFP-Atb2 was imaged in these cells in 2%G every 5mins for 15mins, followed by a change in medium to 0.03%G-imaged every 5min for 30mins.

To induce the expression of Pka1, from the nmt1 promoter cells were first grown in a medium containing 5µg/ml thiamine from a 2000x stock, to repress the promoter, washed three times in the same medium without thiamine and incubated for 18-20 hours prior to imaging (Maundrell K, 1990). All temperature sensitive strains were first grown at their permissive temperature of 25°C then shifted to their restrictive temperature of 36°C in either 2%G, 0.08%G or 0.03%G and imaged using a heated objective at 36°C, except the *cdc25-22* which was grown at the semi-permissive temperature of 30°C. All other strains were grown at 30°C and imaged at room temperature (around 23-25°C) unless stated otherwise. For cell-length measurements (Table 2) all strains used were prototrophs and grown in EMM, except for *cdr2$^{S755A-758A}$, pom1Δ cdr2^{S755A-}758A* and corresponding control strains, which were grown in EMM-ALU, with either 2%G or 0.08%G to mid-log before imaging.

Inhibitor treatment

The MAPK inhibitor SP600125 (Sigma) was added at a final concentration of 25µM from a stock of 1mM dissolved in DMSO (Hartmuth *et al.*, 2009). The TOR inhibitor Torin1 (Selleckchem) was added at a final concentration of 25µM from a stock of 2.5mM dissolved in DMSO (Atkin *et al.*, 2014). Adenosine 3', 5'-cyclic monophosphate (cAMP) (Sigma A9501), was used at final concentrations as indicated from a stock of 30mM dissolved in the same medium as used for imaging. 4-Amino-1-tert-butyl-3-(3-methylbenzyl)pyrazolo[3,4-d]pyrimidine, (3MB-PP1) (Toronto Research Chemicals Inc.) was added at final concentrations as indicated from a stock of either 5mM or 1mM in methanol (MeOH). MeOH addition had no effect on cell length or Pom1 localization. Methyl-benzidazole-carbamate (MBC, Sigma, St. Louis,

MO) was used at a final concentration as indicated, from a stock of 2.5 mg/ml in DMSO. Calcofluor (Sigma) was added at a final concentration of 5μg/ml from a 200X stock solution. Hoechst (Sigma) was added at a concentration of 1μg/ml for about 15-20 minutes prior to imaging.

Microscopy

Microscopy was performed on live cells, either on a spinning disk confocal microscope or on a DeltaVision epifluorescence system. Spinning disk microscopy was carried out using a Leica DMI4000B inverted microscope equipped with HCX PL APO X100/1.46 (NA) oil objective and a PerkinElmer Ultraview Confocal system (including a Yokagawa CSU22 real-time confocal scanning head, and solid-state laser and a cooled 14-bit frame transfer EMCCD C9100-50 camera), as described in (Bendezu and Martin, 2013). Stacks of z-series confocal sections were acquired at 0.3 μm intervals with the Volocity software. For quantifications of Pom1 and Tea4 using Cellophane (Bhatia *et al.*, 2013) 5 images were taken over 30 seconds and summed. To measure microtubule dynamics (Table 1), images were acquired on the spinning-disk microscope as 3 medial Z-stacks at an interval of 0.5 μm every 5 seconds for 10 minutes and analysis was done on maximum projections. Fluorescence recovery after photobleaching, (FRAP) experiments were performed on the spinning disk using the PerkinElmer photokinesis module. One full tip was bleached and post-bleach images were acquired at 5 s intervals for the first 60 s followed by 10 s intervals for the next 140 s and finally 30 s intervals for the last 600 s to minimize bleaching during image acquisition as described in (Hachet *et al.*, 2011). For Fig 2.4A-B, wide-field fluorescence microscopy was performed on a DeltaVision platform (Applied Precision) composed of a customized Olympus IX-71 inverted microscope and a UPlan Apo 100X/1.4 NA oil objective, a CoolSNAP HQ2 camera (Photometrics), and an Insight SSI 7 color combined unit illuminator. 7 Z-stacks were acquired at an interval of 0.6μm and a maximum projection was taken and deconvolved. For cell-length measurements (Table 2), images of calcofluor-stained cells were taken using the same setup with a Plan Apo 60x/1.42 NA objective. Figures were prepared with ImageJ64 and Adobe Photoshop CS5 and assembled using Adobe Illustrator CS5.

Biochemistry

For Western blots protein extracts were prepared in CXS buffer (50 mM HEPES, pH 7.0, 20 mM KCl, 1 mM MgCl, 2 mM EDTA, pH 7.5 and protease inhibitor cocktail) from cells grown in EMM with appropriate glucose concentrations, using glass beads and a bead beater. 25μg of the soluble protein extract was loaded and resolved on a SDS-PAGE gel. Primary antibodies used were anti-GFP (Roche) and anti-tubulin (TAT1), secondary antibody was anti-mouse-HRP (Promega). The concentrations of the antibodies used were 1:3000.

Image Analysis

Image analysis for cortical quantification of Pom1, Cdr2 and Tea4 in Fig 2.1C-D, Fig2.3C-D, FigS2.1G and FigS2.4D was done using the manual mode of the ImageJ plugin-Cellophane as previously described (Bhatia *et al*., 2013). The profiles depicted span from one cell tip to the other. The mean fluorescence intensity measured in the medial 2μm region from all the cells was used for the bar and whisker plots as shown in the panels. Cortical Pom1 and Tea4 measurements in Fig 2.5E-F and Fig 2.6E-F were done manually using the segmented line tool plugin of ImageJ on images taken as for Cellophane analysis. A 3-pixel line was drawn along the cell periphery from the center of one tip to the other for 20 cells and fluorescence intensities were obtained using the Plot profile tool. The intensities were corrected for background obtained from profiles of the same line dragged just outside the cell and the corrected intensities in the middle 2μm of each cell was selected. The mean fluorescence intensity of the medial 2μm region of 20 cells was used for the bar and whisker plots shown.

To calculate global fluorescence intensities (FigS2.1D and FigS2.7A), a sum projection of 14 z-stacks on the spinning disk confocal microscope was done for each cell. The polygon tool of ImageJ was used to draw a line manually around the cell periphery and the mean fluorescence intensity inside the cell was obtained using the Measure tool. The fluorescence intensity was corrected for background intensity taken just outside the cell and for cells not expressing GFP or td-Tomato. To measure the ratio of cls1 over microtubules in FigS2.7B, a sum intensity projection of the 14 z-

stacks was done on individual cells imaged on the spinning disk microscope. A 5-pixel line was drawn along a microtubule, using the Straight Line tool in ImageJ and the intensities were obtained using the Plot profile tool. The maximum intensity for each cell was obtained for >27 cells for both the GFP and RFP channels and a ratio of GFP/RFP was calculated. An average of the ratios is shown on the graph. To measure the average fluorescence intensities of western blots, a rectangular box of a fixed size was drawn around each band and its mean intensity was measured using the ROI manager of ImageJ. This was corrected for background intensity by moving the same box outside the band. This procedure was done for both the sample and the loading control (tubulin). The intensity of the sample was normalized to that of the intensity of the loading control for each sample.

FRAP quantifications were done as previously described (Martin and Chang, 2006). The data was plotted and fit to an exponential and t1/2 derived using the Igor Pro 6 software (Wavemetrics).

For measurements of microtubule dynamics, the ImageJ Manual Tracking plugin was used to measure the growth and shrinkage velocities. Microtubule dynamicity was calculated as described (Fu *et al*., 2011; Walker *et al*., 1988). Briefly growth and shrinkage rates were calculated as the change in microtubule length (growth or shrinkage) in time and averaged. Frequency of catastrophe and rescue were measured on a per microtubule basis over 5 min of imaging, and averaged. Dynamicity was calculated by using the following formula: Dynamicity = [(Growth rate/Freq. catastrophe) + (Shrinkage rate/Freq. rescue)] x (Freq. catastrophe + Freq. rescue) (Fu *et al*., 2011).

For cell length measurements done on calcofluor stained cells in FigS2.2C and Table 2, a line was drawn manually across the length of septated cells from the middle of one tip to the other and the length measured using the ImageJ Measure tool. To derive the adaptation index (Table2) the difference between the length in 2%G and 0.08%G was normalized to the length in 2%G. All the graphs represent mean values and the error bars indicate standard deviations except for Fig2.1D, 2.3D, 2.5E-F and S2.4D where box and whisker plots are shown. The middle line in the box represents the median value. The upper and lower edges of the box show the upper and lower quartile respectively. The whiskers/bars represent the greatest and the lowest value in

the given dataset.

Statistical analysis

Student *t-test* was used throughout to test statistical significance of differences in pairwise comparisons. The level of significance is shown with asterisks with * indicating $p < 0.05$, ** $p < 0.01$ and *** $p < 0.001$. N.S indicates not significant ($p > 0.05$).

Table S1: List of strains used in this thesis

Strain number	Genotype	Source
Figure 2.1		
YSM1292	*h- pom1-tdTomato:natMX cdr2-mEGFP:kanMX ade6- leu1-32 ura4-D18*	Martin *et al.*, 2009
YSM1554	*h+ pka1::ura4+ pom1-tdTomato-kanMX leu1-32 ura4-D18*	Lab stock
YSM1617	*pom1-tdTomato-natMXcdr2-GFP-kanMX git3::kanMX leu1-32*	Lab stock
YMK400	*gpa2::ura4+ pom1-tdTomato-natMX ade6- leu1-32 ura4-*	This study
YSM 1553	*cyr1::LEU2+ pom1-tdTomato-kanMX leu1-32 ura4-D18*	Lab stock
YSM 1622	*pom1-tdTomato-natMX cgs1::ura4+ ade6- leu1-32 ura4-D18*	Lab stock
Figure 2.2		
YSM2417	*h+ pka1-GFP-kanMX ade6-M210 leu1-32 ura4-D18*	Matsuo *et al.*, 2008
YMK311	*h- cgs2::ura4+ cyr1::LEU2+ pom1-tdTomato-natMX leu1-32 ura4-*	This study
YMK371	*pka1^{as1} pom1-tdTomato-natMX leu1- ura4-*	This study
Figure 2.3		
YMK149	*h- tea4-tdTomato-natMX ade6-M210 leu1-32 ura4-D18*	This study
YMK183	*pka1::ura4+ tea4-tdTomato-natMX leu1- ura4-*	This study
Figure 2.4		

YSM2370	*h- leu1-32::pSV40-GFP-atb2:leu1+ ura4-*	Lab stock
YMK136	*h+ pka1::ura4+ leu1-32::pSV40-GFP-atb2:leu1+ ura4-*	This study
YMK357	*leu1-32::pSV40-GFP-atb2:leu1+ Tea4-tdTomato-natMX ura4-*	This study
Figure 2.5		
YMK359	*Klp5:: kanMX klp6::ura4+ GFP-Atb2-leu1+ leu1- ura4-*	This study
YMK361	*Klp5:: kanMX klp6::ura4+ pka1::ura4+ GFP-Atb2-leu1+ leu1- ura4-*	This study
YSM2370	*h- leu1-32::pSV40-GFP-atb2:leu1+ ura4-*	Lab stock
YMK136	*h+ pka1::ura4+ leu1-32::pSV40-GFP-atb2:leu1+ ura4-*	This study
YMK452	*klp5::kanMX klp6::ura4+ atb2-GFP-leu1+ tea4-td-tomato-natMX*	This study
YMK454	*klp5::kanMX klp6::ura4+ atb2-GFP-leu1+ tea4-td-tomato-natMX*	This study
YMK362	*klp5::kanMX klp6::ura4+ Pom1-td-Tomato-natMX*	This study
YMK364	*klp5::kanMX klp6::ura4+ pka1::ura4+ Pom1-td-Tomato-natMX*	This study
Figure 2.6		
YMK428	*h+ cls1-36:ura4+ leu1-32::SV40-GFP-atb2:leu1+ ura4-*	This study
YMK427	*pka1::ura4+ cls1-36:ura4+ leu1-32::SV40-GFP-atb2:leu1+ ura4-*	This study
YSM2370	*h- leu1-32::pSV40-GFP-atb2:leu1+ ura4-*	Lab stock
YMK136	*h+ pka1::ura4+ leu1-32::pSV40-atb2-GFP:leu1+ ura4-*	This study
YMK458	*cls1-36:ura4+ leu1-32::pSV40-atb2-GFP:leu1+ Tea4-tdTomato-natMX ura4-*	This study
YMK457	*cls1-36:ura4+ pka1::ura4+ leu1-32::pSV40-atb2-GFP:leu1+*	This study

	Tea4-tdTomato-natMX ura4-	
YMK429	*h+ cls1-36:ura4+ Pom1-tdTomato-natMX*	This study
YMK430	*cls1-36:ura4+ pka1::hphMX Pom1-tdTomato-natMX*	This study
Figure 2.7		
YMK425	*cls1-3GFP-kanMX mcherry-atb2 leu1-*	This study
YMK424	*h- pka1::ura4+ cls1-3GFP-kanMX mcherry-atb2*	This study
YMK475	*leu1-32::pSV40-GFP-atb2:leu1+ [pNnmt1-mcherry-cls1(1-500)]*	This study
YMK476	*natMX-3nmt1-GFP-Pka1 leu1-32::pSV40-GFP-atb2:leu1+ [pNnmt1-mcherry-cls1(1-500)]*	This study
YMK460	*natMX-3nmt1-GFP-Pka1 leu1-32::GFP-atb2:leu1+ ura4-*	This study
Figure S2.1		
YSM1261	*h+ pom1-tdTomato-natMX ade6-M216 leu1-32 ura4-D18*	Lab stock
YSM1554	*h+ pka1::ura4+ pom1-tdTomato-kanMX leu1-32 ura4-D18*	Lab stock
YSM119	*h- pom1-GFP-kanMX ade6+ leu1+ura4+*	Lab stock
YMK038	*pka1::ura4+ pom1-GFP-kanMX ade6+ leu1+*	This study
YSM1556	*Wis1-DD pom1-td-Tomato-kanMX leu1-32 ura4-D18*	Lab stock
YSM1563	*sty1::ura4+ pom1-tdTomato-kanMX leu1-32 ura4-D18*	Lab stock
YMK390	*tor1D-hphMX pom1-tdTomato-natMX*	This study
YMK394	*tor2S-kanMX pom1-tdTomato-natMX*	This study
YSM1292	*h- pom1-tdTomato:natMX cdr2-mEGFP:kanMX ade6- leu1-32 ura4-D18*	Martin *et al.*, 2009
YMK055	*pka1::ura4+ cdr2-GFP:kanMX*	This study
YSM1286	*h+ cdr2-GFP-kanMX pom1Δ::ura4+*	Lab Stock

	ade6- leu1- ura4-	
Figure S2.2		
YMK046	*cgs1Δ::ura4+ pka1-GFP-kanMX ade6- ura4-*	This study
YMK365	*cgs2::ura4+ pka1::kanMX pom1-tdTomato-natMX ura4-*	This study
YMK311	*h- cgs2::ura4+ cyr1::LEU2+ pom1-tdTomato-natMX leu1-32 ura4-*	This study
YSM1180	*h- ade6-M210 leu1-32 ura4-D18*	Lab stock
YMK155	*h- pka1^{as1}(M278G) leu1-32 ura4-D18*	This study
YMK371	*pka1^{as1} pom1-tdTomato-natMX leu1- ura4-*	This study
Figure S2.3		
YSM119	*h- pom1-GFP-kanMX ade6+ leu1+ ura4+*	Bahler *et al.*, 1998
YSM1511	*h- pom1^{KD}-GFP-kanMX ade6+ leu1+ ura4+*	Hachet *et al.*, 2011
YSM165	*h- tea4::kanMX pom1-GFP-kanMX ura4-*	Padte *et al.*, 2006
YMK027	*tea4::kanMX6 pom1-GFP-kanMX6 pka1::ura4+ ura4-*	This study
Figure S2.4		
YSM2370	*h- leu1-32::pSV40-GFP-atb2:leu1+ ura4-*	Lab stock
YMK414	*cdc25-22 aur-mcherry-atb2 leu1-*	This study
YMK140	*h- kanMX-3nmt1-GFP-pka1 aur-mCherry-atb2 leu1- ura4-*	This study
YMK063	*h+ kanMX-3nmt1-GFP-pka1 Pom1-tdTomato-natMX ade6-M216 leu1-32 ura4-D18*	This study
YMK069	*cdc25-22 pom1-tdTomato-NatMX leu1-32*	This study
YSM1554	*h+ pka1::ura4+ pom1-tdTomato-kanMX*	Lab stock

	leu1-32 ura4-D18	
YMK183	*pka1::ura4+ tea4-tdTomato-natMX leu1- ura4-*	This study
YMK330	*tea2::his3 mal3::his3 tip1::kanMX pom1-tdTomato-natMX ura4-*	This study
YMK328	*tea2::his3 mal3::his3 tip1::kanMX pka1::ura4+ pom1-tdTomato-natMX ura4-*	This study
Figure S2.6		
YMK398	*h- kanMX: nmt41-cls1 leu1-32::SV40-GFP-atb2:leu1+ pom1-tdTomato-natMX ade6-M216 ura4-D18*	This study
YMK404	*h- kanMX: nmt41-cls1 leu1-32::SV40-GFP-atb2:leu1+ pom1-tdTomato-natMX pka1::hphMX*	This study
Figure S2.7		
YMK425	*cls1-3GFP-kanMX mcherry-atb2 leu1-*	This study
YMK424	*h- pka1::ura4+ cls1-3GFP-kanMX mcherry-atb2*	This study
Table 1		
YSM2370	*h- leu1-32::pSV40-GFP-atb2:leu1+ leu1- ura4-*	Lab stock
YMK136	*h+ pka1::ura4+ leu1-32::pSV40-GFP-atb2:leu1+ura4-*	This study
YMK428	*h+ cls1-36:ura4+ leu1-32::SV40-GFP-atb2:leu1+ ura4-*	This study
YMK427	*pka1::ura4+ cls1-36:ura4+ leu1-32::SV40-GFP-atb2:leu1+ ura4-*	This study
YMK452	*klp5::kanMX klp6::ura4+ atb2-GFP-leu1+ tea4-td-tomato-natMX*	This study
YMK454	*klp5::kanMX klp6::ura4+ atb2-GFP-leu1+ tea4-td-tomato-natMX*	This study
YMK414	*cdc25-22 aur-mcherry-atb2 leu1-*	This study
YMK140	*h- kanMX-3nmt1-GFP-Pka1 aur-mCherry-atb2 leu1- ura4-*	This study

YMK265	*mal3::his3+ leu1-32::SV40-GFP-atb2:leu1+ ura4-*	This study
YMK237	*mal3::his3+ pka1::ura4+ leu1-32::SV40-GFP-atb2:leu1+ ura4-*	This study
YMK267	*tea2::his3+ leu1-32::SV40-GFP-atb2:leu1+ ura4-*	This study
YMK269	*tea2::his3+ pka1::ura4+ leu1-32::SV40-GFP-atb2:leu1+ ura4-*	This study
YMK263	*tip1::KanMX6+ leu1-32::SV40-GFP-atb2:leu1+ ura4*	This study
YMK239	*tip1::KanMX6 pka1::ura4+ leu1-32::SV40-GFP-atb2:leu1+ ura4*	This study
YMK302	*tea2::his3 mal3::his3 tip1::kanMX leu1-32::SV40-GFP-atb2:leu1+*	This study
YMK293	*tea2::his3 mal3::his3 tip1::kanMX pka1::ura4+ leu1-32::SV40-GFP-atb2:leu1+*	This study
YMK337	*alp14::kanMX leu1-32::SV40-GFP-atb2:leu1+*	This study
YMK335	*alp14::kanMX pka1::ura4+ leu1-32::SV40-GFP-atb2:leu1+ ura4*	This study
YMK271	*ase1::kanMX leu1-32::SV40-GFP-atb2:leu1+ ura4-*	This study
YMK274	*h+ ase1::kanMX pka1::ura4+ leu1-32::SV40-GFP-atb2:leu1+ - ura4-*	This study
YMK524	*dhc1::ura4+ leu1-32::SV40-GFP-atb2:leu1+ pom1-tdTomato-natMX*	This study
YMK525	*dhc1::ura4+ pka1::hphMX leu1-32::SV40-GFP-atb2:leu1+ pom1-tdTomato-natMX*	This study
Table 2		
YSM1372	*h- WT ade6+ leu1+ ura4+*	Lab stock
YMK173	*h- pka1::kanMX ade6+ leu1+ ura4+*	This study

YMK222	*h+ sty1::ura4+ ade6+ leu1+ ura4+*	This study
YMK219	*h+ sty1::ura4+ pka1::kanMX ade6+ leu1+ ura4+*	This study
YMK168	*h- pom1::kanMX ade6+ leu1+ ura4+*	This study
YMK190	*pom1::kanMX pka1::kanMX ade6+ leu1+ ura4+*	This study
YMK243	*pom1::KanMX6 sty1::ura4+ ade6+ leu1+ ura4+*	This study
YSM1476	*cdr2::ura4+ ade6+ leu1+ ura4+*	Lab stock
YSM1499	*pom1::kanMX cdr2::ura4+*	Lab stock
YSM2706	*pom1^{6A} ade6+ leu1+ ura4+*	Lab stock
YSM1495	*pom1^{KD} ade6+ leu1+ ura4+*	Martin *et al.*, 2009
YMK601	*tea4::kanMX ade6+ leu1+ ura4+*	This study
YMK603	*tea4$^{222-225RVXF-RAXA}$ ade6+ leu1+ ura4+*	This study
YSM2226	*cdr2 $^{S755A-758A}$ ade6+ leu1-32 ura4-D18*	Bhatia *et al.*, 2013
YSM2234	*pom1Δ cdr2$^{S755A-758A}$ ade6+ leu1-32 ura4-D18*	Bhatia *et al.*, 2013
YSM2224	h- *ade6+ leu1-32 ura4-D18*	Bhatia *et al.*, 2013
YSM2229	*pom1Δ::kanMX6 ade6+ leu1-32 ura4-D18*	Bhatia *et al.*, 2013
YMK605	*ssp1::ura4+ ade6+ leu1+ ura4+*	This study
YSM2436	*h- cdr2^{T166A} ade6+ leu1+ ura4+*	Deng *et al.*, 2014

Table S2: List of plasmids used in this thesis

Systematic name	Developed name	Details of construct expressed
pSM1590	*pSP72-(pka1ORF-^{M278G}-3'utr 618bp)*	Pka1ORF-^{M278G}+ 3'utr 618bp
pSM1043	*pFA6a-KanMX6-P3nmt1-GFP-pka1ORF(1-547) + pka1promoter (last 500bp)*	Pka1ORF+ Pka1 promoter
pSM1317	*pFA6a-NatMX6-P3nmt1-pka1ORF(1-547bp) + pka1promoter (last500bp)*	Pka1ORF+ Pka1 promoter
pSM1480	*pNmt1-mcherry-cls1(1-500)*	Cls1 (1-500)

References

1. Akhmanova A*, et al.* Clasps are CLIP-115 and -170 associating proteins involved in the regional regulation of microtubule dynamics in motile fibroblasts. *Cell* **104**, 923-935 (2001).

2. Al-Bassam J, Chang F. Regulation of microtubule dynamics by TOG-domain proteins XMAP215/Dis1 and CLASP. *Trends Cell Biol* **21**, 604-614 (2011).

3. Al-Bassam J, Kim H, Brouhard G, van Oijen A, Harrison SC, Chang F. CLASP promotes microtubule rescue by recruiting tubulin dimers to the microtubule. *Dev Cell* **19**, 245-258 (2010).

4. Al-Bassam J, Kim H. Flor-Parra I, Lal N, Velji H, Chang F. Fission yeast Alp14 is a dose-dependent plus end-tracking microtubule polymerase. *Mol Biol Cell* **23**, 2878-90 (2012).

5. Alvarez-Tabares I, Grallert A, Ortiz JM, Hagan IM. Schizosaccharomyces pombe protein phosphatase 1 in mitosis, endocytosis and a partnership with Wsh3/Tea4 to control polarised growth. *J Cell Sci* **120**, 3589-3601 (2007).

6. Ambrose C, Allard JF, Cytrynbaum EN, Wasteneys GO. A CLASP-modulated cell edge barrier mechanism drives cell-wide cortical microtubule organization in Arabidopsis. *Nat Commun* **2**, 430 (2011).

7. Aranda, S., Laguna, A., and de la Luna, S. DYRK family of protein kinases: evolutionary relationships, biochemical properties, and functional roles. *FASEB J.* **25***, 449–462 (2011).

8. Atkin J, Halova L, Ferguson J, Hitchin JR, Lichawska-Cieslar A, Jordan AM, Pines J, Wellbrock C, Petersen J. Torin1-mediated TOR kinase inhibition reduces Wee1 levels and advances mitotic commitment in fission yeast and HeLa cells. *J Cell Sci* **127**, 1346-56 (2014).

9. Bähler J, Pringle JR. Pom1p, a fission yeast protein kinase that provides positional information for both polarized growth and cytokinesis. *Genes Dev* **12**, 1356-1370 (1998).

10. Bähler J, Wu JQ, Longtine MS, Shah NG, McKenzie A 3rd, Steever AB, Wach A, Philippsen P, Pringle JR. Heterologous modules for efficient and versatile PCR-based gene targeting in Schizosaccharomycs pombe. *Yeast* **14**, 943-51 (1998).

11. Behrens R, Nurse, P. Roles of fission yeast tea1p in the localization of polarity factors

and in organizing the microtubular cytoskeleton *J Cell Biol* **157**, 783-93 (2002).

12. Beinhauer JD, Hagan IM, Hegemann JH, Fleig U. Mal3, the fission yeast homologue of the human APC-interacting protein EB-1 is required for microtubule integrity and the maintenance of cell form. *J Cell Biol* **139**, 717-728 (1997).

13. Bendezu FO, Martin SG. Cdc42 Explores the Cell Periphery for Mate Selection in Fission Yeast. *Curr Biol* **23**, 42-47 (2013).

14. Bhatia P, *et al*. Distinct levels in Pom1 gradients limit Cdr2 activity and localization to time and position division. *Cell Cycle* **13**, (2013).

15. Bishop AC, Buzko O, Shokat KM. Magic bullets for protein kinases. *Trends Cell Biol* **11**, 167-172 (2001).

16. Bratman SV, Chang F. Stabilization of overlapping microtubules by fission yeast CLASP. *Dev Cell* **13**, 812-827 (2007).

17. Breeding CS, Hudson J, Balasubramanian MK, Hemmingsen SM, Young PG, Gould KL. The cdr2 gene encodes a regulator of G2/M progression and cytokinesis in Schizosaccharomyces pombe. *Mol Biol Cell* **9**, 3399-3415 (1998).

18. Browning H, Hackney DD, Nurse P. Targeted movement of cell end factors in fission yeast. *Nat Cell Biol*. **5**, 812-8 (2003).

19. Browning H, Hayles J, Mata J, Aveline L, Nurse P, McIntosh JR. Tea2p is a kinesin-like protein required to generate polarized growth in fission yeast. *J Cell Biol* **151**, 15-28 (2000).

20. Brunner D, Nurse P. CLIP170-like tip1p spatially organizes microtubular dynamics in fission yeast. *Cell* **102**, 695-704 (2000).

21. Busch KE, Brunner D. The microtubule plus end-tracking proteins mal3p and tip1p cooperate for cell-end targeting of interphase microtubules. *Curr Biol* **14**, 548-559 (2004).

22. Busch KE, Hayles J, Nurse P, Brunner D. Tea2p kinesin is involved in spatial microtubule organization by transporting tip1p on microtubules. *Dev Cell* **6**, 831-843 (2004).

23. Byrne SM, Hoffman CS. Six git genes encode a glucose-induced adenylate cyclase activation pathway in the fission yeast Schizosaccharomyces pombe. *J Cell Sci* **105** (Pt 4), 1095-1100 (1993).

24. Chiron S, Bobkova A, Zhou H, Yaffe MP. CLASP regulates mitochondrial distribution in Schizosaccharomyces pombe. *J Cell Biol* **182**, 41-49 (2008).

25. Coleman TR, Tang Z, Dunphy WG. Negative regulation of the wee1 protein kinase by direct action of the nim1/cdr1 mitotic inducer. *Cell* **72** 919-29 (1993).

26. Costello, G., Rodgers, L. & Beach, D. Fission yeast enters the stationary phase G0 state from either mitotic G1 or G2. *Curr. Genet.* **11**, 119–125 (1986).

27. Coulon A, Chow CC, Singer RH, Larson DR. Eukaryotic transcriptional dynamics: from single molecules to cell populations. *Nature reviews Genetics* **14**, 572-584 (2013).

28. Daga RR, Yonetani A, Chang F. Asymmetric microtubule pushing forces in nuclear centering. *Curr Biol.* **16**, 1544-50 (2006).

29. Deng L, Baldissard S, Kettenbach AN, Gerber SA, Moseley JB. Dueling kinases regulate cell size at division through the SAD kinase Cdr2. *Curr Biol* **24**, 428-433 (2014).

30. Desai A, Mithison TJ. Microtubule polymerization dynamics. *Annu Rev Cell Dev Biol* **13**, 83-117 (1997).

31. DeVoti J, Seydoux G, Beach D, McLeod M. Interaction between ran1+ protein kinase and cAMP dependent protein kinase as negative regulators of fission yeast meiosis. *Embo J* **10**, 3759-3768 (1991).

32. Drummond DR, Cross RA. Dynamics of interphase microtubules in Schizosaccharomyces pombe. *Curr Biol* **10**, 766-75 (2000).

33. Erent M, Drummond DR, Cross RA. S. pombe kinesins-8 promote both nucleation and catastrophe of microtubules. *PLoS One* **7**, (2012).

34. Fantes P, Nurse P. Control of cell size at division in fission yeast by a growth-modulated size control over nuclear division. *Exp Cell Res* **107**, 377-86 (1977).

35. Fantes, P.A. Control of cell size and cycle time in *Schizosaccharomyces pombe. J. Cell Sci.* **24**, 51-67, (1977).

36. Feierbach B, Verde F, Chang F. Regulation of a formin complex by the microtubule plus end protein tea1p. *J Cell Biol* **165**, 697-707 (2004).

37. Fingar D. C. and Blenis J. Target of rapamycin (TOR): an integrator of nutrient and growth factor signals and coordinator of cell growth and cell cycle progression *Oncogene* **23**, 3151–3171 (2004).

38. Franco-Sanchez A, Fleig U, Toda T, Millar J. The DASH complex and Klp5/Klp6

kinesin coordinate bipolar chromosome attachment in fission yeast. *EMBO J,* 24 2931-43 (2005).

39.   Fu C, Jain D, Costa J, Velve-Casquillas G, Tran PT. mmb1p binds mitochondria to dynamic microtubules. *Curr Biol* **21**, 1431-1439 (2011).

40. Garcia MA, Koonrugsa N, Toda T. Spindle-kinetochore attachment requires the combined action of Kin I-like Klp5/6 and Alp14/Dis1-MAPs in fission yeast. *EMBO J* **21**, 6015-24 (2002).

41. Gardner MK, Odde DJ, Bloom K. Kinesin-8 molecular motors: putting the brakes on chromosome oscillations *Trends Cell Biol* **18**, 307-10 (2008).

42.   Grallert A*, et al.* S. pombe CLASP needs dynein, not EB1 or CLIP170, to induce microtubule instability and slows polymerization rates at cell tips in a dynein-dependent manner. *Genes Dev* **20**, 2421-2436 (2006).

43. Grissom PM, Fiedler T, Grishchuk EL, Nicastro D, West RR, McIntosh JR. Kinesin-8 from fission yeast: a heterodimeric, plus-end-directed motor that can couple microtubule depolymerization to cargo movement. *Mol Biol Cell*. **20**, 963-72 (2009).

44. Gupta DR, Paul SK, Oowatari Y, Matsuo Y, Kawamukai M. Multistep regulation of protein kinase A in its localization, phosphorylation and binding with a regulatory subunit in fission yeast. *Curr Genet* **57**, 353-365 (2011).

45. Gupta ML, Carvalho P, Roof DM, Pellman D. Plus end-specific depolymerase activity of Kip3, a kinesin-8 protein, explains its role in positioning the yeast mitotic spindle. *Nat Cell Biol,* **8**, 913-23 (2006).

46. Hachet O, Berthelot-Grosjean M, Kokkoris K, Vincenzetti V, Moosbrugger J, Martin SG. A phosphorylation cycle shapes gradients of the DYRK family kinase Pom1 at the plasma membrane. *Cell* **145**, 1116-1128 (2011).

47. Hagan IM. The fission yeast microtubule cytoskeleton. *J Cell Sci* **111**, 1603-12 (1998).

48. Hanyu Y, Imai KK, Kawasaki Y, Nakamura T, Makaseko Y, Nagao K, Kokubu A, Ebe M, Fujisawa A, Hayashi T, Obuse C, Yanagida M. Schizosaccharomyces pombe cell division cycle under limited glucose requires Ssp1 kinase, the putative CaMKK, and Sds23, a PP2A-related phosphatase inhibitor. *Genes Cells* **14**, 539-54 (2009).

49. Hartmuth S, Petersen J. Fission yeast Tor1 functions as part of TORC1 to control mitotic entry through the stress MAPK pathway following nutrient stress. *J Cell Sci* **122**, 1737-1746 (2009).

50. Hersch M, Hachet O, Dalessi S, Ullal P, Bhatia P, Bergmann S, Martin SG. Pom1 gradient buffering through intermolecular auto-phosphorylation. *Mol Syst Biol* **11**, 1-7 (2015).

51. Higuchi T, Watanabe Y, Yamamoto M. Protein kinase A regulates sexual development and gluconeogenesis through phosphorylation of the Zn finger transcriptional activator Rst2p in fission yeast. *Mol Cell Biol* **22**, 1-11 (2002).

52. Hiraoka, Y., Toda, T., and Yanagida, M. The *nda3* gene of fission yeast encodes beta-tubulin: a cold-sensitive *nda3* mutation reversibly blocks spindle formation and chromosome movement in mitosis. *Cell* **39***,* 349–358 (1984).

53. Hoffman CS, Winston F. Glucose repression of transcription of the Schizosaccharomyces pombe fbp1 gene occurs by a cAMP signaling pathway. *Genes Dev.* **5**, 561–71 (1991).

54. Hoffman C.S. Glucose sensing via the protein kinase A pathway in *Schizosaccharomyces pombe. Biochem Soc Trans.* **33**, 257-60 (2005).

55. Howard J, Hyman AA. Microtubule polymerases and depolymerases. *Curr Opin Cell Biol* **19**, 31-35 (2007).

56. Hyman, A.A., Salser, S., Drechsel, D.N., Unwin, N., and Mitchison, T.J. Role of GTP hydrolysis in microtubule dynamics: information from a slowly hydrolyzable analogue, GMPCPP. *Mol. Biol. Cell* **3***,* 1155– 1167 (1992).

57. Ikai N, Nakazawa N, Hayashi T, Yanagida M. The reverse, but coordinated, roles of Tor2 (TORC1) and Tor1 (TORC2) kinases for growth, cell cycle and separase-mediated mitosis in Schizosaccharomyces pombe. *Open biology* **1**, (2011).

58. Inoue YH, Savoian MS, Suzuki T, Máthé E, Yamamoto MT, Glover DM. Mutations in orbit/mast reveal that the central spindle is comprised of two microtubule populations, those that initiate cleavage and those that propagate furrow ingression. *J Cell Biol* **166**, 49-60 (2004).

59. Jorgensen P, Tyers M. How cells coordinate growth and division. *Curr Biol* **14**, 1014-1027 (2004).

60. Kanoh J, Russell P. The protein kinase Cdr2, related to Nim1/Cdr1 mitotic inducer, regulates onset of mitosis in fission yeast. *Mol Biol Cell* **9**, 3321-34 (1998).

61. Katsuki M, Drummond DR, Osei M, Cross RA. Mal3 masks catastrophe events in Schizosaccharomyces pombe microtubules by inhibiting shrinkage and promoting rescue. *J Biol Chem.* **284**, 29246-50 (2009).

62. Kishimoto N, Yamashita I. Cyclic AMP regulates cell size of Schizosaccharomycs pombe through Cdc25 mitotic inducer. *Yeast* **16**, 523-29 (2000).

63. Kunitomo H, Higuchi T, Iino Y, Yamamoto M. A zinc-finger protein, Rst2p, regulates transcription of the fission yeast ste11(+) gene, which encodes a pivotal transcription factor for sexual development. *Mol Biol Cell* **11,** 3205-17 (2000).

64. Laporte D, Courtout F, Pinson B, Dompierre J, Salin B, Brocard L, Sagot I. A stable microtubule array drives fission yeast polarity reestablishment upon quiescence. *J Cell Biol*. **210**, 99-113 (2015).

65. Li Y, Chang EC. Schizosaccharomyces pombe Ras1 effector, Scd1, interacts with Klp5 and Klp6 kinesins to mediate cytokinesis. *Genetics* **165**, 477-88 (2003).

66. Lochhead, P.A., Sibbet, G., Morrice, N., and Cleghon, V. Activation- loop autophosphorylation is mediated by a novel transitional intermediate form of DYRKs. *Cell* **121***,* 925–936 (2005).

67. Loiodice I, Staub J, Setty TG, Nguyen NP, Paoletti A, Tran PT. Ase1p organizes antiparallel microtubule arrays during interphase and mitosis in fission yeast. *Mol Biol Cell* **16**, 1756-1768 (2005).

68. MacNeill S.A. and Nurse P. Cell cycle control in fission yeast. The Molecular and Cellular Biology of the Yeast Saccharomyces: Vol.III. *Cell Cycle and Cell Biology* 697–763, Cold Spring Harbor Laboratory Press. (1997).

69. Maeda T, Mochizuki N, Yamamoto M. Adenylyl cyclase is dispensable for vegetative cell growth in the fission yeast Schizosaccharomyces pombe. *Proc Natl Acad Sci* **87**, 7814–18 (1990).

70. Maeda T, Watanabe Y, Kunitomo H, Yamamoto M. Cloning of the pka1 gene encoding the catalytic subunit of the cAMP-dependent protein kinase in Schizosaccharomyces pombe. *J Biol Chem* **269**, 9632-9637 (1994).

71. Magasanik B. *Cold Spring Harb Symp Quant Biol*. **26**, 249–56 (1961).

72. Maiato H, Fairley EA, Rieder CL, Swedlow JR, Sunkel CE, Earnshaw WC. Human CLASP1 is an outer kinetochore component that regulates spindle microtubule dynamics. *Cell*. **113**, 891–904 (2003).

73. Marks J, Hagan IM, Hyams JS. Growth polarity and cytokinesis in fission yeast: the role of the cytoskeleton. *J Cell Sci,* **5**, 229-41 (1986).

74. Martin SG, Arkowitz RA. Cell polarization in budding and fission yeasts. FEMS Microbiol Rev, **38**, 228-53 (2014).

75. Martin SG, Berthelot-Grosjean M. Polar gradients of the DYRK-family kinase Pom1 couple cell length with the cell cycle. *Nature* **459**, 852-856 (2009).

76. Martin SG, Chang F. Dynamics of the formin for3p in actin cable assembly. *Curr Biol* **16**, 1161-1170 (2006).

77. Martin SG, McDonald WH, Yates JR, 3rd, Chang F. Tea4p links microtubule plus ends with the formin for3p in the establishment of cell polarity. *Dev Cell* **8**, 479-491 (2005).

78. Mata J, Nurse P. tea1 and the microtubular cytoskeleton are important for generating global spatial order within the fission yeast cell. *Cell* **89**, 939-949 (1997).

79. Matsuo Y, McInnis B, Marcus S. Regulation of the subcellular localization of cyclic AMP-dependent protein kinase in response to physiological stresses and sexual differentiation in the fission yeast Schizosaccharomyces pombe. *Eukaryot Cell* **7**, 1450-1459 (2008).

80. Maundrell K. nmt1 of fission yeast. A highly transcribed gene completely repressed by thiamine. *J Bio Chem* **265**, 19857-64 (1990).

81. Mayr M, Hummer S, Bormann J, Gruner T, Adio S, Woehlke G, Mayer TU. The human kinesin Kif18A is a motile microtubule depolymerase essential for chromosome congression. *Curr Biol* **17**, 488-98 (2007).

82. Mitchison T, Kirschner M. Dynamic instability of microtubule growth. *Nature* **312**, 237 – 242 (1984).

83. Mitchison, J. M. Growth during the cell cycle. *Int Rev Cytol,* **226**, 165-258 (2003).

84. Moseley JB, Mayeux A, Paoletti A, Nurse P. A spatial gradient coordinates cell size and mitotic entry in fission yeast. *Nature* **459**, 857-860 (2009).

85. Navarro FJ, Nurse P. A systematic screen reveals new elements acting at the G2/M cell cycle control. *Genome Biol* **13**, R36 (2012).

86. Niccoli T. and Nurse P. Different mechanisms of cell polarisation in vegetative and shmooing growth in fission yeast. *J Cell Sci* **115**, 1651-1662 (2002).

87. Nurse P. Genetic control of cell size at cell division in yeast. *Nature, 256,* 547-51 (1975).

88. Pan KZ, Saunders TE, Flor-Parra I, Howard M, Chang F. Cortical regulation of cell size by a sizer cdr2p. *eLife* **3**, e02040 (2014).

89. Parker LL, Walter SA, Young PG, Piwnica-Worms H. Phosphorylation and inactivation of the mitotic inhibitor Wee1 by the nim1/cdr1 kinase. *Nature* **363**, 736-

38 (1993).

90. Pereira G, Schiebel E. Centrosome-microtubule nucleation. *J Cell Sci* **110** 295-300 (1997).

91. Petersen J, Hagan IM. Polo kinase links the stress pathway to cell cycle control and tip growth in fission yeast. *Nature* **435**, 507-512 (2005).

92. Petersen J, Nurse P. TOR signalling regulates mitotic commitment through the stress MAP kinase pathway and the Polo and Cdc2 kinases. *Nat Cell Biol* **9**, 1263-1272 (2007).

93. Pluskal T, Hayashi T, Saitoh S, Fujisawa A, Yanagida M. Specific biomarkers for stochastic division patterns and starvation-induced quiescence under limited glucose levels in fission yeast. *FEBS J* **278**, 1299-1315 (2011).

94. Pringle J.R., Hartwell L.H. *The Saccharomyces cerevisiae cell cycle. The Molecular Biology of the Yeast Saccharomyces: Life Cycle and Inheritance* Cold Spring Harbor Laboratory Press, 97-142 (1981).

95. Radcliffe P, Hirata D, Childs D, Vardy L, Toda T. Identification of novel temperature-sensitive lethal alleles in essential beta-tubulin and nonessential alpha 2-tubulin genes as fission yeast polarity mutants. *Mol Biol Cell.* **9**, 1757-71 (1998).

96. Rickard, J.E., and Kreis, T.E. Identification of a novel nucleo- tide-sensitive microtubule-binding protein in HeLa cells. *J Cell Biol* **110***, 1623–1633 (1990).

97. Rincon SA*, et al.* Pom1 regulates the assembly of Cdr2-Mid1 cortical nodes for robust spatial control of cytokinesis. *J Cell Biol,* (2014).

98. Rupes I, Jochová J, Young PG. Markers of cell polarity during and after nitrogen starvation in Schizosaccharomyces pombe. *Biochem Cell Biol.* **75**, 697-708 (1997).

99. Rupes I. Checking cell size in yeast. *Trends in Genetics* **18**, 479-485 (2002).

100. Russell P, Nurse P. Negative regulation of mitosis by wee1+, a gene encoding a protein kinase homolog. *Cell* **49**, 559-67 (1987).

101. Saitoh S and Yanagida M. Does a shift to limited glucose activate checkpoint control in fission yeast? *FEBS Lett* **15**, 2373-78 (2014).

102. Saitoh S, Mori A, Uehara L, Masuda F, Soejima S, Yanagida M. Mechanisms of expression and translocation of major fission yeast glucose transporters regulated by CaMKK/phosphatases, nuclear shuttling, and TOR. *Mol Biol Cell* **26,** 373-86 (2014).

103. Sammak P, Borisy G. Direct observation of microtubule dynamics in living cells *Nature* **332**, 724 - 726 (1988).

104. Sanchez-Perez I, Renwick SJ, Crawley K, Karig I, Buck V, Meadows JC, Sandblad L, Busch KE, Tittmann P, Gross H, Brunner D, Hoenger A. The Schizosaccharomyces pombe EB1 homolog Mal3p binds and stabilizes the microtubule lattice seam. *Cell*. **127**, 1415-24 (2006).

105. Saunders TE*, et al.* Noise reduction in the intracellular pom1p gradient by a dynamic clustering mechanism. *Dev Cell* **22**, 558-572 (2012).

106. Sawin KE, Snaith HA. Role of microtubules and tea1p in establishment and maintenance of fission yeast cell polarity. *J Cell Sci*. **117**, 689-700 (2004).

107. Shiozaki K, Russell P. Cell-cycle control linked to extracellular environment by MAP kinase pathway in fission yeast. *Nature* **378**, 739-743 (1995).

108. Shiozaki K, Shiozaki M, Russell P. Heat stress activates fission yeast Spc1/StyI MAPK by a MEKK-independent mechanism. *Mol Biol Cell* **9**, 1339-1349 (1998).

109. Shiozaki K. Nutrition-minded cell cycle. *Science signaling* **2**, 74 (2009).

110. Stettler S, Warbrick E, Prochnik S, Mackie S, Fantes P. The wis1 signal transduction pathway is required for expression of cAMP-repressed genes in fission yeast. *J Cell Sci* **109,** 1927-1935 (1996).

111. Su LK, Burrell M, Hill DE, Gyuris J, Brent R, Wiltshire R, Trent J, Vogelstein B, Kinzler KW. APC binds to the novel protein EB1. *Cancer Res* **55,** 2972-7 (1995).

112. Su, S. S., Tanaka, Y., Samejima, I., Tanaka, K. & Yanagida, M. A nitrogen starvation-induced dormant G0 state in fission yeast: the establishment from uncommitted G1 state and its delay for return to proliferation. *J. Cell Sci*. **109**, 1347–1357 (1996).

113. Tatebe H, Shimada K, Uzawa S, Morigasaki S, Shiozaki K. Wsh3/Tea4 is a novel cell-end factor essential for bipolar distribution of Tea1 and protects cell polarity under environmental stress in S. pombe. *Curr Biol* **15**, 1006-1015 (2005).

114. Tischer C, Brunner D, Dogterom M. Force- and kinesin-8-dependent effects in the spatial regulation of fission yeast microtubule dynamics. *Mol Syst Biol* **5**, 250 (2009).

115. Tran PT, Marsh L, Doye V, Inoué S, Chang F. A mechanism for nuclear positioning in fission yeast based on microtubule pushing. *J Cell Biol* **153**, 397-411 (2001).

116. Umesono, K., Toda, T., Hayashi, S., and Yanagida, M. Two cell division cycle genes *nda2* and *nda3* of the fission yeast *Schizosaccharomyces pombe* control microtubular organization and sensitivity to anti-mitotic benzimidazole compounds. *J Mol Biol.* **168,** 271–284 (1983).

117. Unsworth A, Masuda H, Dhut S, Toda T. Fission yeast kinesin-8 Klp5 and Klp6 are interdependent for mitotic nuclear retention and required for proper microtubule dynamics. *Mol Cell Biol* **19**, 5104-15 (2008).

118. Vale RD, Reese TS, Sheetz MP. Identification of a novel force-generating protein, kinesin nvolved in microtubule-based motility. *Cell* **42**, 39-50 (1985).

119. Varga V, Helenius J, Tanaka K, Hyman AA, Tanaka TU, Howard J. Yeast kinesin-8 depolymerizes microtubules in a length-dependent manner. *Nat Cell Biol,* **8**, 957-62 (2006).

120. Wachtler V, Rajagopalan S, Balasubramanian MK. Sterol-rich plasma membrane domains in the fission yeast Schizosaccharomyces pombe. *J Cell Sci* **116**, 867-74 (2003).

121. Walker RA*, et al.* Dynamic instability of individual microtubules analyzed by video light microscopy: rate constants and transition frequencies. *J Cell Biol* **107**, 1437-1448 (1988).

122. Welton RM, Hoffman CS. Glucose monitoring in fission yeast via the Gpa2 galpha, the git5 Gbeta and the git3 putative glucose receptor. *Genetics* **156**, 513-21 (2000).

123. West RR, Malmstrom T, Troxell CL, McIntosh JR. Two related kinesins, klp5+ and klp6+, foster microtubule disassembly and are required for meiosis in fission yeast. *Mol Biol Cell*. **12**, 3919-32 (2001).

124. Wood E, Nurse P. Pom1 and cell size homeostasis in fission yeast. *Cell Cycle* **12**, (2013).

125. Wordeman L. Microtubule-depolymerizing kinesins. *Curr Opin Cell Biol* **1**, 82-88 (2005).

126. Wu L, Russell P. Nim1 kinase promotes mitosis by inactivating Wee1 tyrosine kinase. *Nature* **363**, 738-41 (1993).

127. Wu M.Y, Cully M, Andersen D, Leevers S.J. Insulin delays the progression of Drosophila cells through G2/M by activating the dTOR/dRaptor complex. *EMBO J.* **26**, 371-379 (2007).

128. Yanagida M, Ikai N, Shimanuki M, Sajiki K. Nutrient limitations alter cell division control and chromosome segregation through growth-related kinases and phosphatases. *Philos Trans R Soc Lond B Biol Sci.* **366** 3508-20 (2011).

129. Yanagida, M. Cellular quiescence: are controlling genes conserved? *Trends Cell Biol*. **19**, 705 – 715 (2009).

130. Young PG, Fantes PA. Schizosaccharomyces pombe mutants affected in their division response to starvation. *J Cell Sci* **88**, 295-304 (1987).

131. Yu G, Li J, Young D. The Schizosaccharomyces pombe pka1 gene, encoding a homolog of cAMP-dependent protein kinase. *Gene* **151**, 215-220 (1994).

132. Zimmerman S, Daga RR, Chang F. Intra-nuclear microtubules and a mitotic spindle orientation checkpoint. *Nat Cell Biol*. **6**, 1245-6 (2004).

Acknowledgments

I would first like to thank my thesis supervisor Prof. Sophie Martin for her constant guidance, support and motivation during the past five years of my thesis. I thank her for providing me the opportunity to work in her lab, which has of course taught me a lot about biology but importantly helped me to develop as a scientist. Her enthusiasm and tolerance have helped me to overcome the lows and cherish the highs of my PhD journey.

Sophie also has the ability to attract some wonderful people in the lab, who I have met, interacted and learnt so much from. Firstly, I would like to thank Felipe Bendezu, Libera LoPresti, Vincent Vincenzetti, Kyriakos Kokkoris and Olivier Hachet for their support, kindness and guidance when I joined the lab and making my initial few months in this new country very pleasant. I would then like to thank Payal Bhatia, Laura Merlini, Pranav Ullal, Omaya Dudin, Daniela Gallo, Aleksandar Vjestica, Cassandre Kinnaer, Thais Reichler and Iker Lamas with whom I spent a lot of my PhD years for their help, encouragement and support. I especially extend my thanks to Felipe, Vincent, Libera, Payal, Laura, Aleks, Pranav, Omaya and Dani for their insights, advice and fruitful discussions about science, philosophy, life and beyond! Finally I would like to thank all the present and past members of the Martin lab for their help and support. I thank also Prof. Serge Pelet for his scientific inputs and advice and members of the Pelet lab for good discussions. Lastly, I would like to thank all the members of the department for making this place so lively, workable, friendly and cooperative, giving a great atmosphere.

I would then like to thank all my family and friends back home who have supported me throughout. I especially thank my parents Ujwala and Ramkrishna Kelkar who have always encouraged me to pursue my dreams, supported all my decisions, stood by me always and cared for my happiness and well being. I dedicate this thesis to the two of you.

Finally my sincere and heartfelt thank you goes to Varun Sreenivasan. With me he has lived two PhD theses! Thank you Varun for your constant support, encouragement and guidance, sharing my joys and frustrations and most importantly for always believing in me. This would not have been possible without you!

Manasi KELKAR

Department of Fundamental Microbiology,

University of Lausanne, Biophore Building

CH-1015 Lausanne, Switzerland

09.07.1987

Indian

Phone: +41 21 692 39 53

E-mail: manasi.kelkar@unil.ch

Education

University of Lausanne (UNIL), Lausanne, Switzerland

- Ph.D (UNIL) PhD in Life Sciences   (2010- present)

University of Pune (UoP), Pune, India

- M.Sc. in Zoology with specialization in Molecular Biology   (2008-2010)

St. Xavier's College (University of Mumbai), Mumbai, India

- B.Sc. Double major in Life Sciences and Biochemistry   (2005-2008)

Research Experience

Department of Fundamental Microbiology, University of Lausanne (UNIL), Lausanne Switzerland

- PhD thesis
  Prof. Sophie Martin

  Thesis Title: *Environmental regulation of the Pom1 cell-size homeostasis system in fission yeast* (2010-present).

Department of Zoology, University of Pune (UoP), Pune, India

- Master Thesis

Molecular Biology Research lab (Prof. Deepti Deobagkar)

Thesis Title: *Evidence for the presence of differential DNA methylation patterns in mouse tissues* (2009-2010).

Indian Institute of Science, Education and Research (IISER), Pune, India

- Indian Academy of Sciences, (IAS), Summer Research Fellowship
  Prof. L.S.Shashidhara

  Project Title: *Expression patterns of warts and Src42A in imaginal discs of Drosophila larvae by RNA in-situ hybridization* (May-June 2009).

Publications

- Manasi Kelkar and Sophie G. Martin. PKA antagonizes CLASP-dependent microtubule stabilization to re-localize Pom1 and buffer cell-size upon glucose limitation. *Nature Communications. (In press).*

Meetings attended

- Conference Jacques Monod: Actin and microtubule cytoskeleton in cell motility and morphogenesis: An integrated view, May 2015, Roscoff, France, *Poster.*

- Poster: Conference Jacques Monod: Cell cycle: Bridging scales in cell division, October 2014, Roscoff, France, *Poster.*

- EMBO conference: Pombe 2013: 7th International Fission yeast meeting, June 2013, London, United Kingdom, *Poster.*

- Changins meeting: Kinases, Proteases: from bench to bedsite, November 2012, Nyon, Switzerland, *Oral presentation.*

- EMBO Young Investigator PhD course, September 2012, Heidelberg, Germany *Poster and Oral presentation*.

- Gordon Research Conference on the Plant and Microbial cytoskeleton, August 2012, New Hampshire, United States of America, *Poster.*

References

Prof. Sophie Martin

Department of Fundamental Microbiology

University of Lausanne

Biophore Building

CH-1015 Lausanne

Switzerland

Phone: +41 21 692 39 31

Email: sophie.martin@unil.ch

Prof. Serge Pelet

Department of Fundamental Microbiology

University of Lausanne

Biophore Building

CH-1015 Lausanne

Switzerland

Phone: +41 21 692 56 21

Email:serge.pelet@unil.ch